UNIVERSITÀ DEGLI STUDI DELLA TUSCIA

Department of Economics, Engineering,
Society and Business

Ph.D. Program

Engineering for Energy and Environment
XXXVII Cycle

Ph.D. Thesis

"TRUST: a New Research and Educational Tokamak to Explore an Alternative Magnetic Layout in Nuclear Fusion Reactors"

S.S.D. IIET-01/A

Ph.D. Candidate
Dr. Simone Carusotti

Ph.D. Coordinator
Prof. Andrea Luigi Facci

Supervisor
Prof. Giuseppe Calabrò

Co-Supervisors
Prof. Pierluigi Fanelli
Prof. Flavio Crisanti

Academic Year 2023 – 2024

Contents

Abstract

The main aim of this study is the design of a new academic tokamak Tuscia Research University Small Tokamak (TRUST), under construction at University of Tuscia (UNITUS), to explore a conceptual Alternative Magnetic Layout (AML) for the future nuclear fusion reactor based on the Tokamak concept. The proposed concept is applied as a large down scaled study. In this proposal the Central Solenoid (CS) placed around the Toroidal Field (TF) coils providing a relevant reduction in the reactor size. In order to compensate the increase of the toroidal filed on the coils, that it is intrinsic in such proposal, High Temperature Superconductor (HTS) material is foreseen for the TF coils. An overview of the proposed design and a possible plasma scenario is presented showing the AML advantages and disadvantages. The electromagnetic and structural characterizations for a preliminary design of the TF coils system is included to prove the engineering feasibility of the solution. Moreover, the involvement of the AML design in the TRUST project framework is presented. TRUST is a flexible and low-cost university-class experiment, to train the next generation of fusion engineers and physicists. Beyond its academic goal, TRUST is designed to allow easy replacement of the plasma facing components and testing innovative technologies (i.e., meta-materials) and materials, including a feasible upgrade the magnetic system from copper to HTS. An overview of the TRUST project and conceptual design will be provided. The main parameters for a first stage of operation to achieve the target single null plasma configuration are the following: R_0 = 0.3 m, A = 2.5, I_{pla} = 0.110 MA, B_t = 0.8 T, q_{95} = 3.2. TRUST will help to train the next generation of fusion engineers and physicists ready to study the technological challenges for the construction of a tokamak, accordingly to the scientific program of EU-DEMO and DTT proposals. Three distinct plasma configurations development in preparation for future TRUST operations are foreseen: Lower Single Null (LSN), Double Null (DN), and Upper Single Null (USN). Detailed analyses are presented for each plasma scenario, with a particular focus on optimizing active coil currents during characteristic pulse phases to achieve the desired magnetic field configuration; while appropriately setting the plasma parameters. A preliminary estimation of the thermal loads and plasma temperatures at the first wall and divertor was made from EM scenario analysis, together with a first analysis on TRUST vertical stability. Additionally, a preliminary plasma disruption database is presented, comprising a collection of EM numerical simulations covering various plasma dynamic conditions within the operational space with a preliminary structural verification of the proposed design. Finally, an overview of the TRUST facility status is reported, including the safety verification performed.

1. Introduction

This section provides the foundational framework for the thesis, addressing the context and significance of the research on nuclear fusion as a transformative solution to global energy challenges. It begins by examining the current energy landscape, emphasizing the limitations of fossil fuels and the pressing need for alternative energy sources that are sustainable, scalable, and environmentally benign. The principles and promise of nuclear fusion are introduced, highlighting its potential to meet these demands with minimal environmental impact. The challenges of achieving practical fusion energy are explored, with a focus on the scientific, engineering, and economic barriers. Tokamaks, as the leading technology for magnetic confinement, are presented in detail. Finally, the objectives of the thesis and the dissemination of research findings are outlined, with the TRUST project discussed as a novel academic platform for advancing reactor design and testing alternative magnetic configurations and providing a clear roadmap for the subsequent sections.

1.1 Nuclear Fusion

Global Energy Landscape

Energy has always been the keystone of human progress, shaping civilizations and driving economic growth. The Industrial Revolution, marked by the large-scale use of coal, catalysed unprecedented advancements in technology and infrastructure, fundamentally altering energy consumption patterns. Since then, global energy demand has grown exponentially, driven by industrialization, urbanization, and population growth. Fossil fuels—coal, oil, and natural gas—have been the primary sources of energy, accounting for over 80% of global energy consumption. These resources have powered industrial machines, transportation systems, and electricity grids, underpinning modern life. However, reliance on fossil fuels comes with significant challenges. They are finite resources, with reserves depleting at a concerning rate, and their extraction and combustion are major contributors to greenhouse gas emissions. According to the International Energy Agency (IEA) [1], the global energy sector is responsible for nearly three-quarters of all anthropogenic CO_2 emissions, exacerbating climate change and threatening environmental stability. The impacts of climate change, including rising temperatures, extreme weather events, and sea-level rise, underscore the urgent need to transition to cleaner energy sources.

In response, a global energy transition is underway, characterized by increasing investment in renewable energy technologies such as solar, wind, and hydropower. These technologies have achieved remarkable progress, with significant reductions in cost and improvements in efficiency.

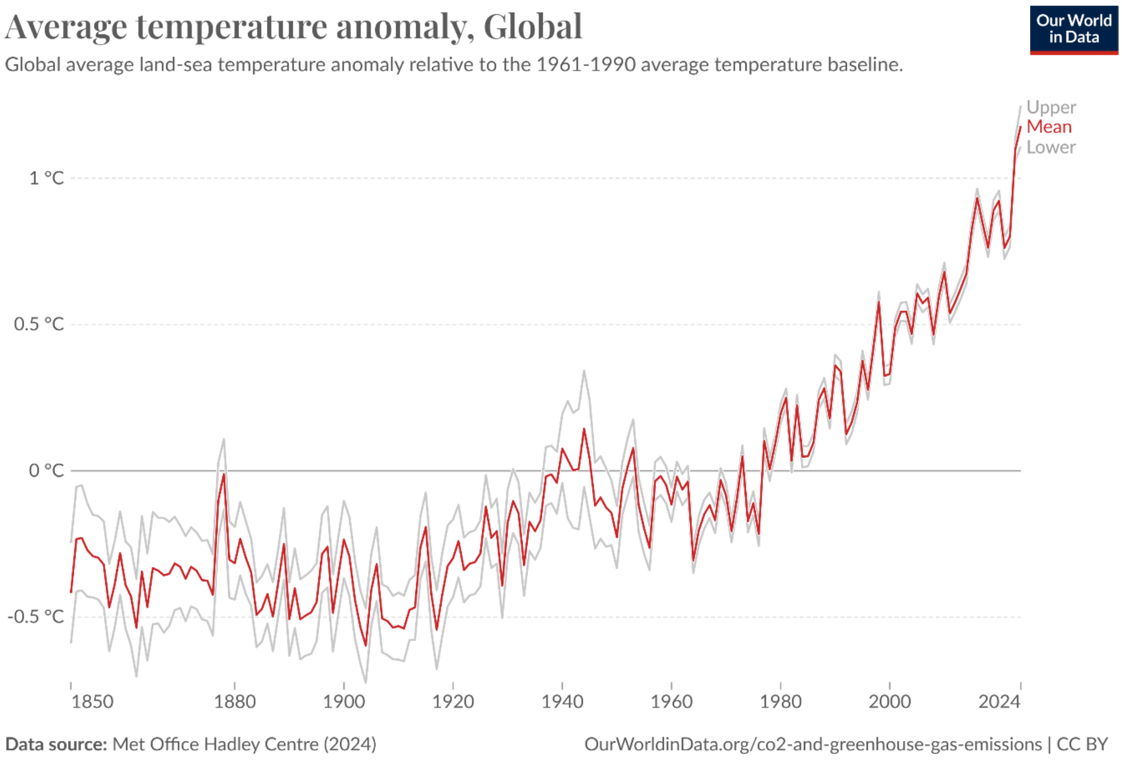

(a)

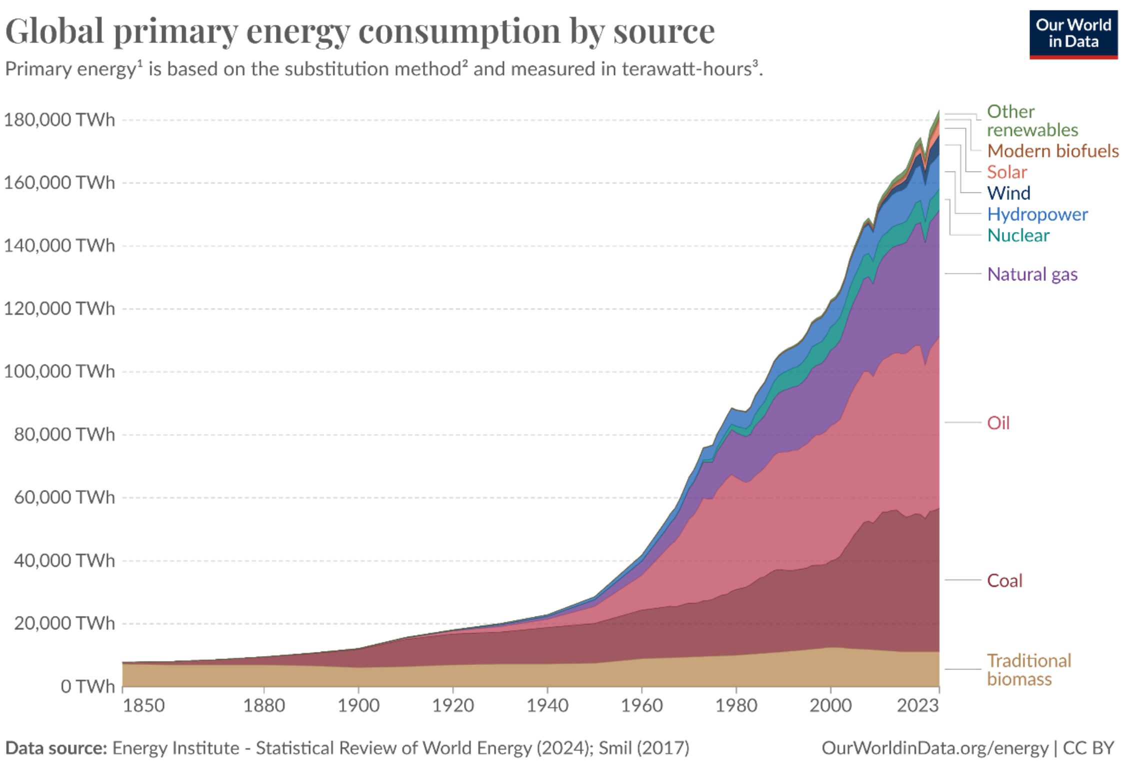

(b)

Fig. 1 (a) Global energy average temperature anomaly and (b) Global primary energy consumption by typology of source

According to the International Renewable Energy Agency (IRENA), renewables accounted for nearly 80% of new electricity generation capacity added globally in 2022. Despite this success, renewables face intrinsic limitations. Their intermittent nature, dependence on weather conditions, and geographic variability hinder their ability to meet the growing global demand for reliable, continuous power [2]. The IEA's *World Energy Outlook 2024* projects that global electricity demand will nearly double by 2050, driven by population growth, urbanization, and the increasing electrification of energy systems. Meeting this demand while achieving climate targets requires the integration of additional energy technologies that can provide consistent, large-scale, and low-carbon power. In this context, nuclear fusion has emerged as a promising solution.

The Promise of Nuclear Fusion

Fusion is the process of combining light atomic nuclei to form heavier nuclei, a reaction that releases substantial energy. This process occurs naturally in the cores of stars, where immense gravitational forces and extremely high temperatures enable hydrogen nuclei to overcome their electrostatic repulsion and fuse. The resulting reactions power stars like the Sun, producing enormous amounts of energy that radiate into space. Replicating these conditions on Earth has been a central focus of scientific research for decades, as nuclear fusion represents a nearly inexhaustible and clean energy source. The most widely studied fusion reaction for terrestrial applications involves deuterium and tritium, isotopes of hydrogen. When these nuclei fuse, they form helium and a high-energy neutron, releasing 17.6 MeV of energy. Unlike chemical reactions, which release energy through the rearrangement of electrons, fusion derives its immense energy yield from mass-to-energy conversion, as described by Einstein's equation $E = mc^2$. The energy carried by the neutron can be harnessed by allowing it to transfer its kinetic energy to a material (e.g., a blanket surrounding the reactor chamber), generating heat that can be used to drive conventional power generation systems. One of fusion's most attractive features is the availability of its fuel sources. Deuterium, a stable isotope of hydrogen, is abundant in seawater, with approximately 33 grams of deuterium in every cubic meter of water. Lithium, used to breed tritium through reactions with fusion neutrons, is widely distributed in Earth's crust and oceans, ensuring a reliable supply. Unlike fossil fuels, which are concentrated in specific regions and often subject to geopolitical tensions, fusion fuel sources are globally accessible and virtually inexhaustible, providing long-term energy security [3][4].

Fusion is inherently clean and safe, addressing many of the concerns associated with traditional energy sources. Unlike nuclear fission, which produces long-lived radioactive waste and poses the risk of catastrophic failures, fusion generates minimal radioactive material, primarily in the form of short-lived isotopes within the reactor components. Additionally, fusion reactors cannot sustain

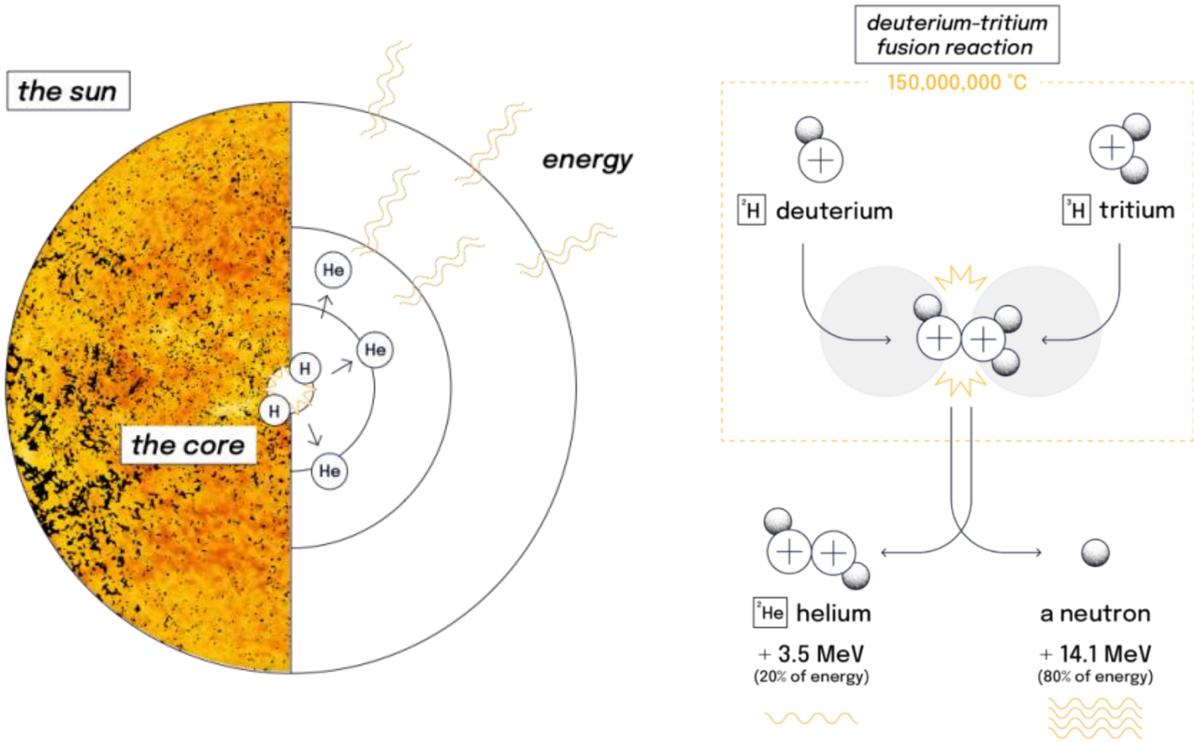

Fig. 2 Schematic view of the nuclear fusion reaction
(Image: ITER Organization)

runaway chain reactions. If the delicate balance of temperature, pressure, or magnetic confinement is disrupted, the fusion reaction ceases immediately, eliminating the risk of large-scale accidents [5]. Fusion also produces no greenhouse gas emissions during operation, making it a critical technology for achieving global climate targets. By replacing fossil fuels with fusion as a primary energy source, humanity could significantly reduce carbon dioxide emissions, mitigating the effects of climate change and supporting the transition to a sustainable, low-carbon future.

Challenges in Fusion Research

Despite its extraordinary promise, achieving controlled nuclear fusion for practical energy generation remains one of the most challenging endeavours in modern science. Fusion requires extreme conditions, including temperatures surpassing 100 million degrees Celsius, adequate particle densities, and sustained confinement times. Under these conditions, matter transitions into a plasma state, where atomic nuclei and electrons are separated. Effectively confining this high-energy plasma and ensuring its stability are essential for maintaining continuous fusion reactions. Magnetic confinement systems, such as tokamaks, employ powerful magnetic fields to trap the plasma within a toroidal chamber, preventing it from contacting the reactor walls. This confinement minimizes energy losses and structural damage. However, achieving and maintaining plasma stability while optimizing confinement efficiency remains a significant hurdle, necessitating sophisticated computational modelling and experimental verification. In addition to scientific challenges, fusion faces substantial engineering and economic barriers. Reactor components must be designed to endure the extreme conditions within a fusion environment, including intense neutron bombardment and severe thermal loads. Advanced materials, particularly those used for plasma-facing components, are essential to ensure the durability and effectiveness of the reactor. Moreover, economic viability is crucial. Fusion systems must not only achieve net energy gain—producing more energy than they consume—but also adopt reactor designs that are scalable and cost-competitive with existing energy technologies [6][7].

Research Context and Objectives

This thesis focuses on addressing key challenges in nuclear fusion research, particularly those related to magnetic confinement and reactor design. The TRUST project serves as the central experimental platform for this work. TRUST is an academic tokamak designed to test innovative magnetic configurations and engineering solutions [8]. Its compact design makes it particularly suited for addressing scalability and economic feasibility, two critical aspects of future fusion systems.

The objectives of this research are to:

1. Investigate alternative magnetic confinement layouts to improve plasma stability and confinement efficiency.
2. Develop scalable and economically viable reactor designs suitable for academic and research applications.
3. Address material and structural challenges posed by fusion environments, with a focus on durability and heat management.

By integrating computational modelling and experimental validation, this thesis aims to advance the understanding of compact fusion reactor technologies and contribute to the broader goal of making fusion energy a practical and sustainable reality.

1.2 Tokamaks

Tokamaks are the most widely studied devices for achieving controlled nuclear fusion, leveraging magnetic confinement to sustain the high-temperature plasma necessary for fusion reactions. Their toroidal (doughnut-shaped) design is central to their ability to trap charged particles using magnetic fields, maintaining the conditions required for fusion. The development of tokamaks represents decades of innovation in plasma physics, materials science, and advanced engineering.

Principle of Operation

At the core of a tokamak's operation is its ability to confine plasma, an ionized gas composed of free electrons and atomic nuclei, at temperatures exceeding 100 million degrees Celsius. Plasma in this state achieves the energy densities needed for the fusion of light nuclei, such as deuterium and tritium, into heavier nuclei, releasing substantial energy. Magnetic fields are essential for confinement

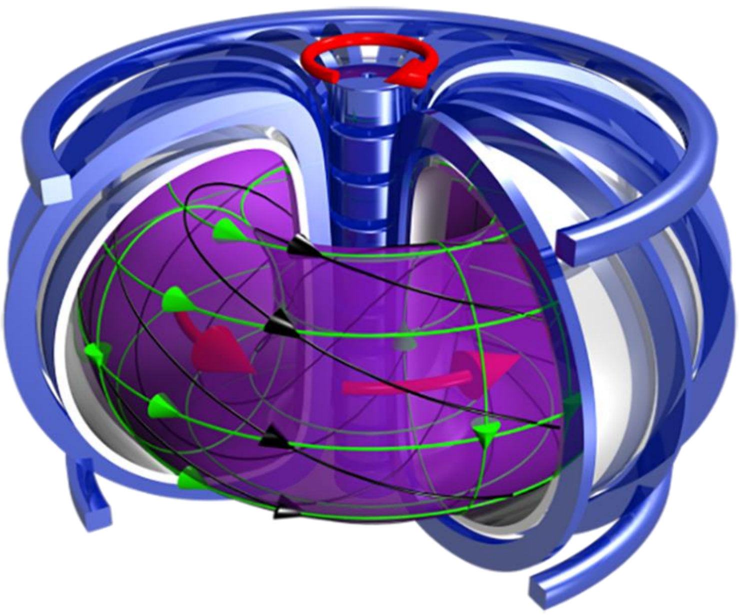

Fig. 3 The electric field induced by a transformer drives a current (big red arrows) through the plasma column. This generates a poloidal magnetic field that bends the plasma current into a circle (green vertical circle). Bending the column into a circle prevents leakage and doing this inside a doughnut-shaped vessel creates a vacuum. The other magnetic field going around the length of the doughnut is referred to as toroidal (green horizontal circle). The combination of these two fields creates a three-dimensional curve, like a helix (shown in black), in which the plasma is highly confined.
(Image: Max Planck Institute for Plasma Physics, Germany)

because they prevent the hot plasma from coming into contact with the reactor walls, where it would rapidly cool and lose its reactive properties. These fields, a combination of toroidal (circular) and poloidal (looping around the cross-section) components, create helical magnetic lines that trap charged particles within the tokamak.

The toroidal magnetic field is produced by a series of toroidal field (TF) coils surrounding the reactor, while the poloidal field is generated by currents induced in the plasma itself, which are driven by a large central solenoid. Together, these fields not only confine the plasma but also maintain its stability and shape within the reactor chamber.

Key Components of a Tokamak

Tokamaks are complex systems that integrate numerous critical components to sustain and control the fusion process:

- **Vacuum Vessel (VV):** The chamber housing the plasma is maintained at an ultra-high vacuum to reduce impurities that could cool the plasma and disrupt fusion reactions. The vessel must also contain diagnostics and cooling systems while withstanding the thermal and mechanical stresses of operation.
- **Magnetic Coils:** The toroidal and poloidal field coils are essential for plasma confinement and stability. High-performance superconducting materials, such as Nb_3Sn or high-temperature superconductors (HTS), are increasingly used in these coils to produce strong magnetic fields efficiently.
- **Central Solenoid (CS):** This large electromagnet, located at the center of the tokamak, induces the plasma current that generates the poloidal magnetic field. It also plays a key role in initiating the plasma and maintaining its current.
- **Plasma-Facing Components (PFCs):** PFCs, including the divertor and limiter, are critical for managing heat and particle loads from the plasma. The divertor, in particular, extracts helium ash and impurities, while also protecting the reactor from excessive heat loads.
- **Breeding Blanket (BB):** Positioned around the plasma chamber, the breeding blanket serves multiple functions. It absorbs high-energy neutrons produced during fusion reactions, converting their kinetic energy into heat that can be used to produce electricity. Additionally, it contains lithium to breed tritium, a key fusion fuel, via neutron interactions. Advanced designs aim to optimize neutron capture, heat transfer, and tritium production, while also providing sufficient shielding to protect the reactor's structural components.

- **Cryogenic Systems:** These systems maintain the superconducting magnets at temperatures near absolute zero, ensuring their efficiency and enabling the generation of high magnetic fields.
- **Auxiliary Heating Systems:** Beyond the ohmic heating generated by the plasma current, tokamaks employ additional methods to reach the required temperatures. Neutral beam injection (NBI) accelerates high-energy neutral particles into the plasma, while radiofrequency (RF) heating uses electromagnetic waves to energize the plasma particles.
- **Diagnostics:** Sophisticated diagnostic systems monitor plasma parameters such as temperature, density, and magnetic field strength in real-time, enabling precise control and optimization of the fusion process.

Large Scale Tokamaks

The development of tokamaks spans decades, with a wide range of devices contributing to the understanding of plasma behavior and the advancement of fusion technology. Among the most prominent is the Joint European Torus (JET), located in the UK [9], which has set records for fusion power output and provided invaluable data for future devices such as ITER. JET has been instrumental in testing deuterium-tritium fuel mixtures, developing advanced plasma scenarios, and exploring materials for plasma-facing components. These contributions have established JET as a cornerstone of fusion research, laying the foundation for the next generation of fusion reactors.

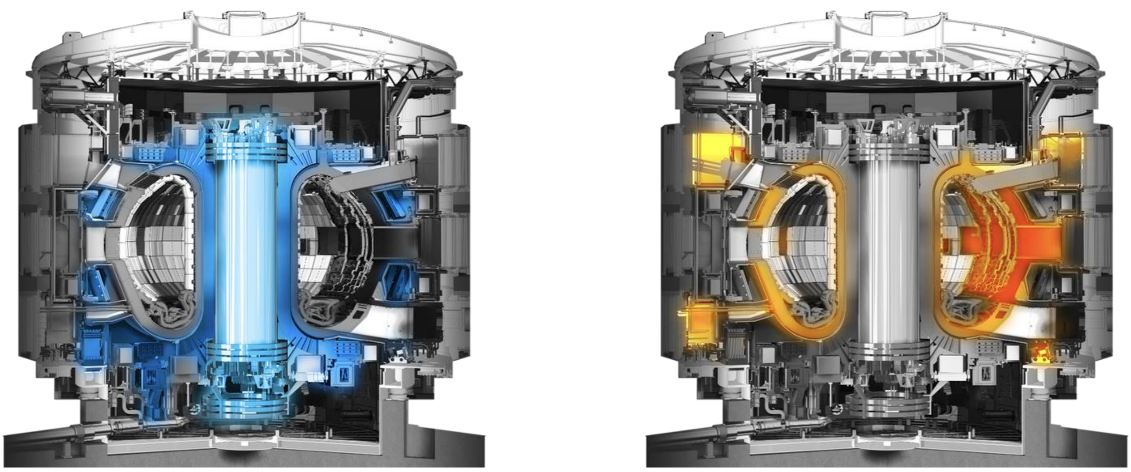

(a) (b)

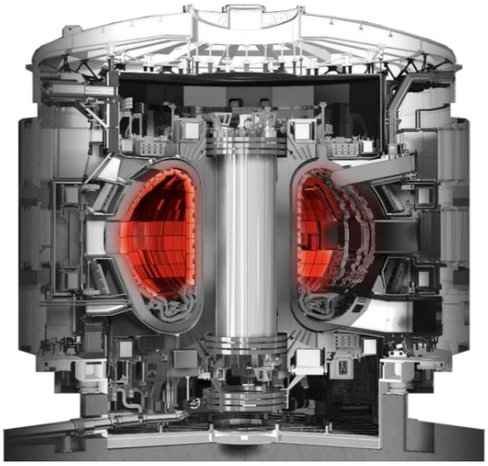

(c)

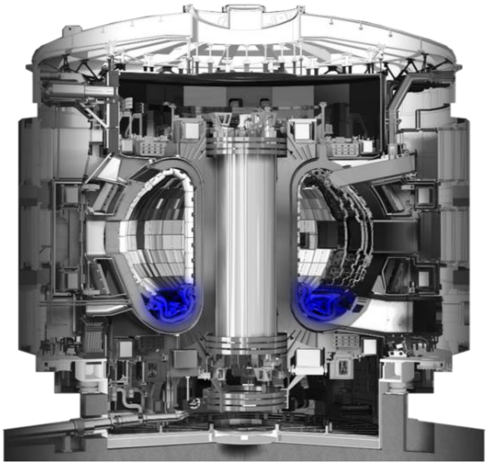

(d)

Fig. 4 Tokamaks main systems: (a) TF and PF coils, (b) VV, (c) BB and (d) Divertor (Image: ITER Organization)

Currently under construction in France, ITER [3][7] represents a significant leap forward, designed to demonstrate the feasibility of achieving net energy gain from fusion at an unprecedented scale. ITER incorporates lessons learned from earlier devices while advancing key areas of fusion science, including magnet technology, plasma control, and the design of the breeding blanket for tritium production. With its massive size and advanced features, ITER is expected to serve as a critical step toward the realization of commercial fusion power plants.

Complementing these large-scale projects are other cutting-edge tokamaks that focus on specific challenges in fusion research. The Divertor Tokamak Test (DTT), located in Italy [10][11], plays a crucial role in testing advanced divertor configurations designed to manage the extreme heat and particle fluxes encountered in fusion reactors. As a dedicated platform, DTT contributes to optimizing heat exhaust solutions for ITER and future reactors. Similarly, the SPARC tokamak, developed by the private company Commonwealth Fusion Systems in collaboration with MIT [12][13], is a compact, high-field device that leverages advanced superconducting magnet technology. SPARC aims to achieve a significant energy gain in a relatively small reactor footprint, demonstrating the potential of compact tokamaks to bridge the gap between research devices and practical fusion power plants.

Academic Tokamaks

Academic tokamaks play a vital role in advancing fusion research, providing platforms to explore innovative technologies, train future scientists, and test experimental setups. These university-level devices contribute to the field by focusing on specialized aspects of fusion research and pushing the boundaries of plasma physics. At the Massachusetts Institute of Technology (MIT), the Alcator C-Mod [14] tokamak has pioneered high-magnetic-field designs, achieving improved plasma confinement and stability in a compact reactor configuration. These advancements underline the potential of high-field tokamaks to achieve higher plasma performance within smaller volumes, reducing the overall scale and cost of reactors. In Japan, Kyushu University's QUEST tokamak [15] emphasizes steady-state plasma operation, a critical milestone for achieving continuous and reliable energy production. QUEST explores advanced radiofrequency (RF) current drive techniques and investigates plasma-wall interactions, contributing to the understanding of long-duration plasma behavior. The Czech Technical University's GOLEM tokamak [16], as one of the oldest operational devices, plays a pivotal educational role. It offers students and researchers hands-on opportunities to study plasma physics, test diagnostic tools, and conduct remote operation experiments, exemplifying its integration into academic curricula and global research networks. At the University of Seville, under the Plasma Science and Fusion Technology (PSFT) group, the SMall Aspect Ratio Tokamak (SMART) [17] is recently starting the operational phase, aiming to explore the effects of negative triangularity in a compact spherical tokamak configuration. This design is anticipated to enhance plasma stability and confinement, contributing valuable insights to the pursuit of efficient fusion energy production. These academic tokamaks collectively advance fusion research by focusing on specific challenges such as plasma stability, steady-state operation, and innovative design configurations. Their contributions are instrumental in progressing toward the realization of practical and sustainable fusion energy.

Spherical Tokamaks

Spherical tokamaks represent a promising avenue in fusion research [18], characterized by their low-aspect-ratio design, which offers potential advantages in terms of compactness, efficiency, and reduced operational costs. Unlike conventional tokamaks with a larger central hole, spherical tokamaks have a more tightly packed core, resembling a cored apple rather than a doughnut. This configuration allows for stronger magnetic fields relative to the size of the device, enhancing plasma pressure and confinement while reducing the overall volume of the reactor. The MAST Upgrade (Mega Amp Spherical Tokamak) in the United Kingdom [19] and the National Spherical Torus Experiment (NSTX) in the United States [20] are leading devices in this category. These projects explore the unique physics of low-aspect-ratio plasmas, focusing on improved confinement, plasma stability, and advanced divertor configurations to manage heat and particle fluxes effectively. Both devices aim to address critical challenges such as controlling plasma instabilities and managing extreme mechanical stresses on the central column, which houses the toroidal field coils. Complementing these efforts is the ST40 tokamak, developed by the private company Tokamak Energy in the UK [21][22][23]. ST40 represents a high-field spherical tokamak that combines compact design principles to achieve fusion-relevant plasma temperatures of over 100 million degrees Celsius, a critical milestone for demonstrating the feasibility of compact and high-performance reactors.

Advancing Tokamak Research

While large experimental facilities like ITER aim to demonstrate the commercial viability of fusion, smaller and academic tokamaks are vital for exploring innovative concepts and providing hands-on training for researchers. These devices enable the study of specific plasma behaviours, testing of new materials, and development of advanced diagnostics and control systems. The synergy between large-scale reactors and smaller experimental devices ensures steady progress in fusion research. By addressing challenges such as plasma stability, magnetic confinement, and efficient breeding blanket design, tokamaks continue to drive the field closer to realizing sustainable, large-scale fusion energy.

1.3 Thesis Objective

The aim of this thesis is the development of TRUST (Tuscia Research University Small Tokamak), a new modular and compact tokamak specifically designed as a research and educational experiment at University of Tuscia (UNITUS) [8]. TRUST aims to deal with some of the critical challenges in fusion reactor design, leveraging its small scale and flexible configuration to support innovative experimentation. By incorporating advanced technologies, such as high-temperature superconductors (HTS) and metamaterials [24], TRUST is positioned to explore the feasibility of next-generation tokamak designs. The educational goal of TRUST is central to its design, providing hands-on training for students and researchers while fostering interdisciplinary collaboration. In addition to its academic role, TRUST emphasizes collaboration with industries to develop and test innovative engineering solutions. This partnership supports the integration of cutting-edge technologies and ensures that the design aligns with practical applications and scalability requirements for future reactors. These collaborations also facilitate the application of advanced manufacturing techniques and modular construction strategies, enhancing the feasibility of compact and efficient tokamak systems. Detailed information on the specific design and objectives of TRUST is provided in Sections 2 and 4. The thesis also introduces the Alternative Magnetic Layout (AML) [25], a pre-conceptual design aimed at simplifying and reducing the size of fusion reactors while maintaining operational efficiency.

TRUST serves as a testbed for AML principles, enabling experimental validation of key features such as the reconfiguration of the central solenoid and toroidal field coils to minimize radial build. The AML concept represents a step toward compact, cost-effective fusion reactors, and its design is elaborated in Section 3.

To evaluate and optimize both TRUST and AML, the thesis employs a combination of computational modelling and experimental validation. Simulations of magnetic equilibrium, plasma behavior, and thermal stresses are conducted to refine design parameters. TRUST plays a critical role in bridging theoretical models with practical outcomes, providing experimental data to validate the feasibility of compact reactor configurations. This thesis not only contributes to the advancement of compact tokamak technology but also emphasizes the importance of integrating educational and industrial objectives. By combining academic training, experimental research, and industrial collaboration, TRUST aims to approach key challenges in fusion technology while fostering innovation and scalability.

1.4 Research Disseminations

Preliminary activities are carried out to understand the tokamak principles of functioning and design through the studies of existing and under construction and design tokamaks. The outcomes of this studies have been presented at the following international conferences:

- FuseNet PhD Event 2022 - S. Carusotti, et al., *Structural behaviour characterization of ST40 Inner Vacuum Chamber (IVC2) during a plasma VDE using ANSYS Workbench.*
- 32nd Symposium on Fusion Technology (SOFT2022) - S. Carusotti, et al., *Structural behaviour characterization of ST40 Inner Vacuum Chamber (IVC2) during a plasma VDE using ANSYS Workbench.*

Moreover, these studies are part of journal publications:

- R. Lombroni, S. Carusotti, et al., *Use of MAXFEA-ANSYS tool to study the Electro-Magnetic behaviour of the new ST40 inner vacuum chamber proposal during a plasma VDE,* Fusion Engineering and Design, 2023, 192, 113611
- S. Carusotti, et al., *Structural behaviour characterization of ST40 Inner Vacuum Chamber (IVC2) during a plasma VDE using ANSYS Workbench*, Fusion Engineering and Design, 2023, 192, 113772.

- M. Scarpari, R. Lombroni, A. Mele, S. Carusotti, et al., *Development of SPARC plasma disruption database through electromagnetic predictive MAXFEA Modelling, Fusion Engineering and Design, 2024, 204, 114469*

The topics proposed in this thesis have been presented at international conferences:

- FuseNet PhD Event 2023 - S. Carusotti, et al., *Overview on the conceptual design of TRUST: the new nuclear fusion experiment of University of Tuscia.*
- 15th International Symposium on Fusion Nuclear Technology (ISNFT 2023) - S. Carusotti, et al., *Overview on the conceptual design of TRUST: the new nuclear fusion experiment of University of Tuscia.*
- 33rd Symposium on Fusion Technology (SOFT2024) - S. Carusotti, et al., *Alternative Toroidal and Poloidal Field Coils Conceptual Design for Tokamaks.*
- 7th International Conference on Frontier in Diagnostic Technologies (ICFDT7) – S. Carusotti, et al., *Alternative toroidal field coils conceptual design for tokamaks in the TRUST project framework.*

Moreover, these studies are part of journal publications:

- S. Carusotti, et al., *Preliminary study on Alternative Magnetic Layout (AML) for tokamaks reactors in the TRUST project framework*, submitted to Fusion Eng. Des., 2024.
- S. Carusotti, et al., *Overview on the conceptual design and preliminary plasma scenario studies of university-class experiment TRUST*, submitted to Fusion Eng. Des., 2024.

2. TRUST Project

The TRUST project idea was conceptualised in the summer 2022 by UNITUS research group on the nuclear fusion (UNITUS4FUSION) and it is based on three main pillars:

- Creation of a new pole on nuclear fusion in Italy capable of training a class of engineers with specific skills on this topic.
- Activation of collaborations with the industrial world for their direct involvement right from the design phase of components and technologies applicable in the world of nuclear fusion.
- Dealing with the frontier of technology and engineering challenges testing innovative materials and alternative solutions for the design of a future nuclear fusion reactors.

The first two aspects arise from the requirements identified by the European Consortium for the Development of Fusion Energy (EUROfusion) of which the UNITUS is a third party through the Italian agency ENEA. The need for more engineers with specific skills in the world of nuclear fusion, and the need to directly involve the industrial and manufacturing world more closely in the development of future tokamaks are key points for speeding up research and development and bridging those technological gaps that could be showstoppers for magnetic confinement fusion energy today [26][27]. This approach is already applied and studied in the United States (US) as set out in the strategic plan of the US Department of Energy (DOE), such as through the recent Innovation Network for Fusion Energy (INFUSE) initiative [28]. The last key point identified the intention to realise a flexible and economic platform to test different technologies under development by the UNITUS4FUSION team and by the International and Italian nuclear fusion community. In fact, considering the current close collaboration between UNITUS and DTT S.C.ar.l. and the EUROfusion Consortium, the TRUST project could contribute to the scientific program of DTT machine [10] and the future EU-DEMO [29].

The industries involvement in TRUST represents one of the key features of this project. The main collaborations range from the physical aspects of the plasma that the experiment will produce to the design of the mechanical components required for the device. One of the first partner that contributed to the definition of the operational parameters for TRUST was Tokamak Energy Ltd [30]; it was essential to develop the TRUST preliminary concept with their cooperation, given their experience in building compact tokamaks. Another key contribution was provided by Walter Tosto Spa [31] one of the most important groups for the construction of pressure equipment. Due to their extensive knowledge in the construction of components for tokamaks, was actively involved in the design of the TRUST vessel to make it feasible according to their standards. In addition, companies such as ASG Superconductors Spa [32] and OCEM Power Electronics [33] are also involved in the TRUST project. These respectively are actively contributing to the design and manufacture of HTS coils and supercapacitor power supplies.

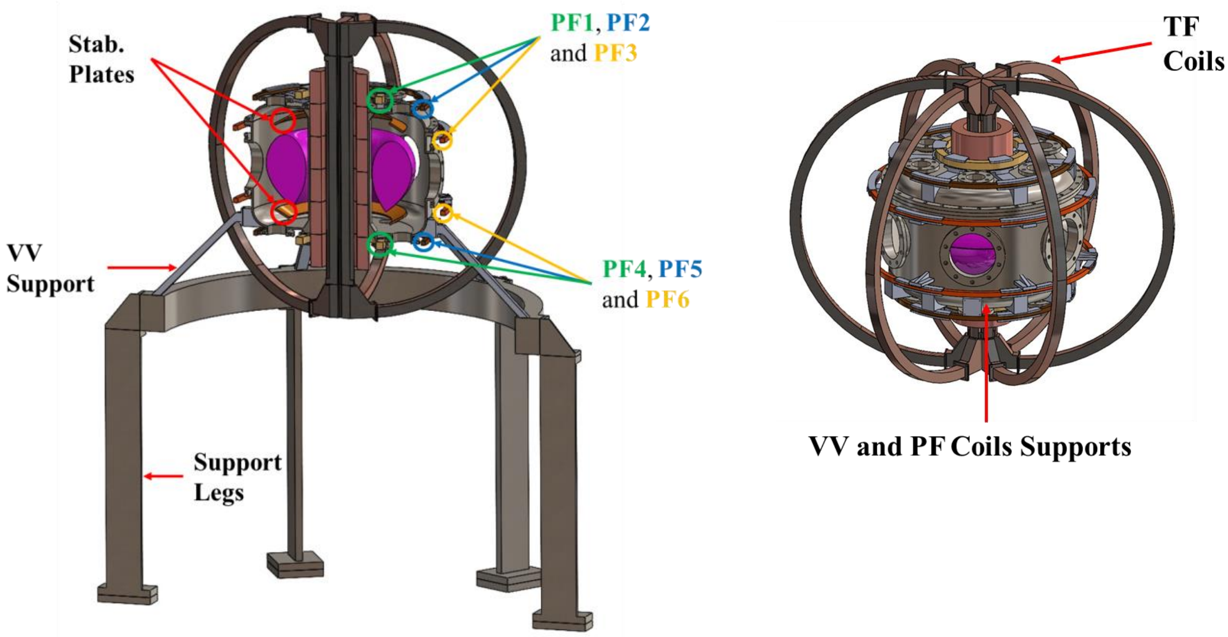

Fig. 5 TRUST conceptual design with its the main components

According to their goals, the starting physics and engineering design drivers for TRUST are the following:

- The target major plasma radius is $R \leq 0.3\ m$.
- The plasma aspect ratio should be $\frac{R}{a} \sim 2.3$.
- The expected plasma safety factor and plasma elongation are respectively $q_{95} > 3.3$ and $k < 1.9$.
- The CS driven discharge is supposed to be in the order of magnitude tenths of a second.
- The CS must be located around to the TF coils central column.
- The integration of HTS coils in the design is foreseen.
- The heat flux on the PFCs should be relevant to test materials and components for a tokamak environment $q_{target} \geq 2 \frac{MW}{m^2}$.

- A Single Null (SN) plasma configuration is foreseen.

This parameters for TRUST are a trade-off between the need to build an academic and economic tokamak fully design and operated by students and the intention to test advanced technologies for nuclear fusion. The major radius of 0.3 m guarantees a compact device affordable for a university in terms of economic resources, facility area and manpower to be involved. In fact the cost of the machine is basically expected to scale like the magnetic energy, i.e. $C_{tot} \sim B^2 R^3$ [34]. The design of a small aspect ratio tokamak (close to a spherical one) is attractive to studies engineering and physical challenges for the nuclear fusion science, such as the integration of all necessary components within the central column of a tokamak. At the same time, with the aimed TRUST performances, it will be possible to reach relevant plasma scenario for testing materials (as described in Section 4.2). The SN configurations is chosen referring to the target plasma scenario planned for DTT [11] and EU-DEMO [35]. Moreover with the SN, it is possible to increase the heat flux on the divertor region for the materials testing. To explore different configurations such as a Double Null (DN) and an Upper Single Null (USN), a symmetric location for the PF coils is foreseen.

Due to its aim, TRUST is designed to operate in three operational phases (OP) along the years. The OP1 includes the achievement of the first plasma and the successful execution of the foreseen target plasma scenario including the commissioning of all the system. In this phase, the device will be equipped with a fully copper magnetic systems with a plasma duration in the order of magnitude tenths of a second. Obliviously, the OP1 covers also the design, manufacturing and test of the TRUST components and mock-ups, as explained in the following paragraphs. So it is possible to affirm that the OP1 is already started, in fact the formation of young engineers and researcher with the direct involvement of the industries remains one of the main goals of this project. In the OP2 the testing of a HTS PF coil is planned by replacing at least one copper PF coil with an HTS one working at 77K. The top divertor coil (PF1, as showed in Fig. 5) is expected to be replaced in HTS material. In fact, the PF1 is the smallest poloidal field coils and the one with the least demands in terms of current and voltage and corresponding derivative (as explained in Section 4.2). This upgrade will allow students and researchers to approach the HTS coil technology and manufacturability. In order to fulfil such goal, a cryogenics laboratory will be set up from the beginning of commissioning of the TRUST facility in the OP1. The possibility to start the operation of HTS coils in a dedicated laboratory, before of their installation on TRUST, is extremely important to reduce errors and possible failures and to train engineers on the design, manufacturing and test of these superconducting coils. On a very long time-scale at third phase OP3 is foreseen where all the TRUST magnetic system will be upgrade from copper to HTS including the TF coils. During the OP3, it is scheduled the addition of an ECH system to upgrade the plasma heating system and to perform plasma discharge with a duration in the order of magnitude hours. The TRUST experiment will be used as testbed for the AML design presenting the same radial positioning for the TF coils and the CS modules. The electromagnetic coupling between the toroidal systems and the poloidal one will be investigated to study the electromagnetic forces acting on the coils. Through TRUST, technological solutions for the AML design will be evaluated such as the design of the TF coils. As explained in Section 3, for the AML configuration different solutions are proposed and with TRUST these can be checked.

The TRUST facility will be located within the UNITUS campus, near the engineering faculty, and directly used and upgraded by PhD students. The site will be arranged with an experimental hall and the several different areas prepared for the auxiliary systems of the experiment. The final design is currently under development and the construction of the facility is scheduled to end within 2025. A detailed explanation of the TRUST facility is given in Section 5. The preliminary design for the facility was approved by the UNITUS Board of Directors with a budget of 350.000,00 € in March 2023 and the Permission to Build, from the Viterbo city municipality, was given in December 2024.

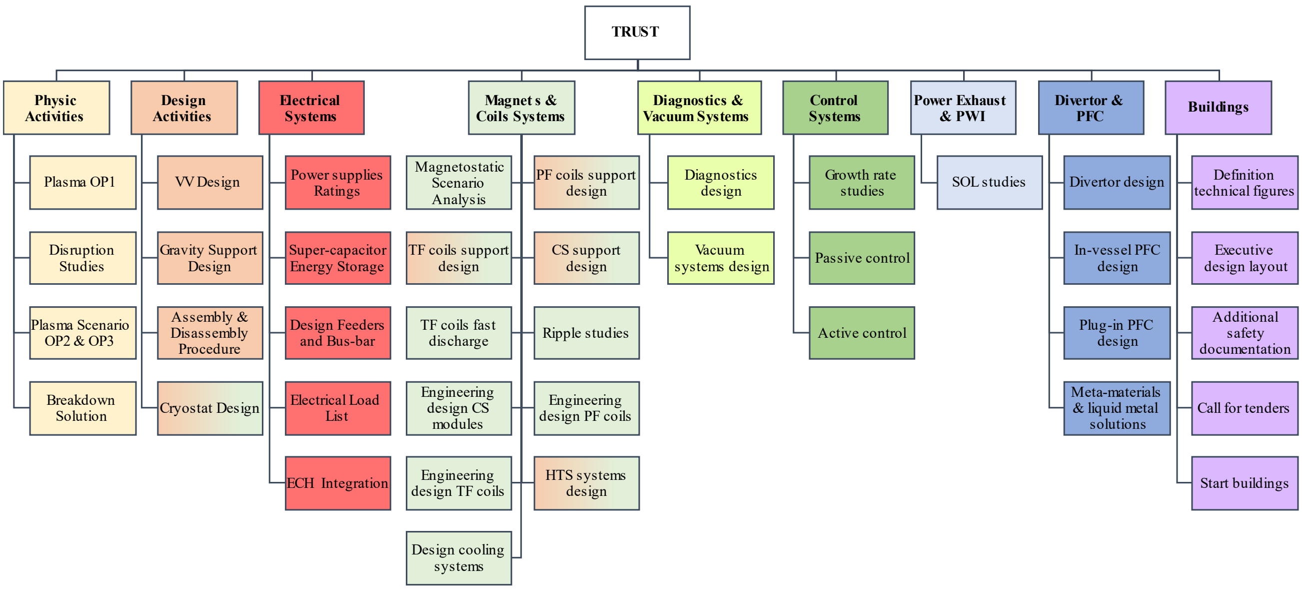

Fig. 6 TRUST work packages structure

For the development of TRUST, an organizational structure for the key activities is carried out. The tasks are divided into several distinct categories, each representing essential aspects of the tokamak's design, operation, and construction. These categories are structured to address both scientific research and engineering challenges while integrating industrial collaboration. The Work Packages (WPs) included in the organizational structure are:

A. Physics Activities, this WP is focuses on developing plasma scenarios and addressing challenges related to plasma operation and stability. Under this activity will be defined the initial plasma operation planning and optimization, the analysis of plasma disruptions and the development of strategies to mitigate their effects, the development of advanced plasma operating phases to ensure stable and efficient performance and the investigation of solutions for plasma startup addressing the critical aspects of achieving stable confinement.

B. Design Activities, this WP deals with the mechanical and structural design of TRUST, ensuring the integration of components. Under this activity will be defined the design of the VV, of the Gravity Support and all the structural supports for the magnetic systems. The latter activity and the Cryostat Design for the HTS coils is developed in parallel with the Magnets and Coils Systems.

C. Electrical Systems, this WP addresses power management and energy supply for the operation of the tokamak. As part of this process, the focus will be on the defining the specifications for power supply systems, designing energy storage solutions for fast discharge requirements including the supercapacitors systems foreseen for TRUST. Moreover, the development of electrical connections for current distribution and the identification and categorizing all electrical loads within the facility including the safety switch-off procedure. Finally, the ECH integration for the OP3 is included in this WP.

D. Magnets & Coils Systems, this WP involves the design, analysis, and optimization of the magnetic systems essential for plasma confinement. Activities include the magnetostatic analysis of operational scenarios, the design of the TF coils and their support of supports, and the engineering of central solenoid (CS) and poloidal field (PF) coils still including the support structures. Additional studies include fast discharge systems for the TF coils, ripple analysis for magnetic field optimization, and the development of HTS systems, supported by corresponding cooling system designs.

E. Diagnostics & Vacuum Systems, this WP addresses the design and implementation of systems for plasma diagnostics and vacuum management. Diagnostics systems are developed to monitor key plasma parameters, such as density and temperature providing real-time feedback during operation. Simultaneously, the vacuum system is designed to maintain ultra-low-pressure conditions in the vacuum vessel, ensuring the proper environment for plasma confinement.

F. Control Systems, this WP focuses on the implementation of passive and active control strategies to manage plasma behavior and ensure operational stability. Growth rate studies are conducted to analyse and mitigate plasma instabilities, while active control systems are developed to provide real-time adjustments to plasma parameters. These systems work together to maintain stable and optimized plasma operation.

G. Power Exhaust & Plasma-Wall Interaction (PWI), this WP examines the power exhaust strategies and plasma-wall interactions necessary for managing the extreme heat and particle fluxes produced during plasma operation. Specific studies focus on the Scrape-Off Layer (SOL), where heat and particles are expelled, to ensure effective exhaust mechanisms and the durability of plasma-facing components.

H. Divertor & PFC, this WP focuses on the development of components that manage the high thermal and particle loads in TRUST. It includes the design of the divertor, in-vessel plasma-facing components, and modular plug-in systems that allow for easy maintenance and replacement. Additionally, advanced material solutions, such as metamaterials and liquid metal technologies, are explored to improve heat resilience and performance.

I. Buildings, this WP deals with the planning and construction of the TRUST infrastructure. It begins with the definition of technical requirements and the preparation of an executive design layout. Safety documentation is developed to ensure compliance with regulations, while procurement processes, including calls for tenders, are initiated. The final phase involves the start of construction to accommodate the TRUST tokamak and its associated systems.

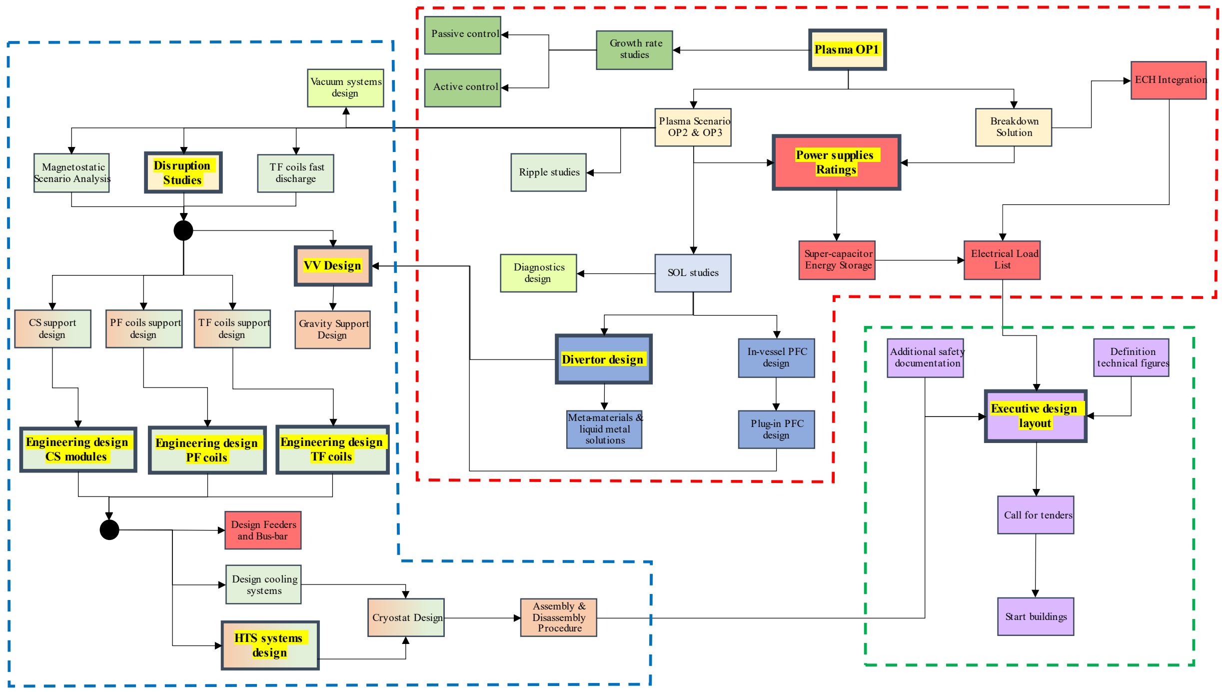

Fig. 7 TRUST work packages flow charts; the highlighted tasks represent the key activities identified for the project.

The TRUST work plan includes a flow chart diagram (Fig. 7) to establish a priority level for each WPs task and to monitoring the activities progress. The current status of the TRUST WP is summarised as showed in Fig. 8.

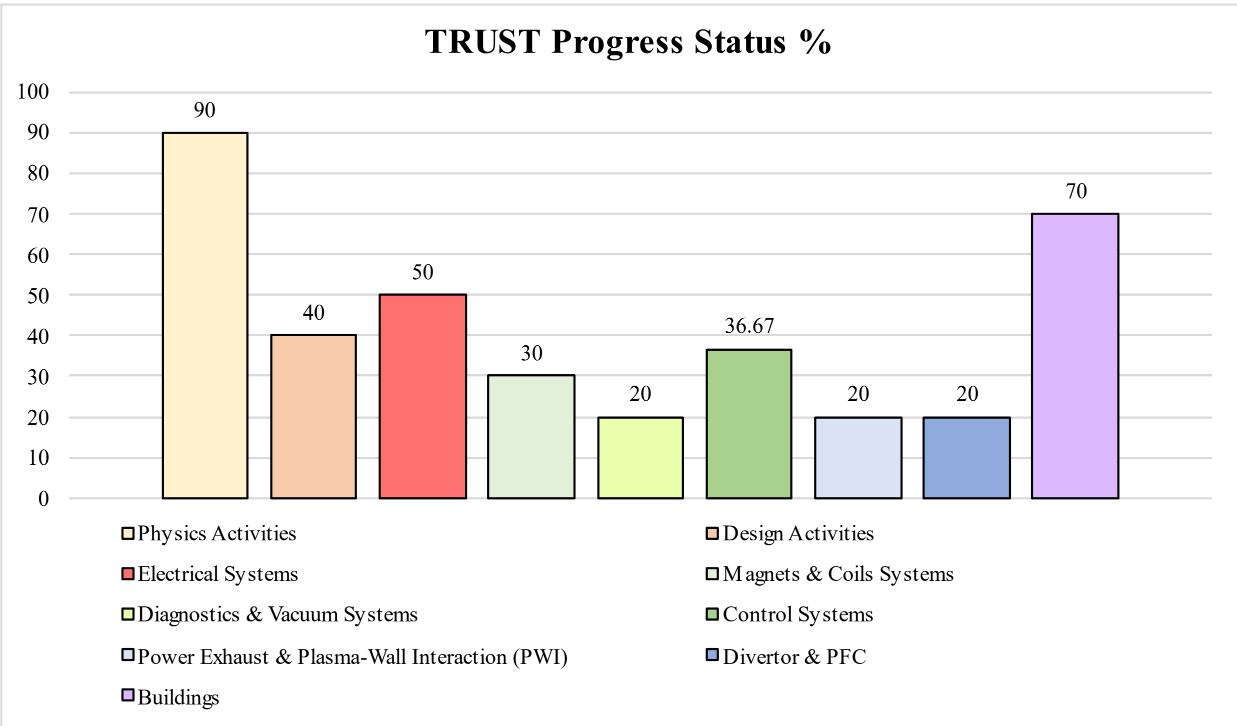

Fig. 8 TRUST progress status for each WP

The total TRUST progress is approx. equal to 40% considering all the WPs tasks to reach the first experimental campaign foreseen for the OP1. The Physics Activities are the most advances, in fact the definition of the target plasma scenario and the analysis of the disruptions load case are the main drivers for the design of a tokamak [36]. In parallel, as explained in Section 5, the design of the TRUST facility is concluded and approved; the remaining activities to complete this WP are related to the preparation of the call for tenders and the starting of construction works. The building activities have been moved ahead of the TRUST design, indeed the space for the realisation of the facility is limited and consequently the design of the experiment for OP1 and OP2 has been adapted. Finally, it can be observed that some WPs are still at an early stage. These include Magnets & Coils Systems, which is one of the most important for the execution of TRUST. Actually, the design of the TF coils, CS modules and PF coils is focused on the AML configurations and in the development phase for TRUST tokamak as explained in the following section.

3. AML Concept

The development of nuclear fusion as a practical energy source depends heavily on advancements in magnetic confinement technologies and reactor compactness. Fusion reactors, such as the EU-DEMO [29], aim to bridge the gap between experimental reactors, such as ITER [3], and full-scale commercial fusion reactors, with the goal of delivering net electricity and enhancing reactor efficiency. However, significant challenges persist, particularly in the areas of magnetic confinement and reactor compactness. As outlined in [37][38], while high magnetic fields can theoretically improve plasma confinement efficiency and enable a more compact reactor design, practical engineering limitations impose strict boundaries on this approach. One of the primary obstacles in realizing a compact, high-field tokamak lies in the structural and thermal demands on the magnetic confinement system. The transition from conventional to AML configurations could introduces significant changes in the overall reactor design, with the primary objective of achieving a reduced radial build while maintaining performance metrics critical to magnetic confinement and plasma stability. This alternative configuration will be tested in TRUST project framework to test and validate the advantages and find possible solution for the disadvantages as explained in the following paragraphs.

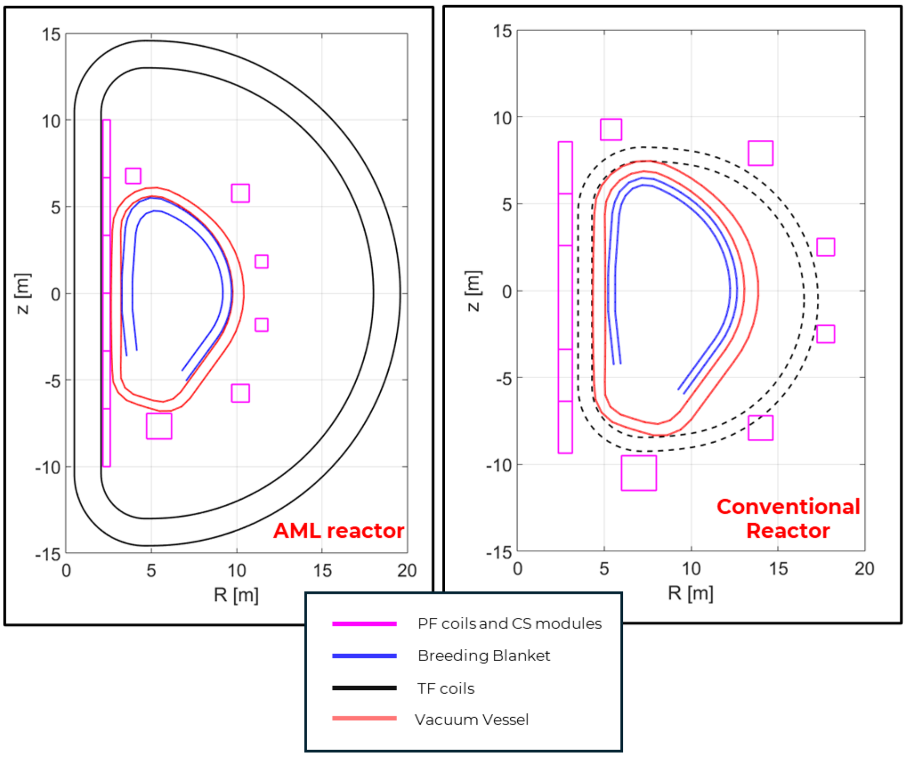

Fig. 9 Comparison between the AML design and a conventional CFTER/DEMO like reactor. The TF coils shape follows the constant tension D-Shape as explained in Section 4

The AML design (illustrated in Fig. 9, compared with a standard possible future reactor) demonstrates a compact arrangement of the PF coils and structural components, achieved by repositioning the CS around the central column of the TF coils. The rearrangement of the CS and TF coils is a strategic design choice that optimizes radial space utilization while maintaining critical magnetic performance. By moving the TF coils central column toward the reactor axis (radial coordinate decreased) and the CS toward the plasma (radial coordinate increased), the AML configuration achieves a more compact radial design. In fact, the target flux ψ_{CS} could be achieved with a thinner CS due to its quadratic dependence with respect to the radial coordinate of its centroid [39]:

$$\psi_{CS} = \frac{\pi B_{CS}}{3}(R_i^2 + R_i R_e + R_e^2) \tag{1}$$

Where B_{CS} is the maximum magnetic field, R_i is the CS inner radius and R_e is the CS outer radius. This flux dependency allows the CS to maintain effective inductive drive even with a reduced footprint, ensuring adequate plasma current generation and duration. The displacement away from the plasma of the TF coils, however, reduces the toroidal magnetic field B_T due to its inverse dependence on the radial position:

$$B_t(R) = \frac{\mu_0 \, N_{TF} \, I_{TF}}{2 \, \pi \, R} \tag{2}$$

Where μ_0 is the magnetic permeability, N_{TF} is the number of TF coils, I_{TF} is the current in the single TF coil and R_0 is the plasma major radius. To maintain a fixed toroidal filed, the TF coils current must be increased and as a result the current density in the magnet will also increase [40]. This requirement underscores the critical role of HTS in the AML design. HTS materials enable the TF coils to sustain high current densities and magnetic fields while maintaining manageable coil dimensions. Unlike Low Temperature Superconductors (LTS), HTS materials could operate at higher magnetic field intensities, higher current density and higher temperatures increasing the electromagnetic load acting on the magnets [41].

From equation 1 and 2 it comes immediately out that, since $B_t \approx 1/R$, whilst $\psi_{CS} \approx R^2$, a clear reduction of the machine dimension can be obtained, whilst maintaining the same engineering parameters. A clear implication of the proposed AML is the necessity of different assembly strategies, respect to conventional tokamak [42], by addressing its design:

- A prominent strategy involves the use of demountable electrical joints for the TF coils, which theoretically allow modular assembly and simplify maintenance. The need of electrical joint may represent a showstopper for the AML configuration, in fact different designs and solutions are under study for a future fusion reactor [43][44][45] but no one reached the maturity level needed yet. At the same time, the AML design presents a significant mechanical advantage by reducing the structural loads on the electrical joints of the TF coils. The design allows the TF coils to be taller and geometrically optimized to reduce their interaction with the poloidal magnetic field. This tailored shaping of the TF coils could mitigate the electromagnetic forces generated by the coupling with poloidal fields. A preliminary quantitative evaluation on the mechanical stress of the TF coils and its implications for the overall AML configuration are discussed and illustrated in Section 3.2.

- An alternative strategy configuration could benefit from the innovative assembly strategies inspired by projects like the Volumetric Neutron Source (VNS). As part of the VNS project, the feasibility of an in-situ winding process will be explored, which could serve as a foundation for AML tokamak assembly [46]. In this approach, the vacuum vessel and Poloidal Field (PF) coils are pre-assembled, and the Toroidal Field (TF) coils are wound directly around these completed structures. This eliminates the need for prefabricated TF coil modules and simplifies alignment and integration.

A clear solution for the assembly of proposed AML design is not provided yet and is currently under investigation, reflecting a broader issue faced by all future fusion reactors under development. For instance, ITER has encountered significant assembly difficulties, including defects identified in major components like thermal shields and vacuum vessel sectors during 2022, which have impacted its construction timeline [47]. Similarly CFETR has faced challenges related to complex interfaces and the integration of physical and engineering requirements, necessitating extensive research and development efforts [48]. These examples underscore the intricate nature of assembling advanced fusion reactors and the necessity for ongoing research to develop effective solutions. Solving this issue could lead to advantages not only related to the assembly and maintenance of the reactor, but also benefits related to its operation and performance. For the proposed AML configuration a concrete example is the possibility to design the PF coils closer to the plasma compared to conventional tokamak configurations. This strategic arrangement enhances the magnetic coupling efficiency, enabling the PF coils to generate stronger shaping and stabilizing fields with lower currents. The shaping field (B_{PF}) produced by the PF coils is inversely proportional to the distance from the plasma, as expressed by:

$$B_{PF} \approx \frac{\mu_0 \, I_{PF}}{2\, \pi \, d_{PF}} \tag{3}$$

Where I_{PF} is the current in the PF coils, and $d_{PF}$is the distance respect the plasma. Reducing d_{PF} increases B_{PF} for a given current, thereby improving the precision of plasma shaping and enabling better control of elongation (κ) and triangularity (δ). Consequently, there is a noticeable space for improving the position of the PF coils in order to minimize their current density. Additionally, the closer positioning of the PF coils enhances the system's ability to counteract vertical displacement events (VDEs). The stabilizing vertical force ($F_{vertical}$) depends on the coupling efficiency, which scales with d_{PF}, and is given by:

$$F_{vertical} \approx \frac{\partial M_{PF}}{\partial z} \delta I_{PF} \tag{4}$$

Where M_{PF} is the mutual inductance between the plasma and the PF coils, and δI_{PF} is the current variation in the coils. Smaller d_{PF} increases $\frac{\partial M_{PF}}{\partial z}$, enabling faster and more effective stabilization of elongated plasmas. The reduced d_{PF} also decreases the response time of the control system, facilitating real-time adjustments to plasma instabilities and improving confinement [49]. These control advantages are further supported by the AML's compact design, which minimizes energy losses and operational costs, as detailed in the subsequent sections. These control advantages are inherently linked to the AML design, in which the PF coils are directly supported to the vessel structure.

3.1 Plasma Scenario

A preliminary investigation of the operational conditions for the AML reactor is reported in this section. The AML plasma parameters are explored to obtain high-performance plasma operation within a compact and efficient tokamak layout. The parameters are evaluated to balance confinement, stability, and engineering constraints while supporting long-pulse operation. The analysis of operational plasma parameters for the AML reactor is developed by the evaluation of critical metrics such as q_{95}, fusion power (P_{fus}), and the normalized heat flux parameter $\frac{P_{sep}\, B_t}{q_{95}\, A\, R}$.

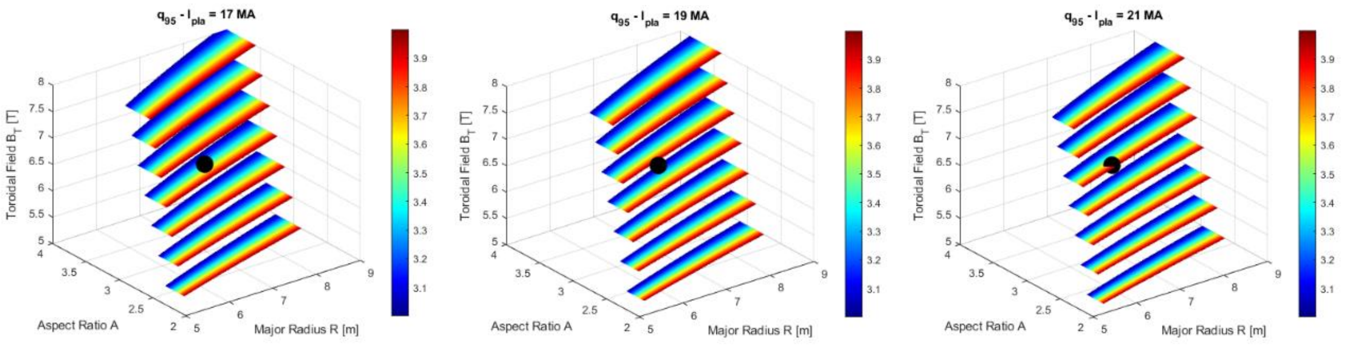

(a) (b) (c)

Fig. 10 The q_{95} variation as function of R, A and B_t plotted varying the reference plasma current I_{pla} between (a) 17 MA, (b) 19 MA and (c) 21 MA. The black point represents the target parameters chosen for the AML design with co-ordinates $R = 6.5\ m$, $A = 2.71$ and $B_t = 7\ T$ and fixed for each I_{pla} considered

The value of q_{95} was confined to the range $3 < q_{95} < 4$ (Fig. 10), which is critical for preventing magnetohydrodynamic (MHD) instabilities such as edge-localized modes (ELMs) and vertical displacement events (VDEs). These stability requirements are well-documented in tokamak research and have been validated in device like JET [9]. Within Fig. 10, as in the following Fig. 11 and Fig. 12, the black point represents the chosen values for R, A and B_t as indicated in Table 1. As evident in Fig. 10 the black point does not intersect any surface by decreasing the current (from plot c to plot a). The only way to work with a lower current (Fig. 10a) could be to modify the aspect ratio or/and the toroidal field. For the design of the plasma scenario the following plasma shape parameters have been assumed: elongation $\kappa \sim 1.65$ and triangularity $\delta \sim 0.29$. These values align with those observed in high-confinement (H-mode) scenarios, providing robust equilibrium conditions that support high plasma performance [35]. Conservative assumptions were made for the Greenwald fraction ($f_{Green} \sim 0.87$) and the confinement enhancement factor relative to ITER scaling ($H_{98} \sim 0.9$) [50]. These values were selected based on operational regimes already achieved in JET, ensuring a realistic baseline for AML's performance projections.

Togher to the plasma stability, a minimum fusion power output of $P_{fus} \geq 1400$ MW is considered for the AML design point. This parameter is essential for economic feasibility and meeting energy production goals. Fig. 11 shows the dependence of P_{fus} on R, A, B_t and I_{pla}. Reducing the main dimension for the reactor (R and A) to reach the same fusion power it's necessary to increase the plasma current and the toroidal magnetic field as clearly indicated by Fig. 11a and Fig. 11b, at lower plasma current the black point does not intersect any surface.

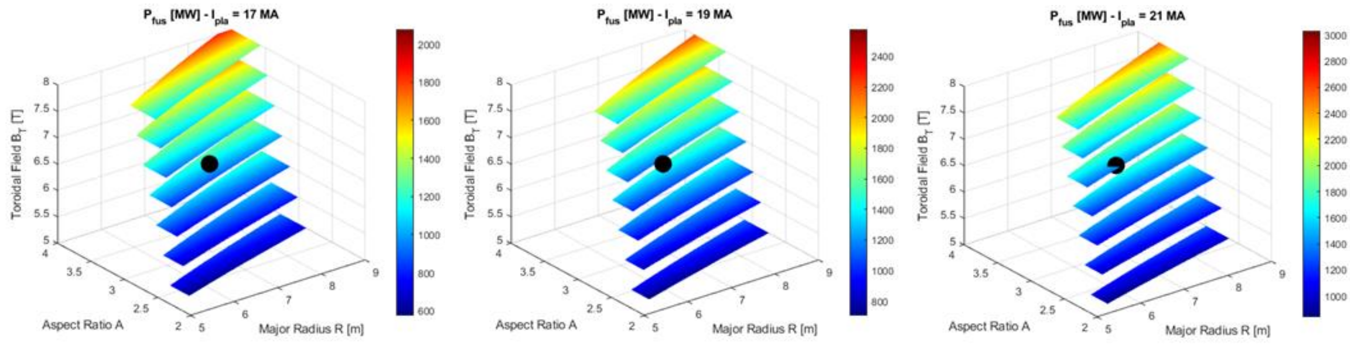

(a) (b) (c)

Fig. 11 The P_{fus} variation as function of R, A and B_t plotted varying the reference plasma current I_{pla} between (a) 17 MA, (b) 19 MA and (c) 21 MA. The black point represents the target parameters chosen for the AML design with co-ordinates $R = 6.5\ m$, $A = 2.71$ and $B_t = 7\ T$ and fixed for each I_{pla} considered.

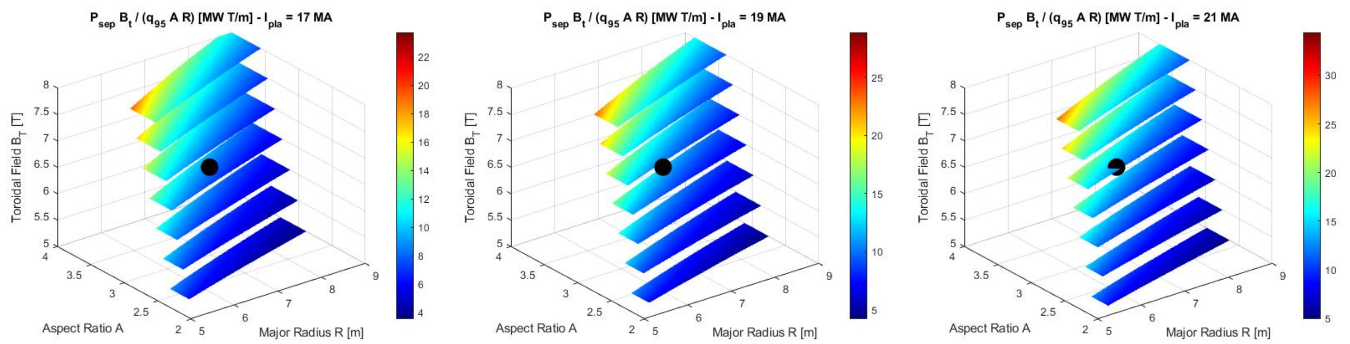

(a) (b) (c)

Fig. 12 The $\frac{P_{sep}\,B_t}{q_{95}\,A\,R}$ variation as function of R, A and B_t plotted varying the reference plasma current I_{pla} between (a) 17 MA, (b) 19 MA and (c) 21 MA. The black point represents the target parameters chosen for the AML design with co-ordinates $R = 6.5\ m$, $A = 2.71$ and $B_t = 7\ T$ and fixed for each I_{pla} considered.

Also the power that flow through the separatrix (P_{sep}) was evaluated to address thermal loads on the divertor. This parameter, scaled by the ratio $\frac{P_{sep}\,B_t}{q_{95}\,A\,R}$, provides a proxy for the heat flux to the divertor [51]. Fig. 12 highlights the parametric evaluation of this metric as a function of R, A, B_t and I_{pla}. Of course, moving the design point to smaller major radius and smaller aspect ratio involves the increase on the normalized heat flux parameter. The aim of this study is not focused on address in detail the heat flux mitigation on the divertor, but different studies are exploring solutions for reactor-class tokamak [52][53].

A possible design point is chosen to analyse its behavior in AML reactor showing a possible compact design respect a conventional tokamak reactor. The main parameters for the design point are indicated in Table 1:

Table 1. Main parameters for the AML reactor design point

R [m]	A	I_{pla} [MA]	B_t [T]	q_{95}	$<n>/n_{GW}$	κ_{95}	δ_{95}	li	β_p	H_{98}
6.5	2.71	21	7	3.78	0.87	1.67	0.36	0.8	0.62	0.9

Pulse length [s]	P_{fus} [MW]	Volume [m^3]	P_{sep} [MW]	$\frac{P_{sep}\,B_t}{q_{95}\,A\,R}$ [MW T/m]	P_{add} [MW]
7200	1460	1037	127	13.33	70

A preliminary plasma scenario and a plasma equilibrium, based on the chosen design point, are designed using MAXFEA code. The PF coils and CS modules position is maintained with a distance of at least 1.5 m respect to the plasma limiter. This space is mandatory to accommodate the VV and the BB under relevant neutronics and electromagnetic load conditions as expected in a nuclear fusion reactor [54]. In addition, the PF coils centroid position and the CS modules extension is obtained to ensure the needed topology to get an optimised quasi null magnetic field during the plasma break down (BD) (Fig. 13).

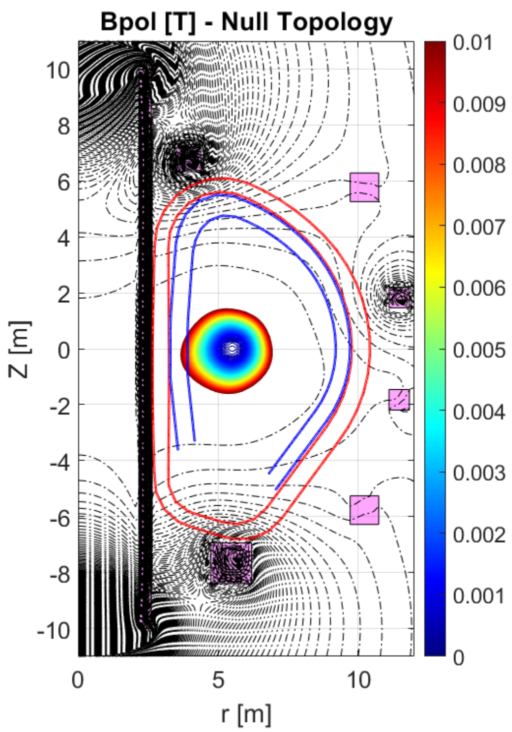

Fig. 13 Poloidal field null generated to reach the plasma breakdown conditions inside the vessel.

An assisted BD is foreseen, indeed different solutions are under development for large scale tokamak as expected for the Divertor Tokamak Test (DTT) [55]. During the non-ohmic breakdown it is assumed no flux consumption. At the end of the breakdown phase a first limiter plasma is considered with CS modules at the maximum current. The equilibrium for the first limiter plasma is reported in Fig. 14 and the main plasma parameters obtained are report in Table 2. The available flux at the start of flattop (SOF) is evaluated according to [56]:

$$\psi_{boundary\ @SOF} = \psi_{boundary\ @BD} - \left(\frac{1}{2}\, li\, \mu_o\, R\, I_{pla} + C_{ejima}\, \mu_0 R\, I_{pla}\right) \tag{5}$$

where the flux available at the SOF $\psi_{boundary\ @SOF}$ depends by the flux available at the breakdown $\psi_{boundary\ @BD}$ (total flux from the CS), the plasma normalized internal inductance li and the Ejima coefficient C_{ejima} assumed equal to 0.4 [56]. The plasma current rise is assumed equal to be 0.4 MA/s, leading to $I_{pla} \approx$ 21MA in 51.25 s. The detailed evolution of the plasma shape needed to reach the target SN configuration is currently neglected.

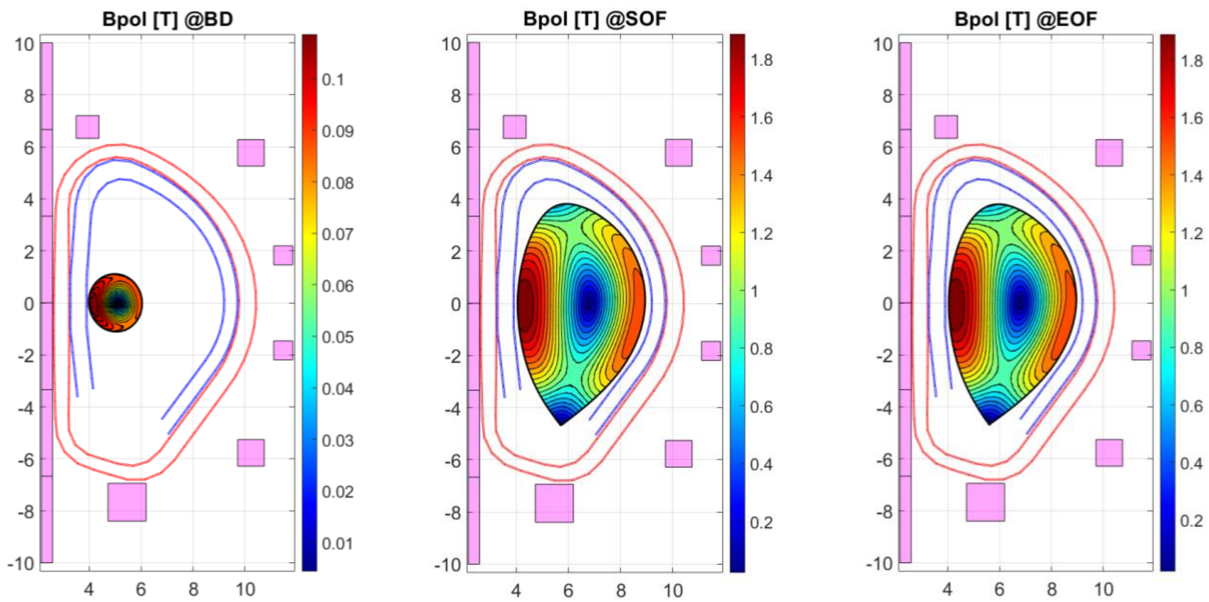

(a) (b) (c)

Fig. 14 Different plasma equilibrium for the three time instant considered in the plasma scenario. Respectively the equilibrium (a) at the breakdown, (b) at the Start of Flattop and (c) at the End of Flattop are reported

A Single Null plasma configuration is considered as target for the AML reactor scenario. The resistive loop voltage during the flattop considering the plasma performance is equal to 0.041 V allowing to reach around 7117 s for the flattop duration.

Table 2. Main parameters for the plasma scenario

	BD	SOF	EOF
I_{pla} [MA]	0.5	21	21
R [m]	5.02	6.50	6.50
a [m]	1.03	2.34	2.35
B_t [T]	9.15*	7.07	7.07
κ	1.08	1.75	1.72
δ_{low}	-0.001	0.26	0.28
β_{pol}	0.10	0.62	0.62
li	0.88	0.73	0.73
q_{95}	20.2	3.52	3.53
Volume [m^3]	112.3	1185.6	1180.9
$\psi_{boundary}$ [Vs]	290.3	150.26	- 144.76

Table 3. CS modules currents during the plasma scenario

	Current @BD [MA· Turns]	Current @SOF [MA· Turns]	Current @EOF [MA · Turns]
CS1	44.861	2.981	-1.712
CS2	44.861	8.328	-33.240
CS3	44.861	7.655	-34.380
CS4	44.861	7.131	-34.460
CS5	44.861	10.260	-35.050
CS6	44.861	4.177	-18.010

Table 4. PF coils currents during the plasma scenario

	Current @BD [MA· Turns]	Current @SOF [MA· Turns]	Current @EOF [MA · Turns]
PF1	4.320	12.110	-1.640
PF2	3.795	-4.049	-7.289
PF3	-1.215	-2.080	-2.035
PF4	1.445	-2.034	-2.442
PF5	0.471	-8.023	-9.931
PF6	6.937	15.120	7.372

3.2 TF Coils Characterization

To check the feasibility of the proposed AML design, a preliminary characterization for the TF coils system is provided. The constant tension D-Shape [57] is used as first design for TF coils to evaluate the overall dimension and the electromagnetic loads acting on the HTS conductors and on the structural materials.

Table 5. Main parameters for the analysed TF coil configuration

I_{TF} [MA]	$B_{t,max}$ [T]	$R_{inb\text{-}ext,TF}$ [m]	A_{HTS} [m^2]	J_{HTS} [MA/m^2]	N_{TF}	$F_{z,TF}$ [MN]	$F_{r,TF}$ [MN/m]
19	22	2.07	0.592	32	12	379	209

From the target toroidal magnetic field (B_t), it is possible to derive the needed current flowing in the TF coils central column, and consequently the current flowing in the single TF coil I_{TF} through the Biot-Savart law (Eq. 2). Given the CS modules geometry from the plasma equilibrium and scenario, the TF coils HTS conductors and the structural material are accommodated in remaining available space in the central column. The proposed solution includes a TF coils cassette composed by a nose, two radial plates and a top plate as showed in Fig. 15. The TF coils Winding Packs (WP) are considered formed by Conductor on Round Core (CORC®) HTS cables [58][59] surrounded with insulation material. Inside each HTS cables the amount of copper needed to perform a safety discharge in case of quench is considered allowing to reach the hot spot temperature at the end of the fast discharge [60]. The adopted procedure is similar to that proposed and well explained in different studies [61][62][63]. The limit time constant τ_{lim}, for the proposed TF coils preliminary design, is approx. equal to 30 s considering 66 MA/m^2 of current density on the stabilizer copper. For each TF coil slightly more than 200 turns are assumed with an operating current around 90 kA. The radial overall dimension for the central column is around 1.5 m located between $R_{inb-ext,TF}$ and $R_{inb-int,TF}$. The electromagnetic forces acting on the TF coil could be roughly estimated [37]:

$$F_z = \frac{1}{4} B_t \, R \, I_{TF} \ln \left(\frac{R_{out,TF}}{R_{inb-ext,TF}}\right) \tag{6}$$

$$F_r = \frac{1}{2} I_{TF} \, B_{t,max} \tag{7}$$

Where F_z (evaluated in N) and F_r (evaluated in N/m) are respectively the vertical and radial force acting on the TF coil, $R_{out,TF}$ is the outboard radial coordinate of the TF coil reference line and $B_{t,max}$ is the maximum toroidal field acting on the TF coils ($B_{t,max} = B_t \frac{R}{R_{inb-ext,TF}}$). These parameters are useful for a first dimensioning and as comparison with different design.

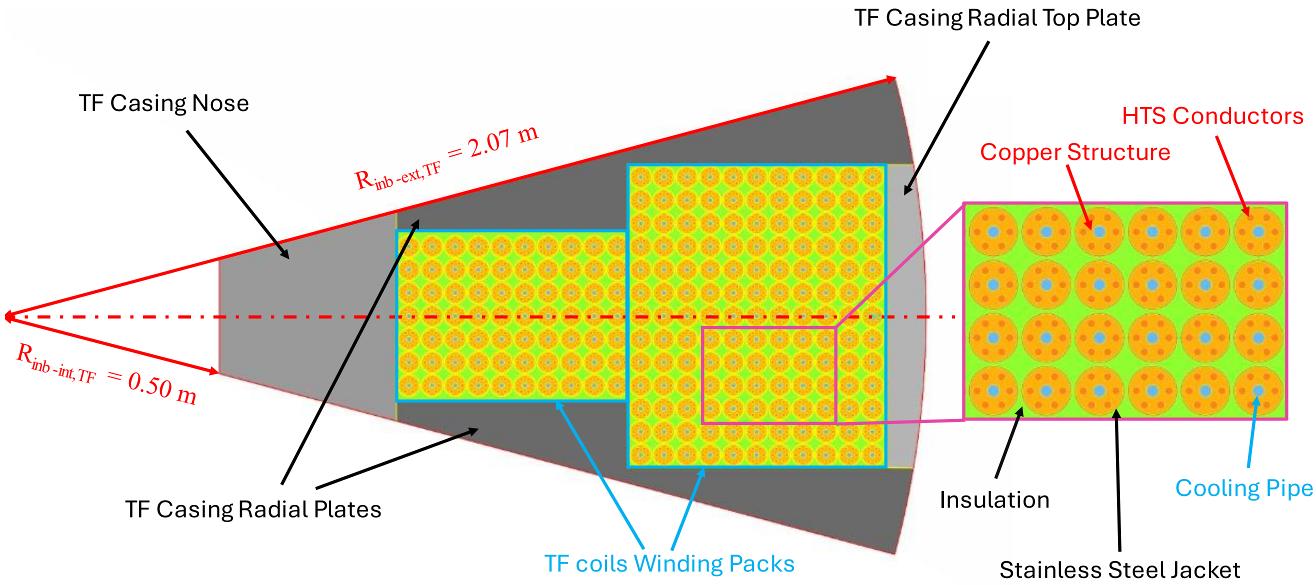

Fig. 15 TF coils design proposed for in the AML design. The preliminary concept includes a stainless-steel casing divided in four components. The HTS cables are encapsulated in an insulating material and bundled in Windings Packs.

An analytical and a Finite Element (FE) model are developed to evaluate in a more precise way the In Plane Forces (IPF), namely F_z and F_r, and the Out of Plane Forces (OPF). The latter will be strictly dependent by the PF coils and CS modules position and current.

The IPF are evaluated considering a filament TF coils model with an analytic approach. The TF coils are modelled as multiple segment filament passing through the midline of the winding pack. For each filament, a current of value equal to I_{TF} is set to evaluate the magnetic field B in the space of interest including maximum toroidal field acting on the winding pack (evaluated on the TF coil reference line).

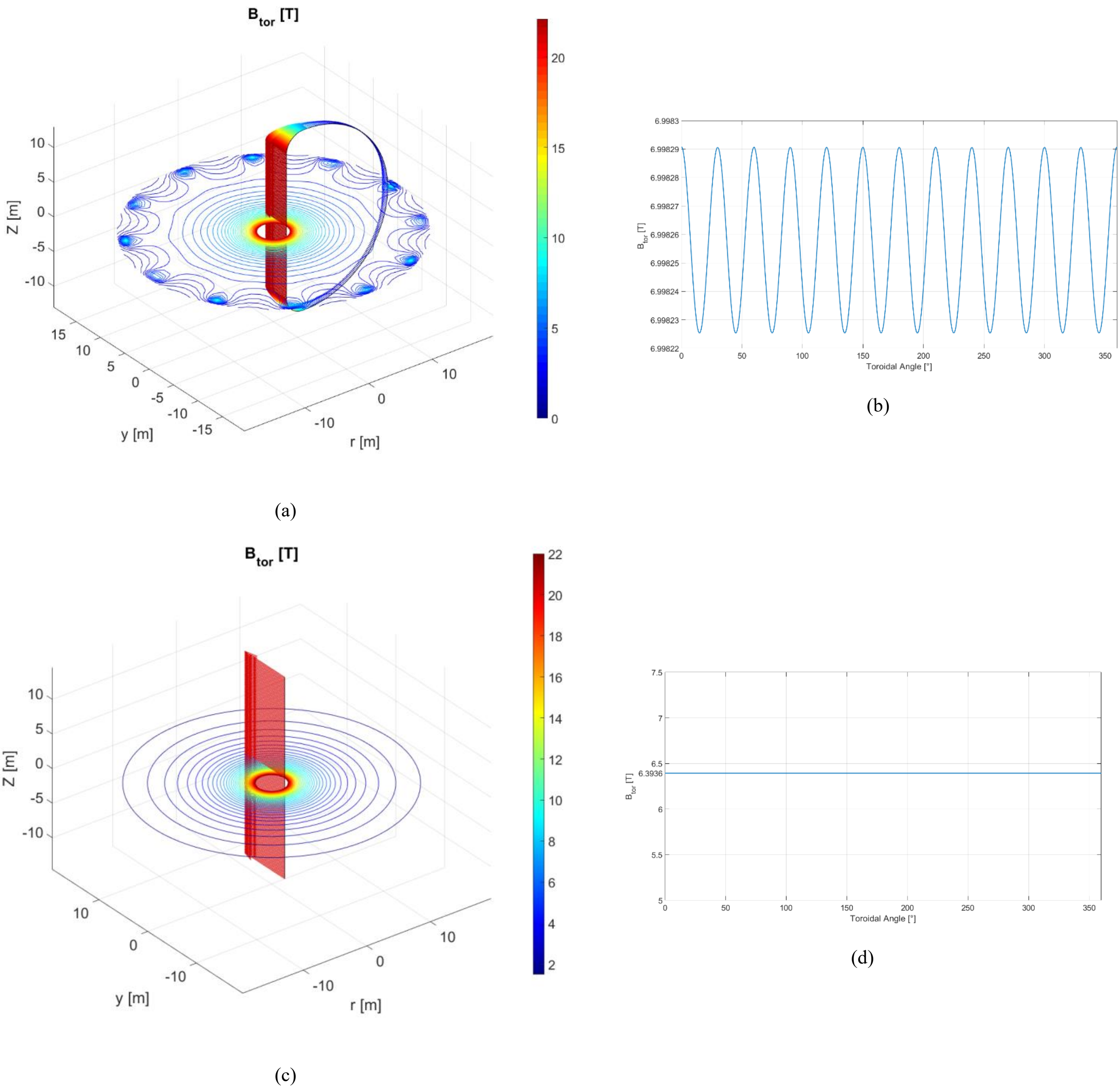

Fig. 16 The toroidal field produced by the magnets is reported in (a) with a focus on the generated ripple (b). The comparison between a conventional D-Shape and the magnetific field produced by a set of vertical filaments is repoterd in (c) with its ripple analysis (d).

The maximum magnetic field acting on the TF coils as expected is $\sim 22\ T$. Also the ripple on the plasma axis is verified reaching a maximum value $< 0.1‰$. The proposed AML design allows to evaluate as the needed toroidal magnetic fields for the plasma confinement is generated only by the TF coils central column. In fact, TF coil outer leg is mandatory to close the conductors winding pack, but it hasn't a relevant impact on the magnitude of the magnetic field on the plasma axis (approx.

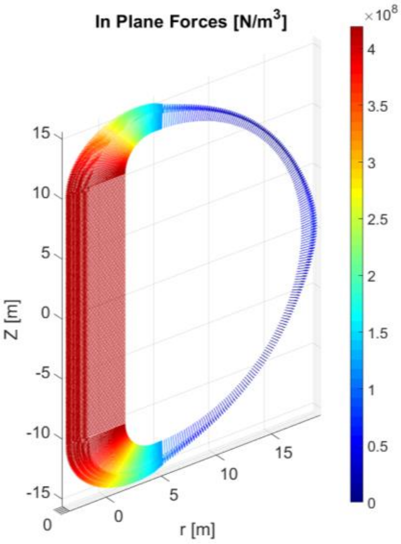

Fig. 17 In plane forces distribution along the TF coil reference line

~ 8.5%) as showed in Fig. 16. Therefore, by increasing the radial extension of the TF coils on the outer side, it is possible to reduce the ripple effect and thus reduce the number of TF coils required.

By the interaction between the current in the TF coils and the toroidal field it is possible to obtain the Lorentz Forces ($J\ x\ B$) acting on the winding pack. The maximum electromagnetic force density acting on the conductors is approx. equal to $420\ MN/m^3$ and it will be considered constant along the TF coil winding pack as conservative choice to evaluate the stress state on the conductor and on the TF coil casing. The poloidal field acting on the TF coil is evaluated with a FE model reproducing the plasma equilibrium configuration in the three-time instants considered and the pre-breakdown phase (PreBD).

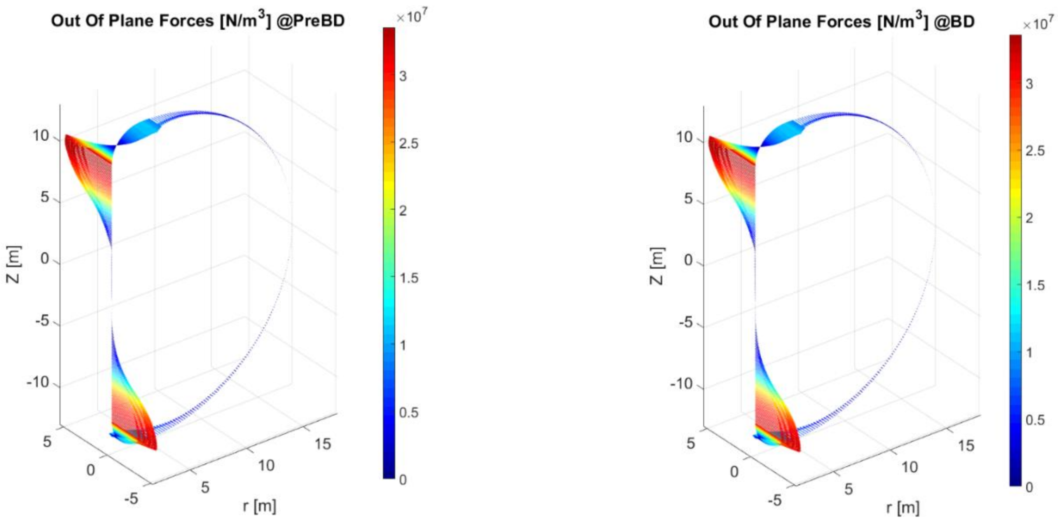

(a)

(b)

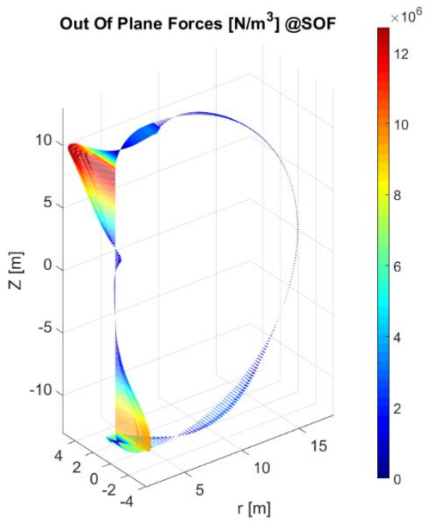

(c)

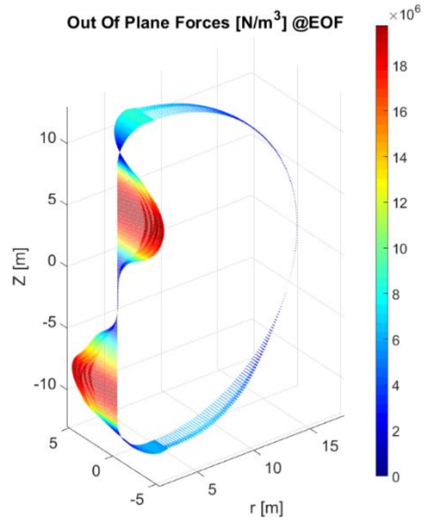

(d)

Fig. 18 Out plane forces distribution along the TF coil reference line for plasma scenario instant studied: (a) pre-breakdown phase, (b) breakdown phase, (c) start of flattop instant and (d) end of flattop instant.

The preliminary stress assessment on the TF central column is provided through a 2D Finite Element (FE) model. Two different configurations are reported and compared: a wedged and a bucked design.

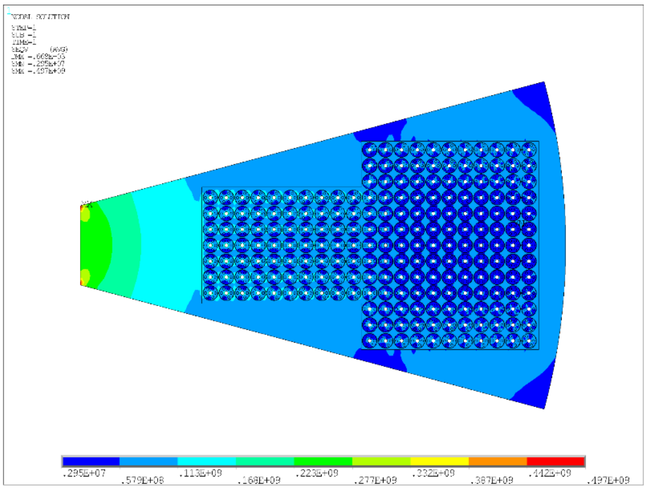

(a)

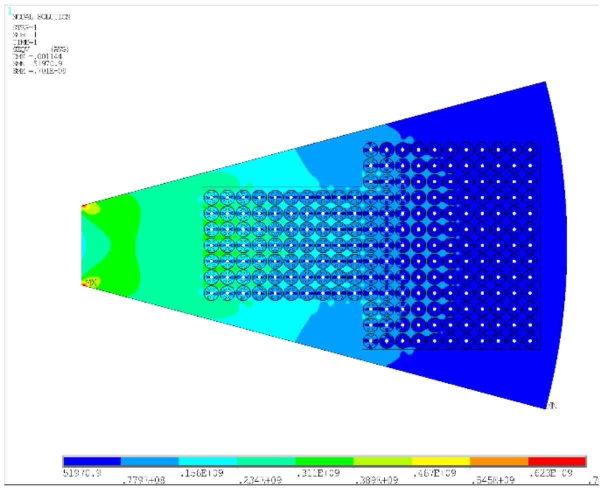

(b)

Fig. 19 Von Mises stress contour plot for the 2D FE model considering the in plane radial force for the (a) wegded solution and (b) bucked solution

The FE analysis includes a 2D model in the condition of plain strain under the radial force load due to the IPF. The radial force acting on the TF coil inner legs is evaluated considering the maximum in plane force density $420\ MN/m^3$. This is applied on the with a linear distribution along the winding pack. In the wedged configuration (Fig. 19a) the stress state in the stainless-steel casing and the WP is better than the bucked solution (Fig. 19b). It is important to notice that respect the conventional reactor design, in the bucked solution, the TF coils radial loads for the AML is decoupled respect with the CS radial expansion improving the stress state on the conductors and on the structural material for both CS and TF coils. Moreover, the positioning of the toroidal magnets in the AML design allows the structural material to be increased, towards the axis of the tokamak, without increasing R or A of the reactor.

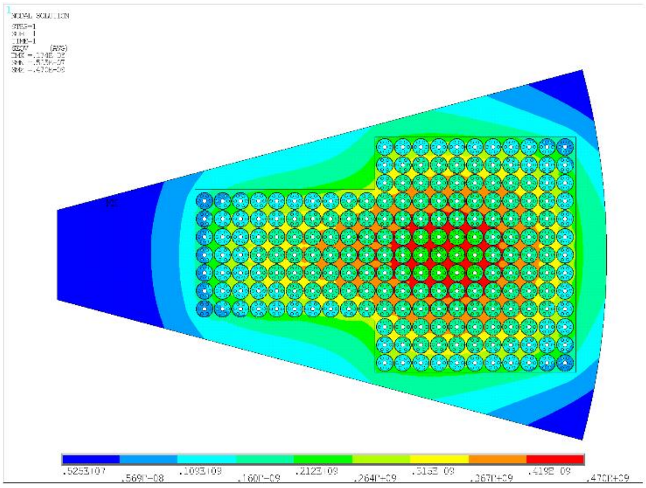

Fig. 20 Von Mises stress contour plot for the 3D FE model considering the in plane vertical force

To complete the stress state characterization also the vertical tension load is considered. A 3D FE model of a section of the TF central column is carried out with $F_z/2$ applied as external load. The maximum Von Mises stress on the FE model are: ~ $500\ MPa$ on the structural material and ~ $120\ MPa$ on the HTS cables for the wedged solution (Fig. 19a); ~ $700\ MPa$ on the structural material and ~ $170\ MPa$ on the HTS cables for the bucked solution (Fig. 19b); ~ $470\ MPa$ on the structural material and ~ $220\ MPa$ on the HTS cables for the 3D tension analysis (Fig. 21). The proposed analyses performed to characterize the TF coils, in the AML design, are a first step to prove the feasibility of the solution included in this work.

4. TRUST Design

4.1 Conceptual Design

The TRUST conceptual design can be subdivided in four sub-assemblies: a) the VV and IVCs system; b) the cryostat system; c) the PF coils and the CS modules system; d) the TF coils system (see Fig. 5). This conceptual design is characterized by some challenging engineering solutions (described in the following sections), for instance a demountable TF coils or an openable VV. In fact, the academic goal of TRUST also includes the design phase itself, allowing students to explore different engineering solutions and addressing issues related to the manufacturing aspects of these components. In this context, the involvement of industry is crucial for several different aspects: the training of students within an industrial framework, reducing the time from the design phase to the manufacturing phase and eventually to prepare the students to the necessary future involvement of the industrial world in the realization of fusion based power plants [64]. This approach has already been used for the TRUST VV design that being in a more moving mature situation has been already realised in cooperation with Walter Tosto Spa. The direct involvement of private manufacturing companies during the design and the realization phase has been recognised to be a key factor to accelerate as much as possible the obtaining of fusion energy [27].

To reach the currents status of maturity level for the TRUST conceptual design, different solutions have been evaluated and studied. From the very first concept the AML configuration was considered as main design drivers with the use of HTS TF coils and CS (Fig. 22).

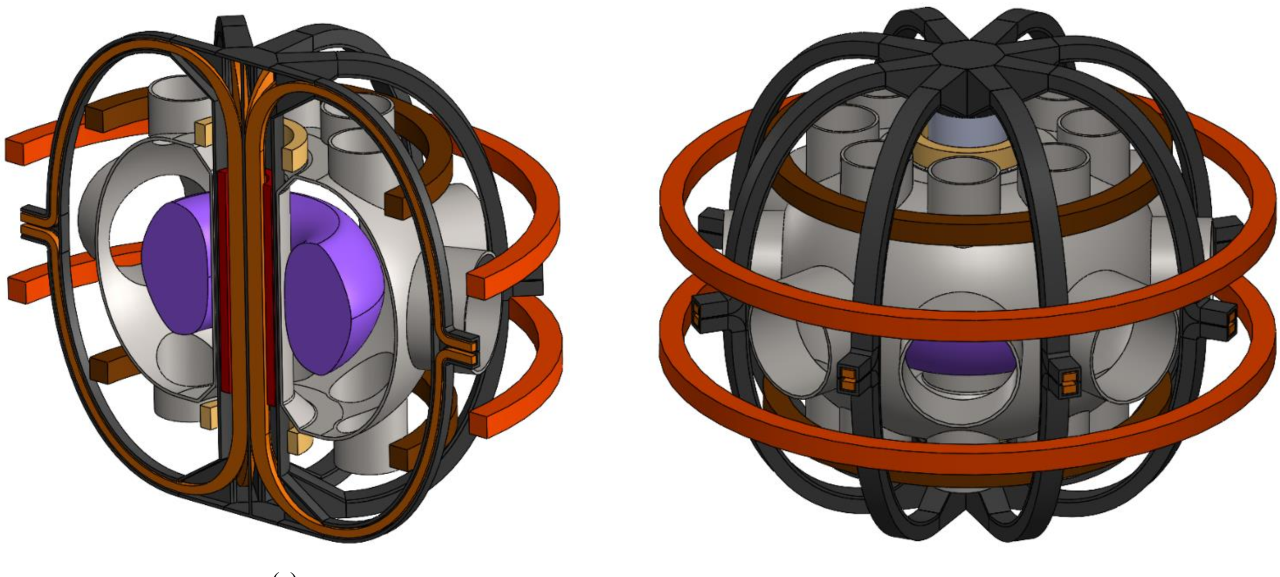

(a) (b)

Fig. 22 First TRUST concept with (a) sectioned view and (b) global view

The first concept included 8 TF coils and a single CS module placed inside a 3D cryostat. In addition 6 PF coils were foreseen to reach the SN plasma equilibrium. The PF3 and PF4 was located outside the TF coils to increase the VV ports dimensions. This first design was designed to operate according to the following parameters:

Table 6. Main parameters for the first TRUST concept

R [m]	A	I_{pla} [MA]	B_t [T]	q_{95}	κ_{95}	H_{98}	Pulse length [s]
0.28	2.15	0.11	0.5	3.3	1.6	0.8	1

Then the first equilibrium was designed and the concept was improved to guarantee the required plasma performance. As showed in Fig. 23, the PF3 and PF4 have been brought closer to the plasma stretching the VV ports shape and by increasing the TF coils dimensions. Respect the first concept, in the second design the plasma performance was increased to allowing to reach the parameters reported in Table 7.

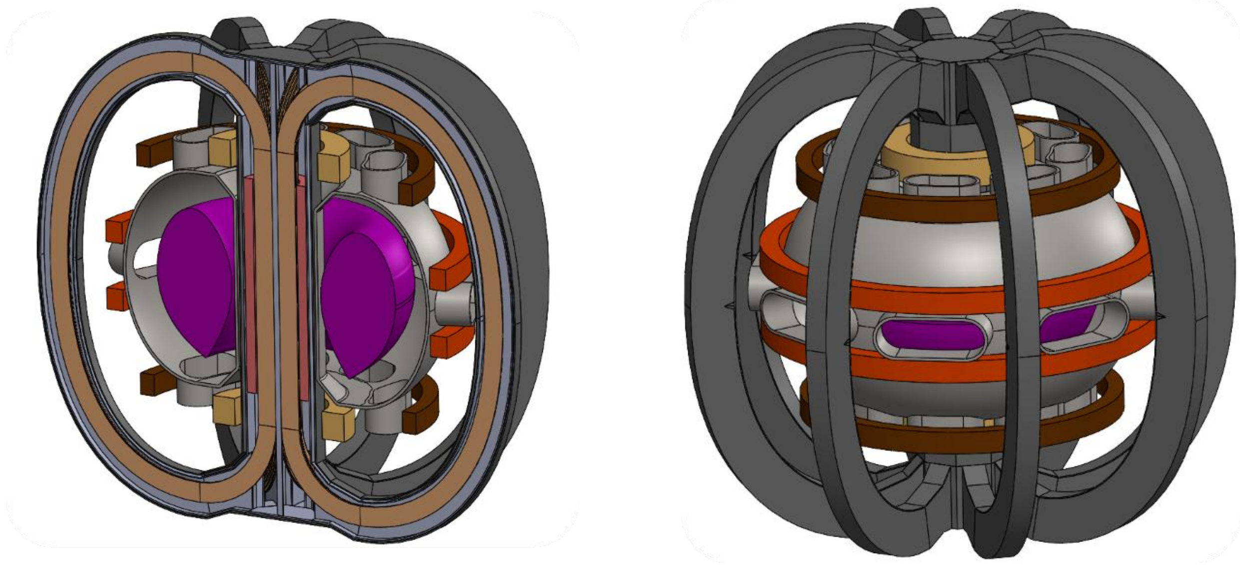

(a) (b)

Fig. 23 Second TRUST concept with (a) sectioned view and (b) global view

From the plasma SN configuration also the first equilibrium currents in the PF coils and CS module were obtained allowing to start the dimensioning of this components. The PF coils was located symmetrically respect the equatorial plane to maintain high flexibility on the plasma configuration. Moreover, a copper material was foreseen without an active cooling system. The PF coils current density was regulated to maintain a temperature variation, on the copper, below 50 K.

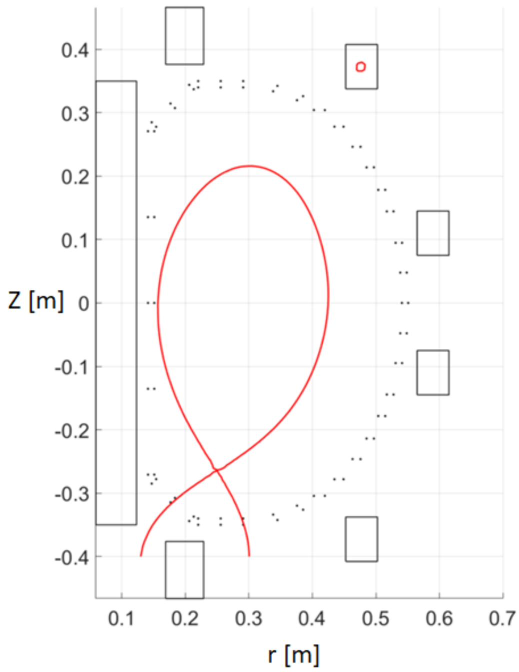

Fig. 24 First plasma SN equilibrium.

Table 7. Main parameters for the second TRUST design

R [m]	A	I_{pla} [MA]	B_t [T]	q_{95}	κ_{95}	Volume [m^3]	Pulse length [s]
0.291	2.17	0.13	0.7	4.59	1.79	0.169	1

A third step of design improvement for TRUST included the introduction of more engineering and economic constraints. In fact, the third TRUST design was obtained considering also:

- Limitation for the electric plant available in the TRUST facility site and economic constraints due to the power supplies provided for the experiment.
- Manufacturability for the structural components, as for the VV.
- Reducing costs and complexity due to HTS for magnetic systems.
- Feasibility of the plasma scenario.

From the previous points, the TRUST design has moved to a more maturity level reaching the configuration showed in Fig. 25.

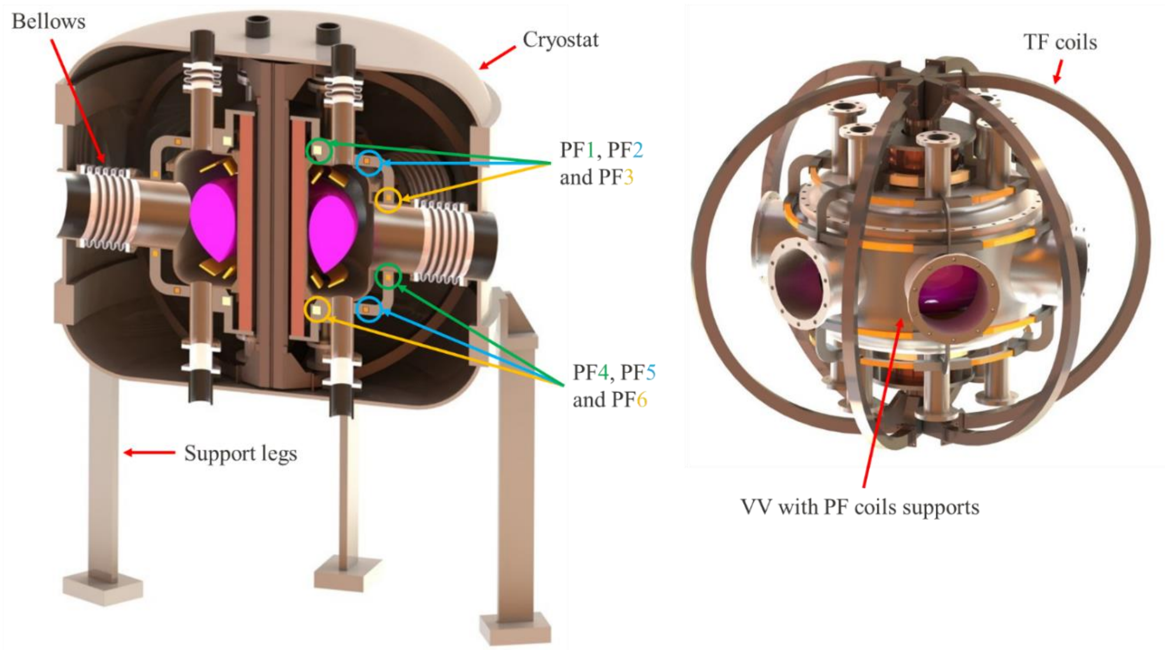

Fig. 25 Third TRUST concept with a sectioned view and focus on the VV design with Walter Tosto Spa and the demountable TF coils.

The third TRUST design includes an openable VV design in collaboration with Walter Tosto Spa, a quasi-axisymmetric cryostat with 6 legs for the ground connection, 6 TF coils bigger respect the previous design and 6 CS modules to reduce the power supplies ratings. In addition, a preliminary design for the bellows, PF coils supports and for the stabilizing passive plate was considered. This TRUST design moves towards the AML configuration starting to present possible engineering solutions for the assembly phase, as demountable TF coils. The plasma parameters considered for the third TRUST concept are reported in *Table 9*, while the null field for the plasma start-up and the equilibrium configuration obtained are reported in Fig. 26. A detailed description for the design of the plasma scenario is reported for the current TRUST design in Section 4.2.

Table 8. Target SN equilibrium main parameters for the third TRUST design

	SOF	EOF
I_{pla} [kA]	110.0	110.0
R [m]	0.3	0.3
a [m]	0.11	0.11
B_t [T]	0.8	0.8
κ	~1.9	~1.9
δ_{low}	~0.3	~0.3
β_{pol}	~ 0.1	~ 0.1
li	~ 0.8	~ 0.8
q_{95}	~3.3	~3.3
Volume [m^3]	~0.125	~0.125
$\psi_{boundary}$ [Vs]	0.126	-0.190

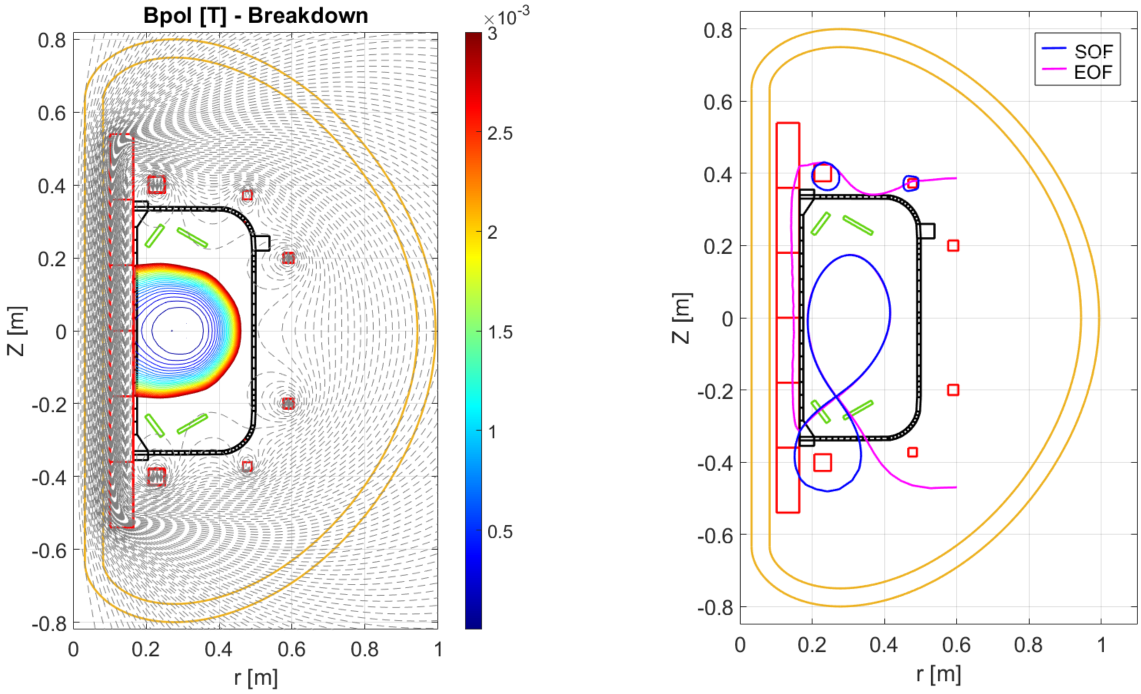

a) b)

Fig. 26 a) Contour plot of the breakdown poloidal null field generated by the currents in the CS modules and the PF coils and magnetic flux lines in grey. b) Target SN equilibrium during the flat-top; in red the PF coils and CS modules, in Orange the TF coils shape, in green the in-vessel passive plate and in black the VV.

VV and IVCs system

The current TRUST design includes, as for the third concept, an openable VV through two flanges. The material considered for the VV and the other structural components is the SS 316 L. The VV is composed of two toro-spherical shells (decinormal) and two cylindrical shells. The equatorial flange on the top decinormal shell (called from here VV dome) to allow an easily maintenance and assembly/disassembly for the PFC. Inside the VV two copper stabilizing plates have been located to improve passive control as already planned for instance in DTT [65]; respect the third configuration, the stabilizing plates are located on the low field side (LFS) and their positioning is under investigation as explained subsequently in the plasma vertical stability section. The divertor is under design to allow a flexible interchange of the tested components. During the second phase of TRUST, a first wall will be required to protect the VV as a consequence of the increasing of the input power. The VV has eighteen ports to accommodate the diagnostics, the vacuum systems, the gas puffing systems and to allow the maintenance and the testing of different PFC. Compared with the previous designs, the ports radial extension was reduced to increase the plasma view for the future diagnostic systems.

Cryostat system

The cryostat, included in the previous design, is currently neglected. Considering the copper coils during the first phase, the design of this components is postponed for the TRUST OP3; this solution will allow to easily upgrade or maintenance the device. Actually, in the first phase the cryostat would be non-mandatory for a discharge of only 400 ms as explained in the following section. The maximum plasma discharge of 400 ms is obtained considering a fully ohmic heating pulse sustained by the CS modules discharge. However, always to best prepare students with cryogenics systems all the copper coils are designed and will be realized to work from room temperature down to nitrogen temperature. For this reason, a casing with cryostat functionality for the PF coils is under development even considering the TRUST OP2. The base of the cryostat is maintained in the current design and it is used to sustain the whole machine through six support legs (Fig. 5).

PF coils and CS modules system

The design includes a set of six PF coils and six modules for the CS. The PF coils are arranged in a symmetrical position respect the equatorial plane of the experiment. The reference equilibrium for SN configuration at the start of flat-top (SOF) and at the end of flat-top (EOF) is showed in Fig. 32a and Fig. 32a. The PF coils position will also make possible to test and study a Double Null (DN) plasma configuration and an Upper Single Null configuration (USN), as showed in Fig. 31d (to avoid redundant figures, the reference waveforms for the USN are not reported – current and voltages are specular respect to the SN). The PF coils are connected directly on the VV through twenty-four poloidal ribs. These supports will be demountable in order to not interfere with the opening of the VV and to allow and easily replacement of the coils. These supports are in a preliminary design phase, but they allow to represent the possible connection from PF coils and vessel. The position of the PF coils centroid is defined to have a trade-off between target plasma equilibrium, the topology of magnetic field null during the plasma breakdown (see Fig. 31a) and the space available for other components (e.g., VV ports). The PF coils characteristic parameters (e.g., number and section of turns) are estimated considering the power supplies limits and the current density limitation to avoid an active cooling during the pulse on the copper coils. The power supplies foresee the use of insulated-gate bipolar transistor (IGBT) systems of four quadrants for the complete independent modulation of current and voltage, with a maximum voltage equal to 1kV and maximum current equal to 1kA. This solution allows to best diversify and exploit the shape control of the different plasma configuration and it presents the advantage to minimize the overall system cost. Set the maximum current from the power supplies, the coils wire dimensions are obtainable considering Joule’s heating limit for copper.

Considering a wire of Ø equal to 4.115 mm by the American Wire Gauge (AWG) standard the Onderdonk fusing current for 1 s is equal to 4 kA. As showed in Fig. 27 the current waveform generates a neglectable Joule's heating on plasma pulse time scale (the estimated temperature variation during the plasma discharge is approx. equal to 30 °C). In Table 8 and Table 10 are reported the main parameters for the PF coils.

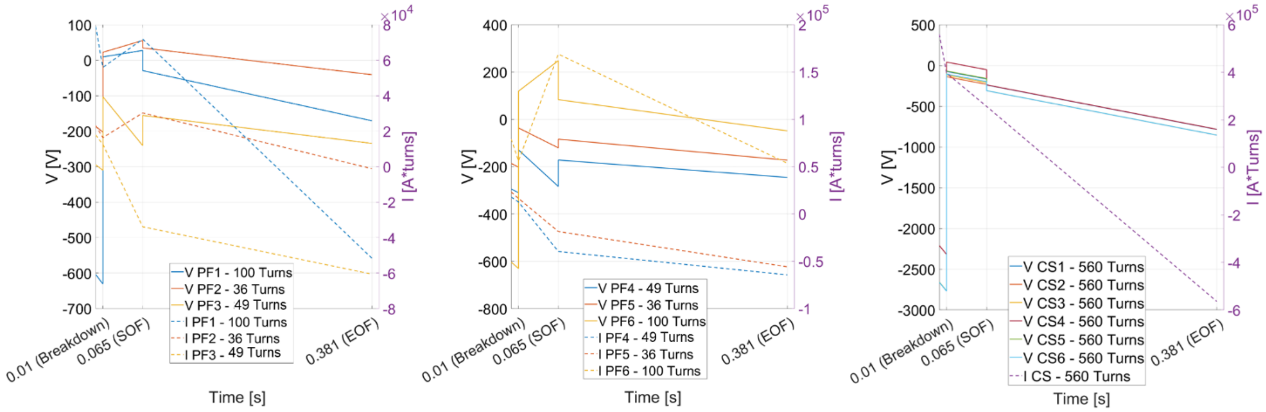

(a)

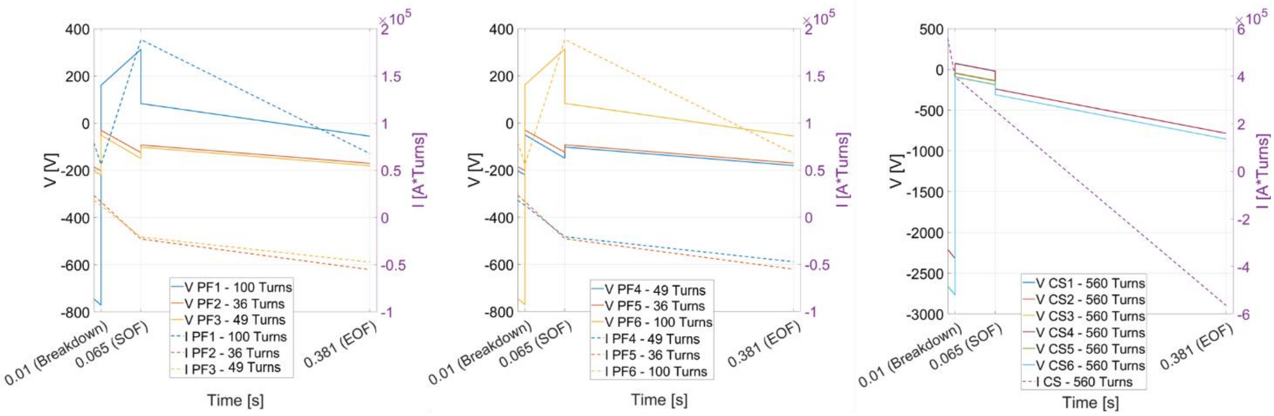

(b)

Fig. 27 Current (Amper-Turns), voltage and number of turns for PF and CS coils during the plasma discharge considering a wire Ø equal to 4.115 mm (AWG6). Figure (a) contain the reference waveforms for the SN target scenario, Image (b) for DN alternative scenario.

The CS is divided in six modules to reduce the voltage of the power supplies and consequently the use of supercapacitors energy storage. In order to get the highest flexibility all the power supply are design with the same voltage and current limits. As for the PF coils, the number of turns and the wire diameter is estimated with trade-off by Joule's heating and power supplies limits (max. voltage 1 kV and max. current 1 kA). The current and voltage waveforms are showed in Fig. 27. In Table 11 and Table 12 are reported the main parameters for the CS modules. Two non-toroidally continuous structure cylindrical plates are located at the top and bottom of the CS modules to pre-compress the CS modules and to support the electromagnetic loads. As explained in Section 3, in the AML configuration the swapped positions between the CS modules and the TF coils allow to gain radial space in the tokamak radial building.

Table 9. PF coils currents during the SN plasma scenario

	Current @0s [MA· Turns]	Current @Breakdown [MA· Turns]	Current @SOF [MA· Turns]	Current @EOF [MA · Turns]
PF1	0.0791	0.0560	0.0592	-0.0496
PF2	0.0232	0.0164	0.0266	-0.0022
PF3	0.0179	0.0126	-0.0360	-0.0603
PF4	0.0179	0.0126	-0.0437	-0.0641
PF5	0.0232	0.0164	-0.0195	-0.0569
PF6	0.0791	0.0560	0.1543	0.0551

Table 10. PF coils geometric parameters considering R and Z respectively the radial and vertical coordinates for the PF coils centroid, and DR and DZ respectively the radial and vertical extension

	Number of Turns	R [m]	Z [m]	DR [m]	DZ [m]
PF1	100	0.2287	0.40130	0.0464	0.0464
PF2	36	0.4775	0.37270	0.0238	0.0238
PF3	49	0.5900	0.20000	0.0282	0.0282
PF4	49	0.5900	-0.20000	0.0282	0.0282
PF5	36	0.4775	-0.37270	0.0238	0.0238
PF6	100	0.2287	-0.40130	0.0464	0.0464

Table 11. CS modules currents during the SN plasma scenario

	Current @0s [MA· Turns]	Current @Breakdown [MA· Turns]	Current @SOF [MA· Turns]	Current @EOF [MA · Turns]
CS1	0.560	0.396	0.173	-0.564
CS2	0.560	0.396	0.173	-0.564
CS3	0.560	0.396	0.173	-0.564
CS4	0.560	0.396	0.173	-0.564
CS5	0.560	0.396	0.173	-0.564
CS6	0.560	0.396	0.173	-0.564

Table 12. CS modules geometric parameters considering R and Z respectively the radial and vertical coordinates for the CS modules centroid, and DR and DZ respectively the radial and vertical extension

	Number of Turns	R [m]	Z [m]	DR [m]	DZ [m]
CS1	560	0.1325	0.450	0.0650	0.180
CS2	560	0.1325	0.270	0.0650	0.180
CS3	560	0.1325	0.090	0.0650	0.180
CS4	560	0.1325	-0.090	0.0650	0.180
CS5	560	0.1325	-0.270	0.0650	0.180
CS6	560	0.1325	-0.450	0.0650	0.180

TF coils system

The TF coils are designed to get the target toroidal field and to minimize the structural stress. As a consequence of their radial extension far from the plasma, it produces a very low toroidal ripple (approximately 0.4%) regardless the low number of toroidal field coils (only six). In fact, maintaining the AML configuration, the number of TF coils moved from eight to six during the development of the TRUST design (increasing the radial outboard coordinates). The toroidal magnetic field and its ripple are evaluated through Ansys APDL and the results are showed in Fig. 28. An obvious consequence to have the PF coils internally to the toroidal ones is the interaction of poloidal magnetic field with the toroidal field current is completely different respect to the standard case. By these considerations the TF coil upper curvature is brought in a region less intense poloidal field. This vertical extension should allow to reduce the interaction with the poloidal field and a consequently reduction of the out of plane forces. In fact, the possibility to increase the vertical dimension brings the TF coils curvature and its current better aligned with the poloidal field direction reducing their coupling. One of the main TRUST goals remains the test and verification of the AML design, studying the electromagnetic loads acting on the TF coils and the possibles engineering solutions to prove the construction feasibility of alternative configuration.

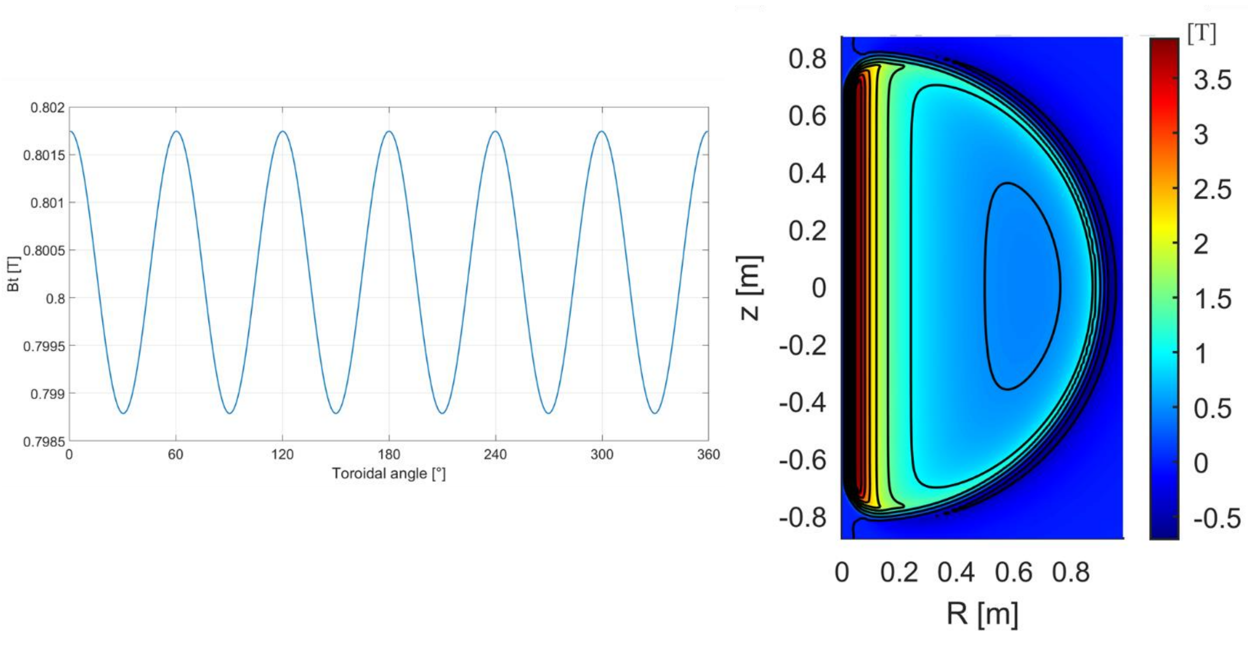

Fig. 28 Ripple of the toroidal magnetic field and toroidal magnetic field showed on the poloidal plane.

The TF coils current geometry is obtained considering the constant tension or bending free shape [57][66]. To assembly and disassembly all the internal components (CS, PF, VV, etc…), for the current TRUST design, two electrical joints are required between the central column and the TF coils outer legs [67][68][69]. The design of this joints is a critical aspect and it is important carefully dealing with it also for the copper TF coils. The TF coils conceptual design is showed in Fig. 29. The TF coils inner leg is composed by a set of cylindrical copper bars held by a steel case filled with epoxy to guarantee the electrical insulation. The TF coils outer part is designed with the same principle. Between the inner legs and the TF coils outer parts a plug-in connector is located to perform a series connection among the copper bars. The plug-in connector is attached through a bolted flange. The foreseen design should simplify the TF coils realization avoiding the winding process and it should ensure an easy assembly/disassembly phase for the experiment.

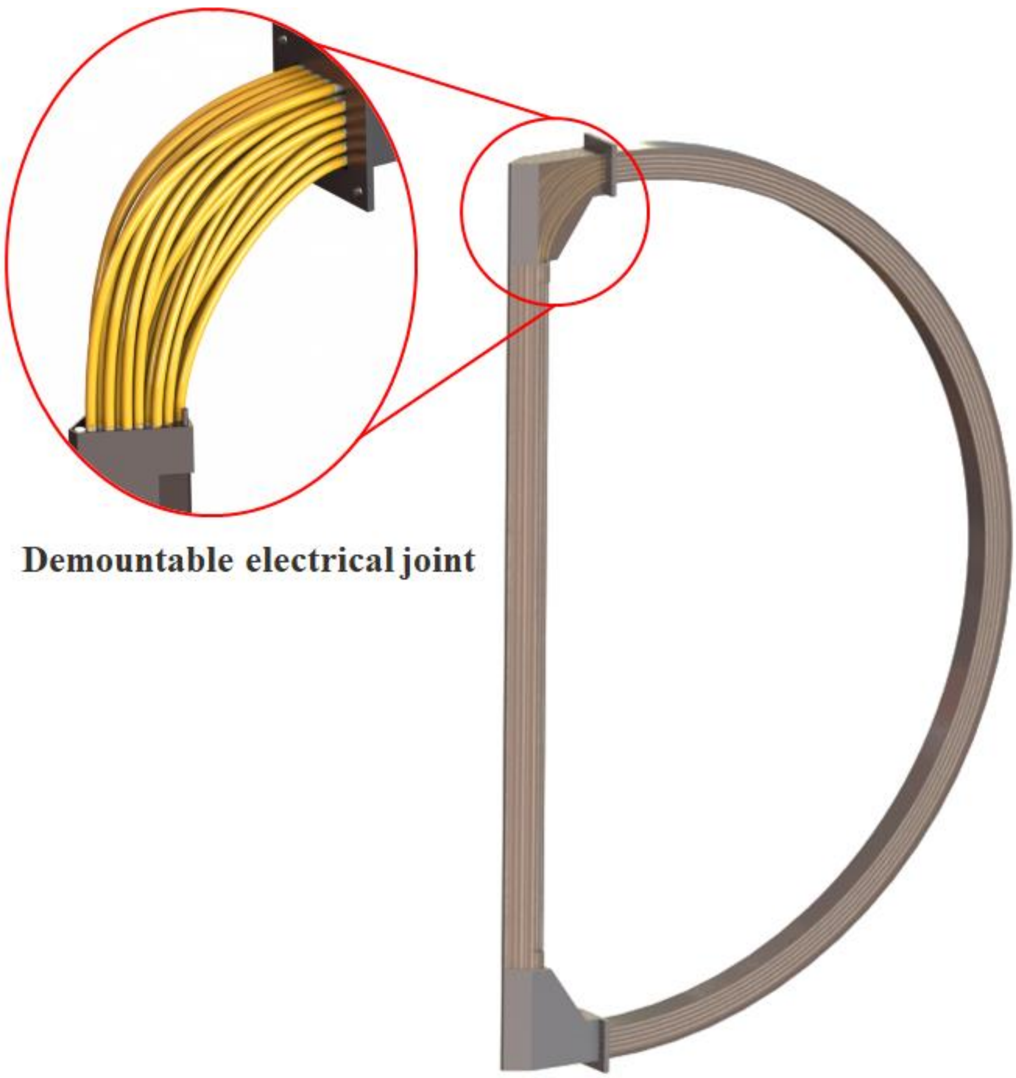

Fig. 29 Current design for the TRUST copper TF coils.

4.2 Plasma Scenario

The target SN plasma configuration was designed considering the TRUST scientific and academic goals. In fact, the target plasma scenario was achievable maintaining the economic feasibility for a university-class experiment and at the same time a scientific relevance to test meta-materials as PFC and HTS coils. An important feature for the scenario design was the use of a four quadrants IGBT power supplies, energized by a supercapacitor energy storage system, as discussed in the previous section. All the power supplies have the same characteristic in terms of maximum voltage and maximum current (1kV and 1 kA). This solution allows high flexibility in the possible plasma shapes and scenarios for TRUST. The reference SN scenario is designed by using MAXFEA code in combination with a MATLAB routine. The plasma current and voltage loop waveforms are showed in Fig. 30. The poloidal field at SOF and EOF is showed in Fig. 32a and Fig. 32b and the main parameters of the plasma equilibrium are report in . The designed plasma equilibrium affords a solid baseline for the PFC testing as explained in the following paragraphs. Therefore considering the power supplies limits and the SN target equilibrium an iterative procedure was developed to combine all the constraints obtaining the PF coils and CS modules parameters need to carry out the required plasma scenario.

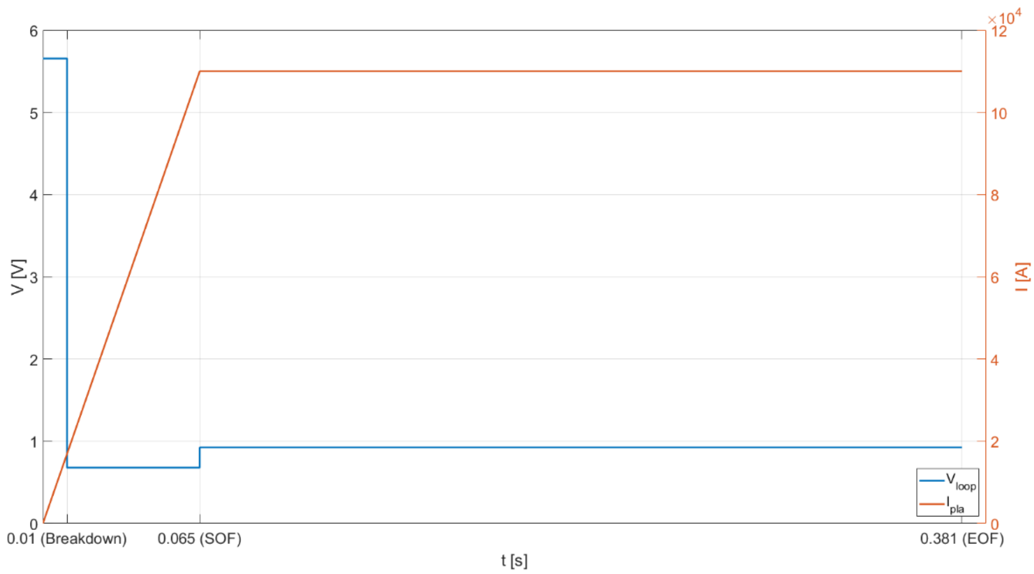

Fig. 30 Plasma current and voltage loop waveforms during the plasma discharge.

Breakdown

The PF coils and the CS modules current are currently designed to guarantee a good magnetic field null for the plasma breakdown as showed in Fig. 31a. The maximum magnetic field at the edge of null area is estimated less than 3 mT, while at plasma magnetic axis (R_0 and Z_0) is estimated less than 0.5 mT. Considering an ohmic breakdown, a toroidal electric field of 3 V/m is imposed at R_0 and Z_0 for 10 ms obtaining a voltage loop of 5.65 V and a flux consumption of 0.0565 Vs. The electric field required for the breakdown $E_{avalanche}$ is evaluated trough the Townsend avalanche theory [70][71]:

$$E_{avalanche} = \frac{1.25 \times 10^4 P}{ln\ (510 P L_c)} \tag{8}$$

Where the P is the gas pressure in in Torricelli and L_c is the connection length:

$$L_c = \frac{a}{4} \frac{B_\varphi}{B_\theta} \tag{9}$$

Given a the minor radius, $B_\varphi$the toroidal field and B_θ the poloidal null field. For an affordable ohmic breakdown an empiric formulation could be used [72]:

$$E_{avalanche} \frac{B_\varphi}{B_\theta} \geq 1000 \tag{10}$$

For the TRUST electric field, toroidal and poloidal field the Eq. 3 is fulfilled. A pre-ionization system based on an electron cyclotron system [73] for the plasma start-up is under investigation, to facilitate the plasma breakdown and to allow more flux availability for longer discharges. A solution like this has been already easily implemented in a similar experiment [73][74].

Ramp-up

Further flux is needed to ramp-up the plasma to the flat-top current and it is evaluated as already explained in Section 3.1 with the equation 5. In the TRUST case the normalised plasma internal inductance li of 0.8, the Ejima coefficient C_{ejima} assumed equal to 0.5 [56]. The plasma current rise is assumed equal to be 2 MA/s, leading to I_{pla} ≈ 0.110 MA in 0.055 s. The detailed evolution of the plasma shape needed to reach target SN configuration is currently neglected and it will be investigated at a more advanced stage of the design. As mentioned before, at least three different plasma configurations are considered for the future operation of TRUST by exploiting the almost up-down symmetry of the machine. For each configuration the breakdown and the ramp-up phases are considered equal. The TRUST design will allow the possibility to test and study also DN and USN plasma configurations.

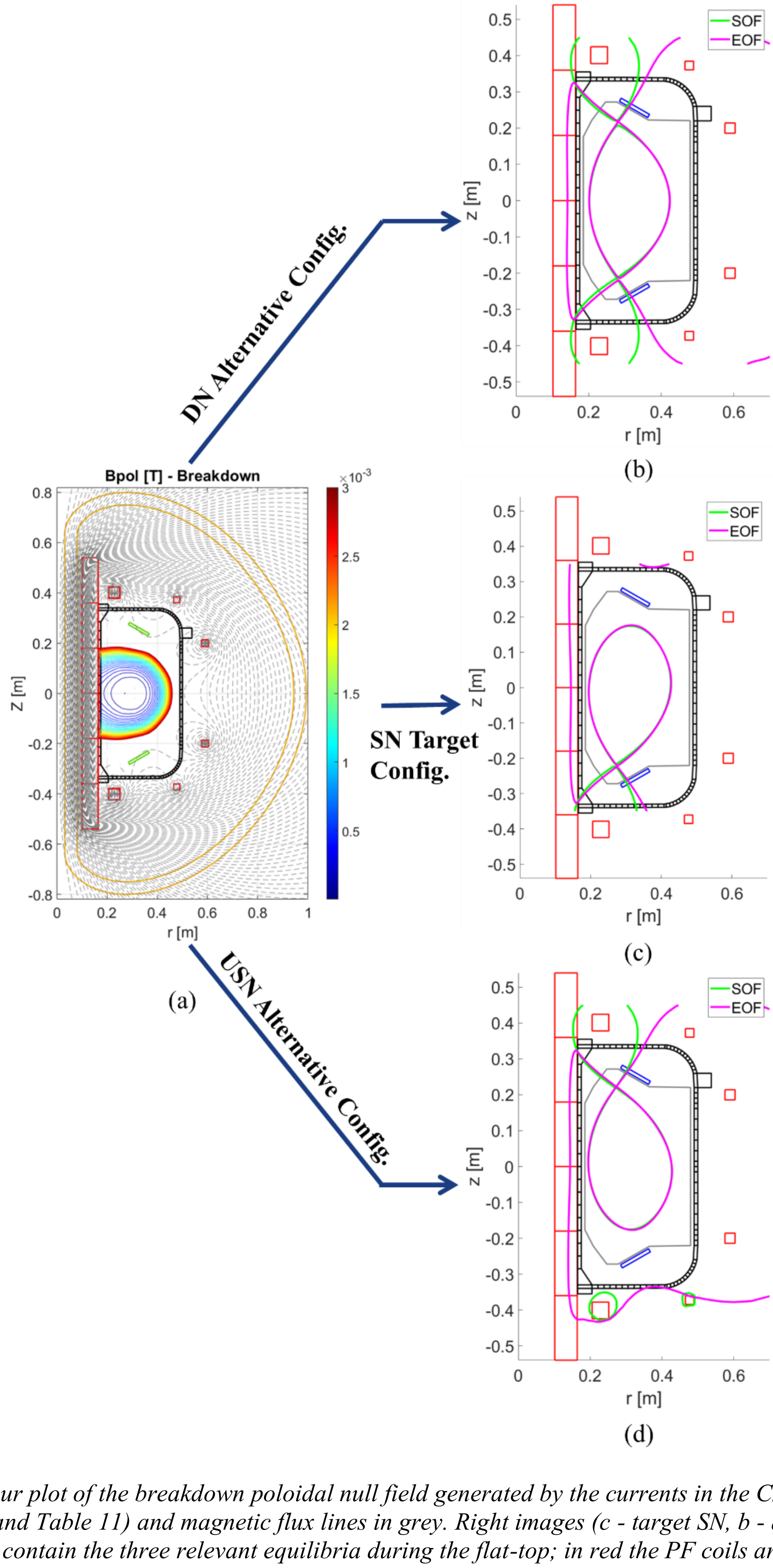

Fig. 31 (a) Contour plot of the breakdown poloidal null field generated by the currents in the CS modules and the PF coils (Table 9 and Table 11) and magnetic flux lines in grey. Right images (c - target SN, b - alternative DN, d – alternative USN) contain the three relevant equilibria during the flat-top; in red the PF coils and CS modules, in blue the in-vessel passive plate, in black the VV, the LCFS at SOF is in green and the LCFS at EOF is in magenta.

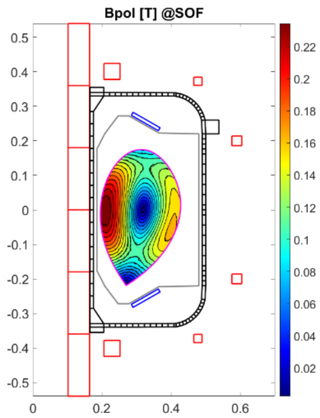

(a)

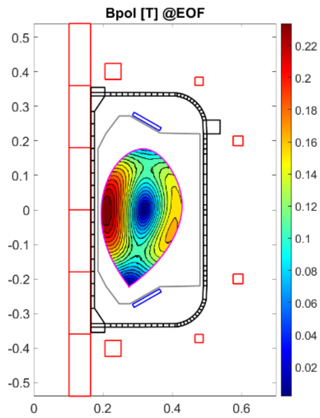

(b)

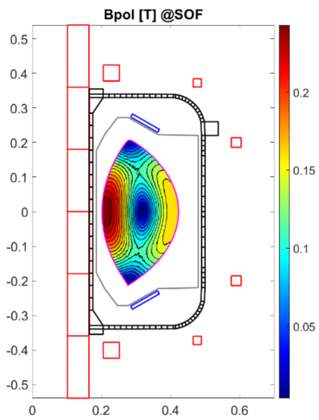

(c)

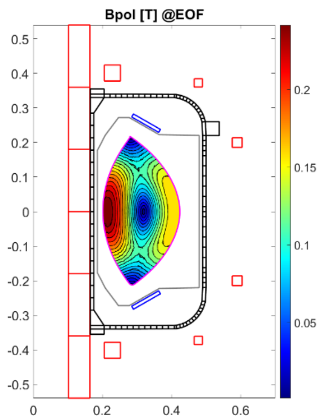

(d)

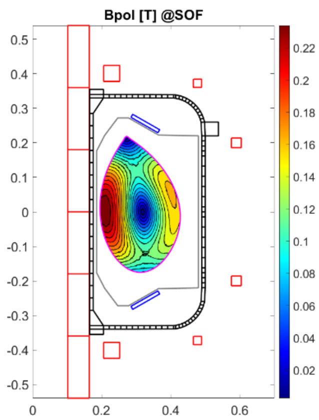

(e)

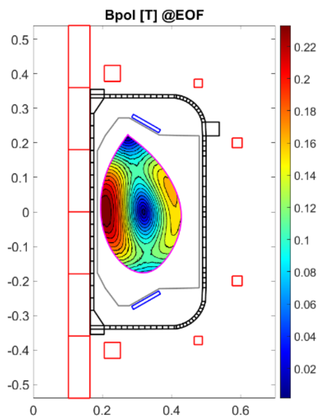

(f)

Fig. 32 Contour plot of the poloidal field for the (a) SN @SOF, (b) SN @EOF, (c) DN @SOF, (d) DN @EOF, (e) USN @SOF, (f) USN @SOF

Table 13. Target SN equilibrium main parameters

	SOF	EOF
I_{pla} [kA]	110.0	110.0
R [m]	0.3	0.3
a [m]	0.11	0.11
B_t [T]	0.8	0.8
κ	~1.9	~1.9
δ_{low}	~0.3	~0.3
β_{pol}	~ 0.1	~ 0.1
li	~ 0.8	~ 0.8
q_{95}	~3.3	~3.3
Volume [m^3]	~0.125	~0.125
$\psi_{boundary}$ [Vs]	0.126	-0.190

Table 14. Target DN equilibrium main parameters

	SOF	EOF
I_{pla} [kA]	110.0	110.0
R [m]	0.3	0.3
a [m]	0.12	0.12
B_t [T]	0.8	0.8
κ	~1.7	~1.7
δ_{low}	~0.3	~0.3
β_{pol}	~ 0.1	~ 0.1
li	~ 0.8	~ 0.8
q_{95}	~3.2	~3.2
Volume [m^3]	~0.125	~0.125
$\psi_{boundary}$ [Vs]	0.123	-0.193

Table 15. Target USN equilibrium main parameters

	SOF	EOF
I_{pla} [kA]	110.0	110.0
R [m]	0.3	0.3
a [m]	0.12	0.12
B_t [T]	0.8	0.8
κ	~1.7	~1.7
δ_{low}	~0	~0
β_{pol}	~ 0.1	~ 0.1
li	~ 0.8	~ 0.8
q_{95}	~3.2	~3.2
Volume [m^3]	~0.125	~0.125
$\psi_{boundary}$ [Vs]	0.123	-0.193

Flat-top

During the flat-top phase a plasma resistive voltage V_p of $\sim$1 V is evaluated by considering the Spitzer resistivity $\eta_s$with an electron temperature T_e of $\sim$350 eV [5]:

$$\eta_s = \frac{2.8 \times 10^{-8}}{T_e^{\frac{3}{2}}} \tag{11}$$

$$V_p = \frac{2q_{95} I_{pla} R}{\kappa a^2 \sigma_s} \tag{12}$$

Where σ_s is the Spitzer conductivity inverse of Spitzer resistivity. To estimate the plasma electron temperature a preliminary scan on the operational TRUST condition is performed for the SN scenario with a two-point model [75][76].

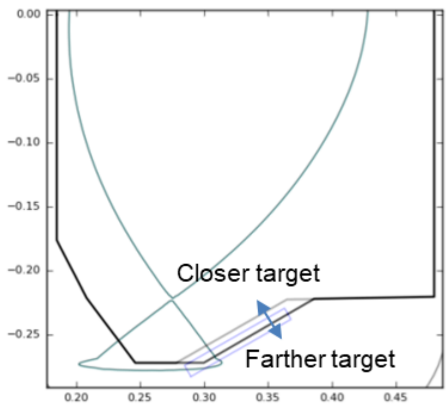

a)

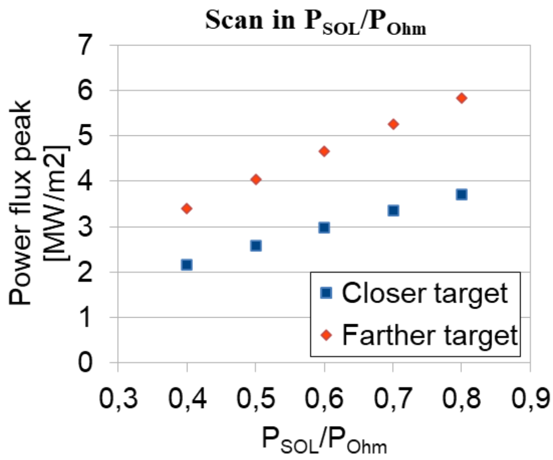

b)

Fig. 33 Preliminary scan on the radiated power fraction with two different positions for the divertor target

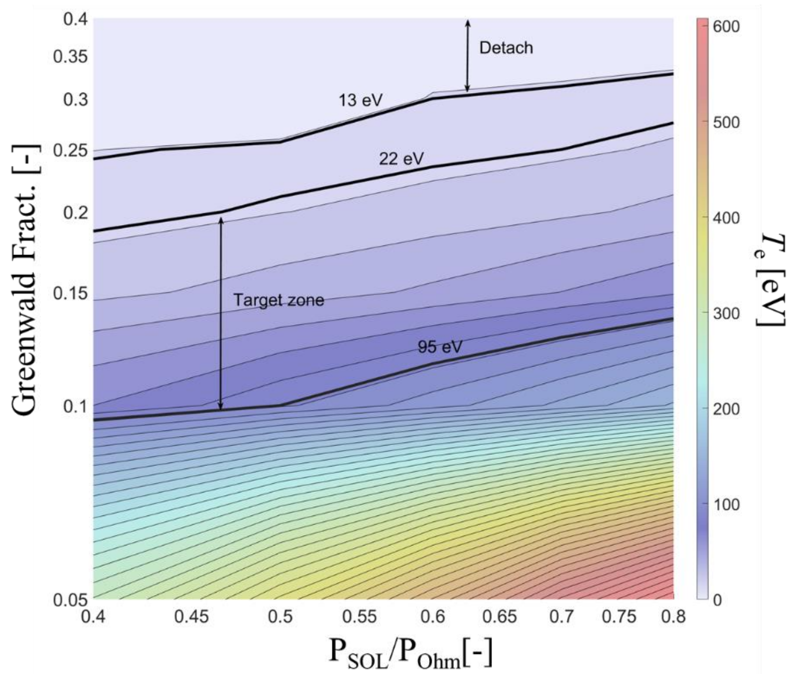

Fig. 34 Operational range of the electron temperature on the outboard divertor as function of the operating density and the radiated power fraction. The operational target zone is individuated (attached condition) to increase the heat flux on the divertor target.

Consequently, it is possible to estimate the maximum duration of the plasma discharge to be of the order to 381ms. In order to validate the possible heat flux achievable also a preliminary analytic model is used. The ohmic power during the flat-top is included between 160 kW and 190 kW. By assuming up to approximately 50% of losses by plasma radiation, it can be roughly considered about 100 kW power will flow through last magnetic surface. According to the Eich scaling [77]:

$$\lambda_q \approx P^{-0.02} R^{0.04} B_{pol}^{-0.92} \varepsilon^{0.42} \tag{13}$$

The scrape off layer (SOL) power decay length λ_q is approx. equal to 6 mm depending essentially only by the poloidal magnetic field B_{pol} and the inverse of the aspect ratio ε. In this operational condition, the parallel power flux in the SOL P_{sol} is around 4 MW/m^2:

$$P_{sol} = \frac{P}{A_{sol}} \tag{14}$$

$$A_{sol} \approx 2\pi R \lambda_q f_a \tag{15}$$

Given A_{sol} the SOL area near the divertor region function of the magnetic surface expansion parameter f_a. Considering a poloidal angle θ of 20° [78] and f_a approx. equal to 4, the perpendicular power flux onto divertor target P_{target} could easily reach 1.3 MW/m^2 which is in accordance with what expected from Fig. 33:

$$P_{target} = P_{sol} sin\,(\theta) \tag{16}$$

Varying the null vertical position during the operation or designing a divertor target with an increased poloidal angle would accomplish the fulfilment of overcome 2 MW/m2. Moreover, using a test module divertor (like what foreseen in DTT [79]) covering a minor toroidal sector of the geometry, it is possible to further increase the power deposition of a factor between 5 and 10. This preliminary evaluation shows the TRUST potential as valid experiment to test innovative PFC. Indeed, testing W metamaterials in an experimental tokamak could aid the research activities [80] and improve the models to predict their behavior in a reactor-like conditions.

Plasma Vertical Stability

Due to the intrinsic vertical instability of elongated plasmas, copper stabilizing plates have been introduced to help control the growth rate. To determine a suitable centroid position for the stabilizing plates, a simplified rigid displacement model (RZIp formulation) has been developed to estimate the growth rate [13]. The area selected for evaluating the placement of the plates has been chosen to avoid interfering with the space reserved for diagnostics inside the machine, while also considering the spatial constraints imposed by the divertor structure. The positioning of the plates on the high-field side (HFS) has been excluded as it has been shown to have a negligible stabilizing effect [81]. The model incorporates the effects of port cuts in the vacuum vessel by assigning appropriate equivalent electrical resistivity values to the affected regions, as explicated in [13]. Fig. 35 illustrates the growth rate values within the viable zone for plate placement in the SN plasma configuration at EOF. The chosen position for the plates results in a growth rate of approximately 990 s^{-1}, a consistent value for elongated plasmas, whose growth rates can reach up to 2500 s^{-1} [82]. Downstream to this calculation the reference position is set considering the best condition in terms of plasma vertical stability. Nevertheless, electromagnetic loads acting on the stabilising plates mast be investigated in further analysis.

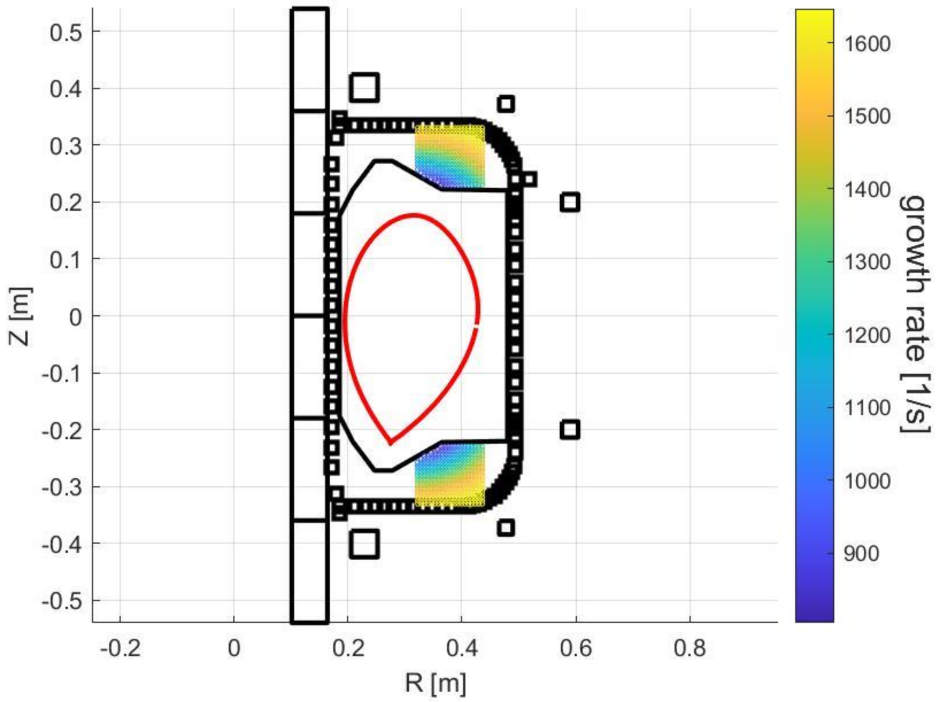

Fig. 35 Growth rate values for plasma SN configuration at EOF instant.

Initial TRUST Disruption Characterization

A preliminary SN plasma disruption database is presented in this section with the aim to evaluate the disruption specification loads for TRUST. The disruption analyses were performed considering the stabilizing plate reference position evaluated in the previous section. As a matter of facts, the increase in disruption case histories is being studied to check the most severe disruption in terms of global loads on passive structures, such as vacuum vessel and stabilising plates, but also for the local effects on the VV Dome end its flanges. In fact, the assessment of the electromagnetic behaviour during a disruption is mandatory for the successful design of a tokamak [83]. A collection of EM numerical simulations is performed by means of 2D MAXFEA evolutionary equilibrium code and reported here, covering various plasma dynamic conditions within the operational space in terms of:

- Starting Time instant: starting from EOF or SOF can have a significant effect on the disruption loads due to the different starting set of currents in the PF coils and, consequently, differences in the evolution of poloidal magnetic field map (it is not possible to say at priori which is the worst case and an investigation is mandatory).
- Plasma trajectory**:** it is common practice that both upward and downward VDE (UVDE and DVDE) be analysed to evaluate the different loads that result from the two trajectories. This is because the machine in question lacks perfect up-down symmetry in terms of plasma configuration and surrounding structures (e.g. VV Dome flanges).
- Current Quench (CQ) duration: the duration of CQ represents a significant discriminating factor in the load resulting from a disruption, and it is typically necessary to consider both Fast and Slow events in this regard. From an initial assessment of the TRUST machine scale end performance, it can be determined that Fast events have a CQ duration of 0.24 ms, while Slow events have a CQ duration of 2.4 ms [13][84].

A total of eight disruptions simulation has collected: two Fast and Slow UVDE and two Fast and Slow DVDE starting from EOF (four in total from EOF); two Fast and Slow UVDE and two Fast and Slow DVDE starting from SOF (four in total from SOF). The methodology applied using MAXFEA ,equilibrium code is fully explained and verified in [22][23][85][86]. Fig. 36 and Fig. 37 contain detailed relevant estimation for two dedicated cases: Fast DVDE starting from EOF and Slow UVDE starting from EOF. In particular, the evolution of plasma in terms of movement, shape evolution and trajectory are reported in Fig. 36 (b and c), while the main relevant EM loads deriving from the specific case of disruption in term of global vertical forces (b1) and Eddy currents (a1) are reported in Fig. 37. The same information was produced for all cases but not reported for avoid repetitive contents.

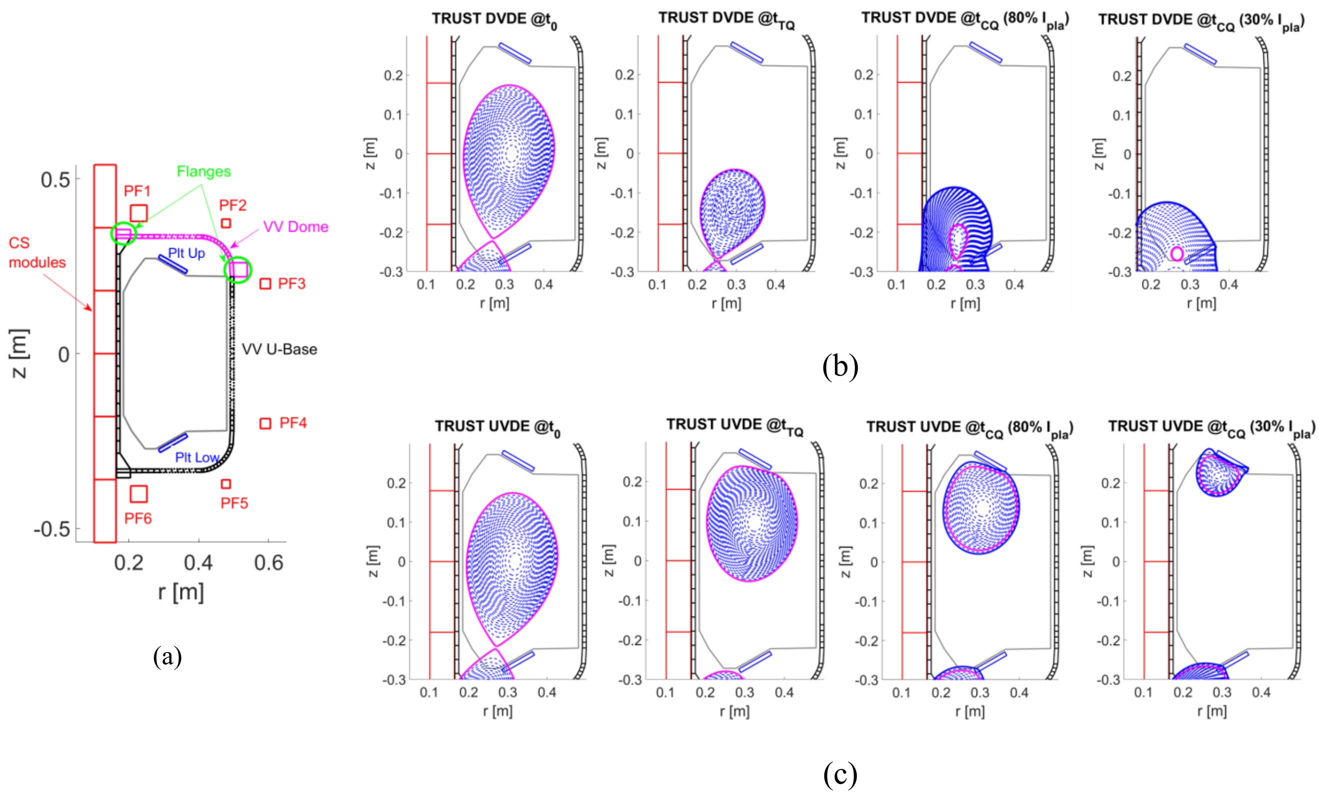

Fig. 36 Labelling of TRUST 2D model structures (a) and evolution of plasma in terms of movement, shape evolution and trajectory for Fast DVDE starting from EOF (b) and Slow UVDE starting from EOF (c). Instants of snapshots in (b) end (c) are referred, considering a left to right order, to the following times: the equilibrium (t_0), start of the thermal quench (t_{TQ}), during CQ when the plasma current is 80% respect to the starting value (t_{CQ} 80% I_{pla}), during CQ when the plasma current is 30% respect to the starting value (t_{CQ} 30% I_{pla}).

Graphs in Fig. 37 (a1)(a2) show: the plasma current and halo currents dynamics (blue and red lines, respectively) with their typical trends [84], the evolution of eddy currents considering the VV structure (yellow trend), the eddy currents trend on the VV Dome (purple curve) and the dynamics of total eddy currents considering the contribute of the upper and lower stabilising plates induced currents (dark red and green respectively). For what concerns the vertical forces (F_z), the trends in Fig. 37 (b1)(b2) contain: force dynamics due to the halo currents effect is reported in blue, the evolution of total forces due to eddy currents on the stabilising plates (light blue for the upper and dark red for the lower), the total loads trend act on the VV structure considering the dynamics of total eddy currents on passives and the halo currents contribute is reported in black, the vertical force considering the VV Dome supports structures (flanges in Fig. 36a) is in magenta, the F_z acting on the VV with the only eddy contribute is represented by the green trend.

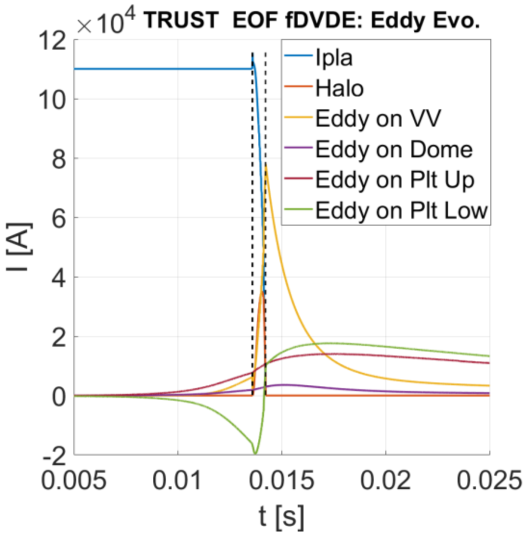

(a1)

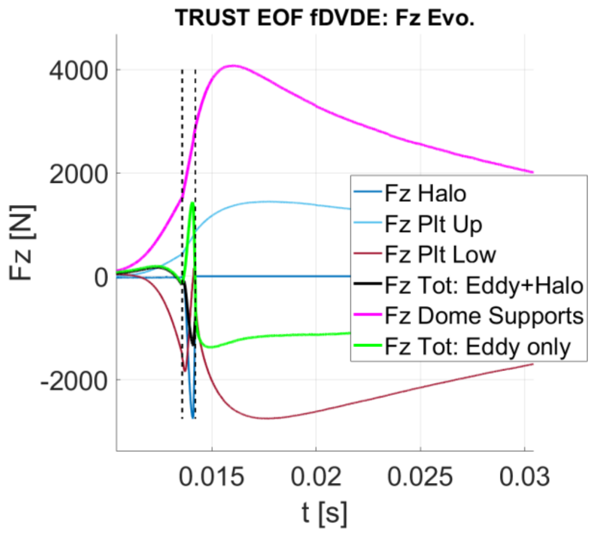

(b1)

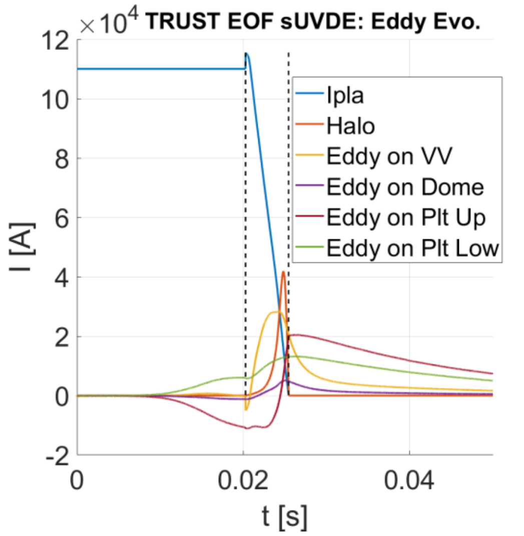

(a2)

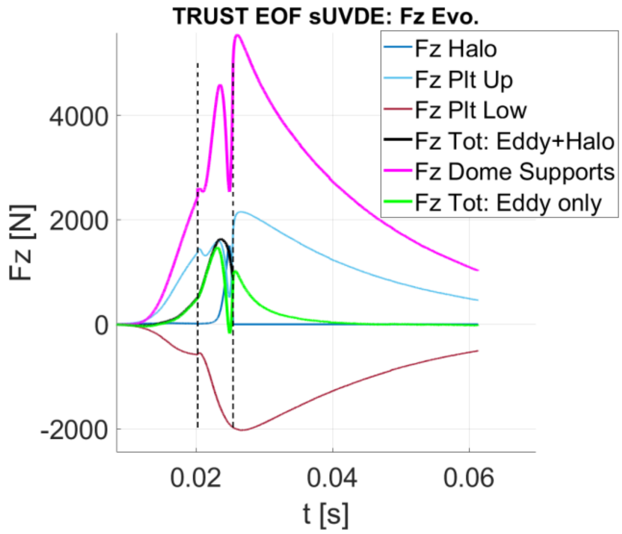

(b2)

Fig. 37 Examples of detailed MAXFEA output in terms of computed eddy currents (a) and 2D vertical forces (b) trends in time on TRUST components for EOF Fast DVDE (a1)(b1) and EOF Slow UVDE (a2)(b2).

Fig. 38 shows a qualitative preview of TRUST numerical disruptions collected to provide EM loads specifications. Additionally, Table 16 contains a summary aimed at outlining the corresponding main outcomes in terms of vertical forces on the different components and plasma trajectory and wall contact point during the VDE, obtained for each case (with reference to Fig. 38). These data will be useful for future structural assessment [82].

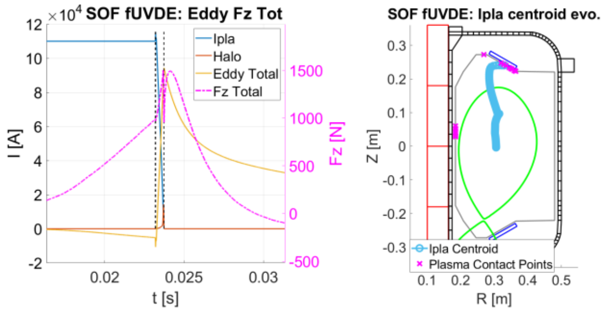

(a)

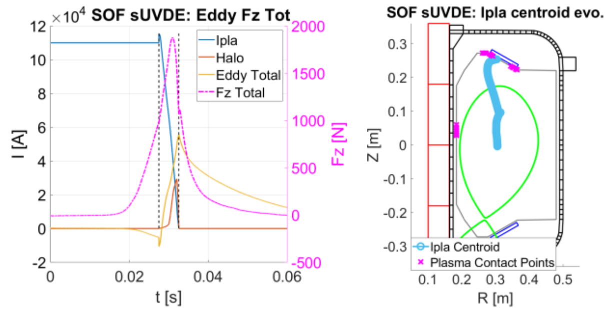

(b)

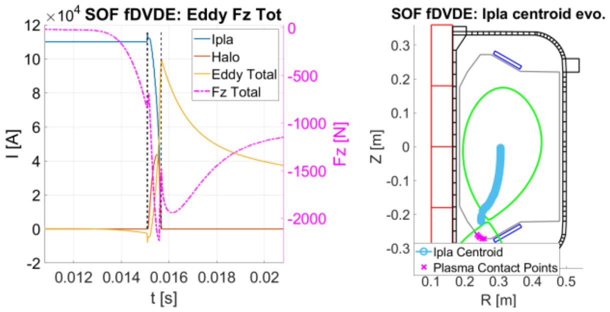

(c)

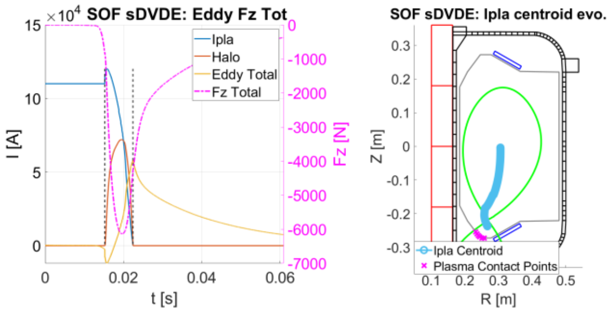

(d)

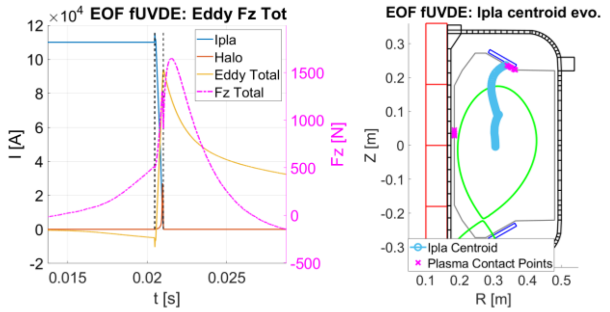

(e)

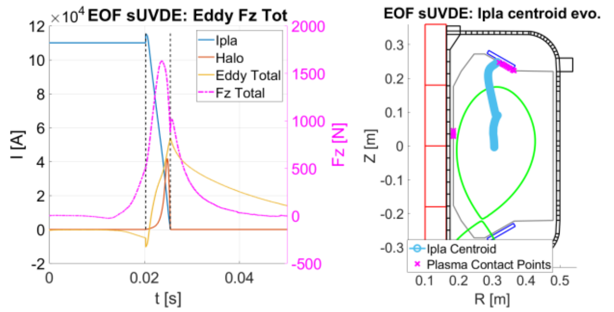

(f)

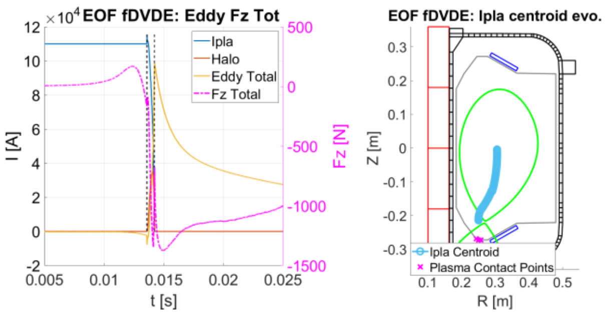

(g)

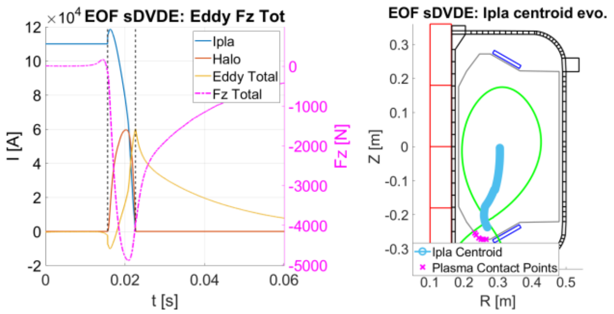

(h)

Fig. 38 Preview of TRUST disruption specification. *The following outcomes are reported: plasma current and halo currents (blue and red lines respectively), total eddy currents for all the passive structures in the model (yellow trends), total loads acting on the VV structure including the supported components (magenta dashed trends, refers to right ordinate axis). In addition, plasma centroid trajectory and wall contact points during the VDE are reported in the poloidal plane images (blue trend and magenta cross, respectively),*

Table 16 TRUST disruption summary table reassuming the main outcomes in terms of vertical forces on the different components for each case. An important focus on the total loads peak act on the VV structure considering the dynamics of total eddy currents on passives and the halo currents contribute is presented (first row), together with the vertical forces peak acting on the VV structure from only eddy contribute (second row). As for the local forces, the vertical force peak considering the VV Dome supports structures and on the stabilizing plates are reported in the third and the fourth row, respectively.

	SOF Fast UVDE (a)	SOF Slow UVDE (b)	SOF Fast DVDE (c)	SOF Slow DVDE (d)	EOF Fast UVDE (e)	EOF Slow UVDE (f)	EOF Fast DVDE (g)	EOF Slow DVDE (h)
F_z PeakTotal - Halo+Eddy [kN]	1.450	1.877	-2.236	**-6.141**	1.650	1.636	-1.376	-4.879
F_z Peak total - Eddy only [kN]	1.492	1.585	-1.942	**-4.271**	1.650	1.471	1.435	-3.928
F_z Peak Dome Supports [kN]	4.614	4.978	3.309	2.520	5.433	**5.537**	4.068	3.078
F_z Peak Plates [kN]	-1.818	1.876	-2.829	**-3.839**	-2.172	2.153	-2.754	-3.650

Looking at Table 16, significant observations can be made regarding the disruption EM load specification for TRUST, together with a preliminary identification of the worst case for the various components. It is evident that the worst disruption case in terms of global vertical forces results to be the SOF Slow DVDE, with an Fz peak of 4.271 kN downward (6.141 kN is also the Halo contribution is considered). The same case result to be the design driver case for the plates supports, with an Fz peak acting on the lower stabilising plates of 3.839 kN downward. In another hand, the target case to be considered for the design of the VV Dome supports is the EOF Slow UVDE, with an Fz peak acting on the flanges of 5.537 kN upward. Although the estimated loads are nowhere near the design driver loads of the world's large tokamaks [13][85][86], the knowledge gained from this data collection on the EM loads from disruption is a necessary step in the design of TRUST. The EM loads obtained will be refined with detailed 3D EM analyses that will also provide information on the 3D effects of the loads not considered in this 2D analysis (such as force concretions or out-of-plane loads). It will then be possible to carry out the first structural analyses for the design of leg supports, stabiliser plates supports and the VV dome flanges, as well as in-vessel components such as the divertor, for which the information provided on Halo currents will a key input [13][85][86].

4.3 Structural Analysis

To evaluate the structural behavior of the VV, an analytical model is carried out considering the circular cylinder and pressure vessels theory [87]. In a small aspect ratio tokamak, the VV central cylinder is one of the most strongly loaded areas during a disruption [22][23][88]. For this reason, the preliminary structural assessment is carried out on this critical component. Considering the VV central cylinder on the equatorial plane, the vertical deformation could be neglected assuming a plane strain problem:

$$\varepsilon_r = \frac{1-\nu^2}{E}\left(\sigma_r - \frac{\nu}{1-\nu}\sigma_t\right) \tag{17}$$

$$\varepsilon_t = \frac{1-\nu^2}{E}\left(\sigma_r - \frac{\nu}{1-\nu}\sigma_t\right) \tag{18}$$

$$\sigma_z = \nu\,(\sigma_r + \sigma_t) \tag{19}$$

The radial strain ε_r and the tangential strain ε_t are function of the radial stress σ_r, tangential stress σ_t and the material properties (Poisson ratio ν and Young modulus E). The axial stress σ_z depends by the Poisson effect. Besides, the vertical force due to the disruption causing an additional axial stress σ_z and the radial expansion of the CS modules is considered. The latter, generated by the magnetic pressure of the CS and the different thermal expansion, acts on the VV central cylinder causing an additional load. The circular cylinder and pressure vessels theory formulation are reported here:

$$\sigma_r = \bar{A} - \frac{\bar{B}}{\rho^2} - \frac{\alpha\,E}{(1-\nu)\rho^2}\int_\beta^\rho T\,\rho\,d\rho \tag{20}$$

$$\sigma_t = \bar{A} + \frac{\bar{B}}{\rho^2} + \frac{\alpha\,E}{(1-\nu)\rho^2}\int_\beta^\rho T\,\rho\,d\rho - T \tag{21}$$

Where $\bar{A}$ and $\bar{B}$ are functions of material properties and boundary conditions, α is the thermal expansion coefficient, ρ is the normalized radial position ($\rho = r/r_{ext}$) and β is the ratio between inner radius r_{inn} and external radius r_{ext}. Considering the thin thickness of the VV (1 cm) and the vacuum on the plasma side, the radial stress results neglectable. The tangential stress σ_t result maximum (57 MPa) at the inner radius of the VV central cylinder, while the axial stress (along the experiment z axis) σ_z is maximum (40 MPa) at the external radius (plasma side). The stress trends are reported in Fig. 39. These preliminary stress value for the structural verification of the mechanical structure are presently under investigation through a 3D analysis using Ansys. It is possible to observe how the preliminary stress state is below the allowable primary membrane stress intensity of materials considering a VV operating temperature of 80 °C (126.7 MPa for the SS 316 L) obtained considering the ITER SDC-IC code for structural analysis of the ITER in-vessel components (Level A criteria) [89].

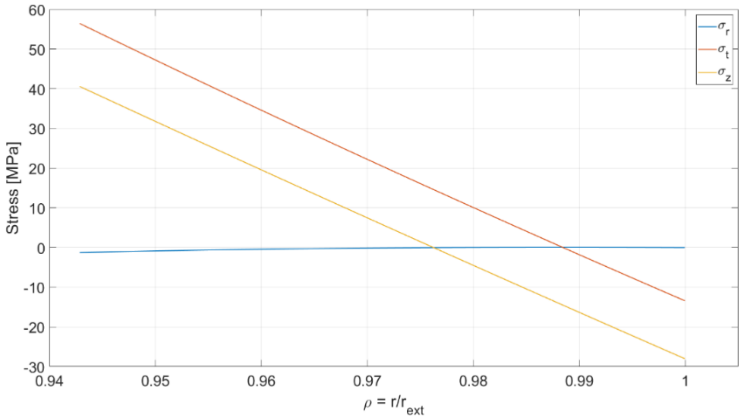

Fig. 39. Stress state on the VV central cylinder along the normalized thickness

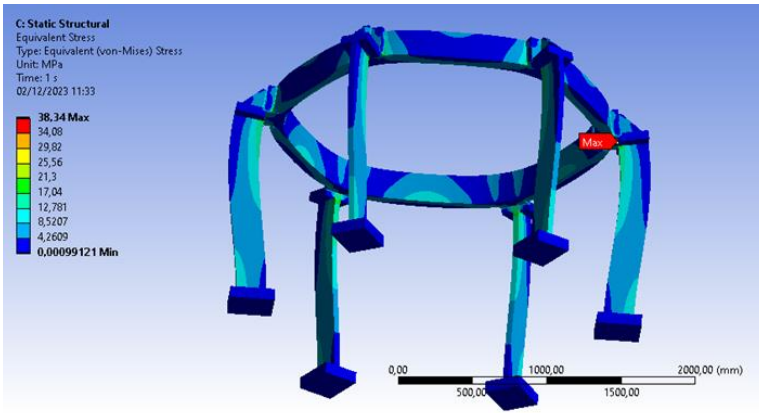

(a)

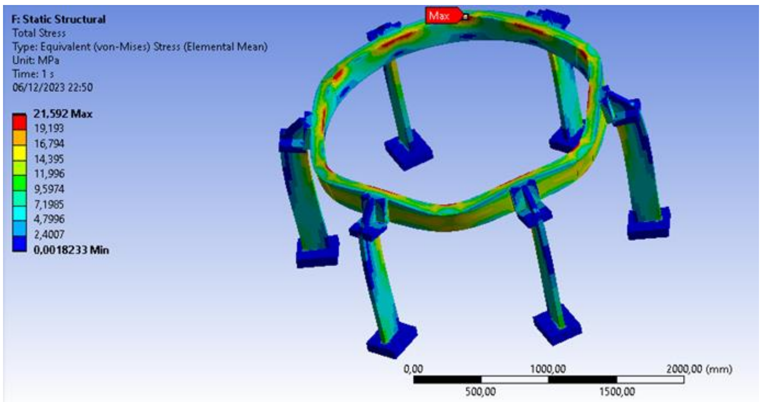

(b)

Fig. 40. Stress state on the gravity support considering the vertical loads acting (a) directly on the support legs and (b) acting between the legs

Moreover, a preliminary structural assessment on the gravity supports legs is performed as showed in Fig. 40. A conservative vertical force of 300 kN is distributed on 6 points, corresponding to the VV and TF coils supporting structure. The VV transmits its vertical force contribution in the area of the support legs, while the TF coils contribution is distributed on the rigid ring between each support legs. The two contributions are evaluated separately (linear elastic regime) and the maximum Von Mises stress is around 60 MPa. Also in this case the maximum stress is well below the allowable primary membrane stress intensity of AISI 316LN [89].

Finally, the PF coils and CS modules support structures are preliminary structurally checked for the SN scenario. Indeed, during the plasma scenario these coils are affected by considerable electromagnetic loads. The worst condition is generated before the BD phase and at the EOF as the currents flowing in the PF coils and CS modules are the highest.

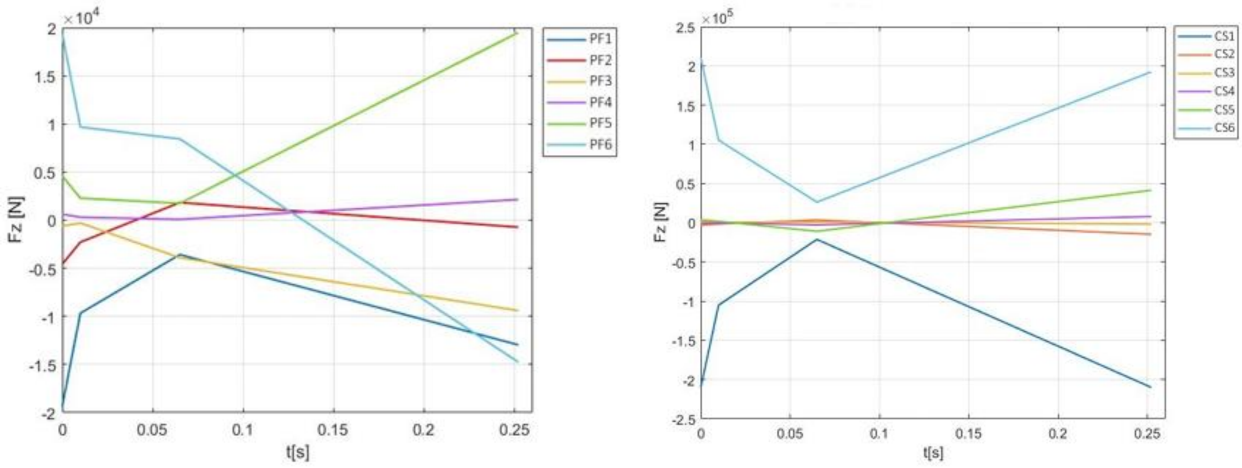

(a) (b)

Fig. 41 Vertical forces acting on (a) the PF coils and on the (b) CS modules during the plasma scenario (third TRUST concept)

The maximum vertical force is generated on the CS1 and CS6 modules with a value of ~200 kN. To sustain this load a solution is currently under investigation; a prominent strategy will include the addition of central support leg with a vertical preload on the CS modules. This analysis was performed for the third TRUST concept, but due to their similarities respect the current design remains relevant to proceed with the improvement and the design of the support structures.

5. TRUST Facility

The present section describes the site and experimental hall layout of the TRUST facility that will be hosted in at the Didactic Experimental Farming Company 'Nello Lupori' of the University of Tuscia located in Viterbo at Via Strada Riello n° 30. The TRUST facility will be realized through partial reconversion of the prefabricated concrete building, now used as a farm equipment shed, into a research laboratory. This reconversion is part of the interventions to be planned to meet the needs and requirements of the Department of Economics, Engineering, Society and Enterprise (DEIM). Indeed, the construction of the TRUST facility is included in the programme of redevelopment, renovation and new construction approved by the UNITUS Board of Directors resolution on March 31, 2023, in which a total amount of 350,000.00 € is foreseen for this work.

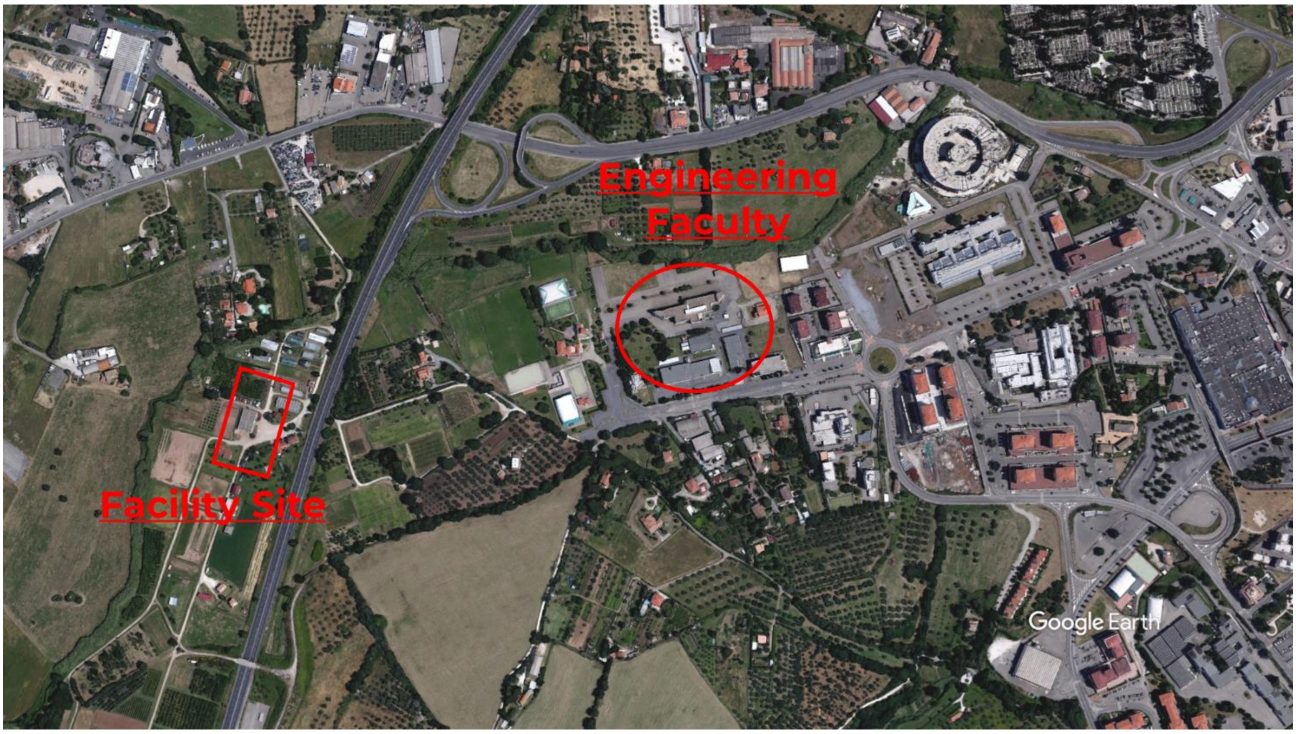

(a)

(b)

Fig. 42 (a) Satellite view on the TRUST facility and (b) West to East view of the warehouse.

The building is subject to several constraints:

- It is located in the “Road and Railway buffer zone”, due to its proximity to the SS675 road according to the Municipal Master Plan (PRG).
- It is in the area “Valuable Agricultural Landscape” and the area of “Archaeological Interest” according to Regional Territorial Landscape Plan (PTPR).

In the contexts of the PRG and PTPR, which are subject to certain constraints, the law permits the realisation of the planned intervention as scientific facilities (falling within the category of scientific facilities, cultural and worship centres and museums, educational activities and adventure parks). New constructions and extensions are permitted, even exceeding 20%, favouring the recovery and renovation of existing artefacts whose use is aimed at ‘promoting agrarian use and traditional cultivation methods, rural culture as well as the study and dissemination of innovative and/or experimental techniques’ (art. 26 of the NTA of the PTPR). In fact, since the property falls within this category of intervention, the law allows the design of building works for adaptation to the new uses (experimental laboratory and vehicle shed) from the technological and functional points of view.

For the previously mentioned motivation the Viterbo City municipality granted UNITUS a building permit on Decembre 5, 2024. The approved design for the facility is described as follows in this section.

5.1 Facility Design

As described above, the intervention on the existing building foresees a partial reconversion of the functions housed within it: one part will host the research laboratory spaces for the TRUST experiment, the other part will maintain the current function as a shed for the agricultural machinery used within the farm. The adaptation and re-functioning of the various planned spaces will be possible through building works that will define a 92 m^2 area for the experimental hall, with annexed a control room of 20 m^2 and service areas of approximately 5 m^2. Moreover, a cryogenic laboratory of 30 m^2 is foreseen to test HTS coils during the TRUST OP1. Next to the space dedicated to DEIM for the research and experimentation activities conducted by the latter, through a masonry made of monolithic blocks in autoclaved cellular conglomerate, a space of 150 m^2 will be maintained to continue to host the work activities carried out today inside the building. Adapting the current state of the building means responding definitively to the objectives discussed above, in particular guaranteeing maximum flexibility between the different functions that will be housed within the structure. The design has as its object the construction of two different spaces through internal building works that partly involve demolition and partly the construction of new ones: an autoclaved conglomerate masonry allows for the division of the two rooms, in which two self-supporting mezzanines are built, both supported by a structure of steel pillars and beams. The mezzanine included in the TRUST facility will be used as utility room for the power supplies of 57 m^2.

The insertion of these internal works defines a non-invasive intervention that is independent of the building's current structure, also envisaging an appropriate covering of the internal walls with plasterboard and rigid expanded polyurethane foam panels. access to the two different functional spaces is guaranteed by different entrances: the laboratory space is accessible through a small existing door and a new one inserted in the design process, which echoes the forms of the large 4-door opening compartments currently present. On the other hand, access to the work and storage area is provided by the two large existing compartments. The project also includes the design of mechanical plant works such as an air conditioning system, a water-sanitary system related to the sanitary service present in the university laboratory area, ventilation and an electrical system.

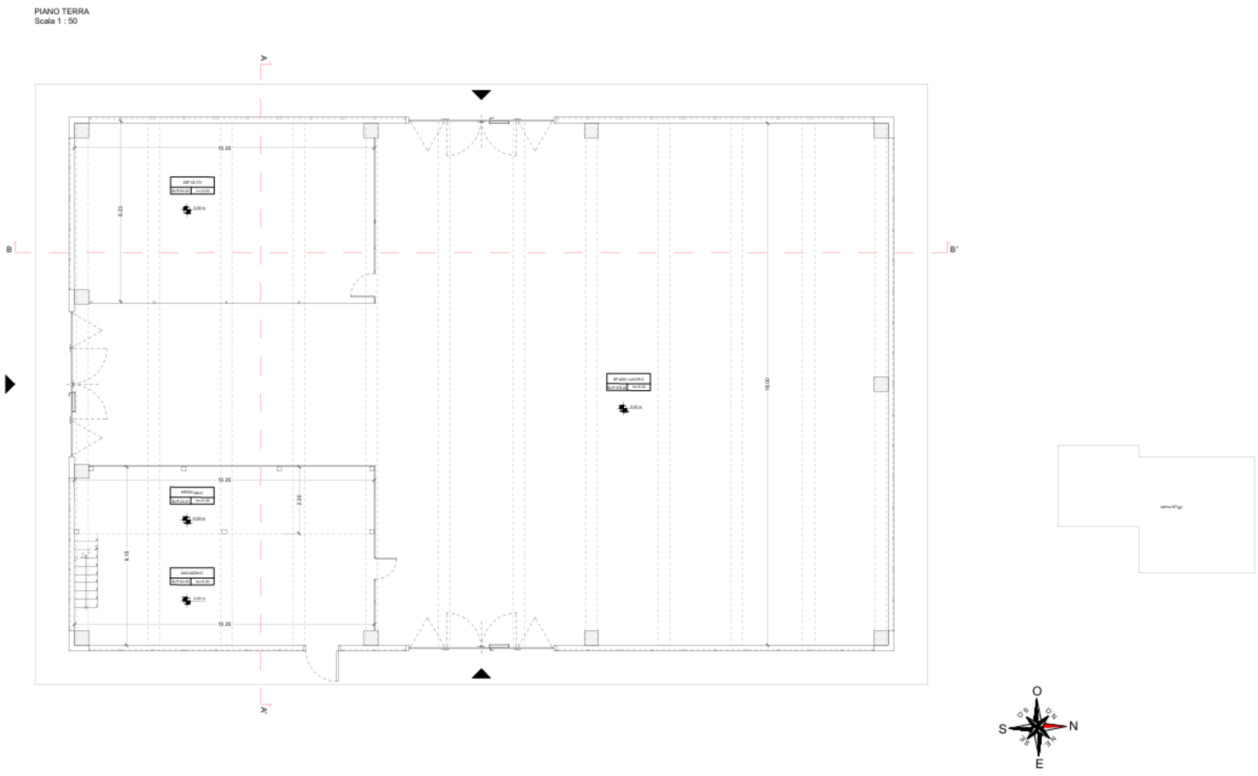
PIANO TERRA
Scala 1 : 50
A
B
B'
10.35
6.23
2.30
6.15
16.00
A'
O
S
N
E

(a)

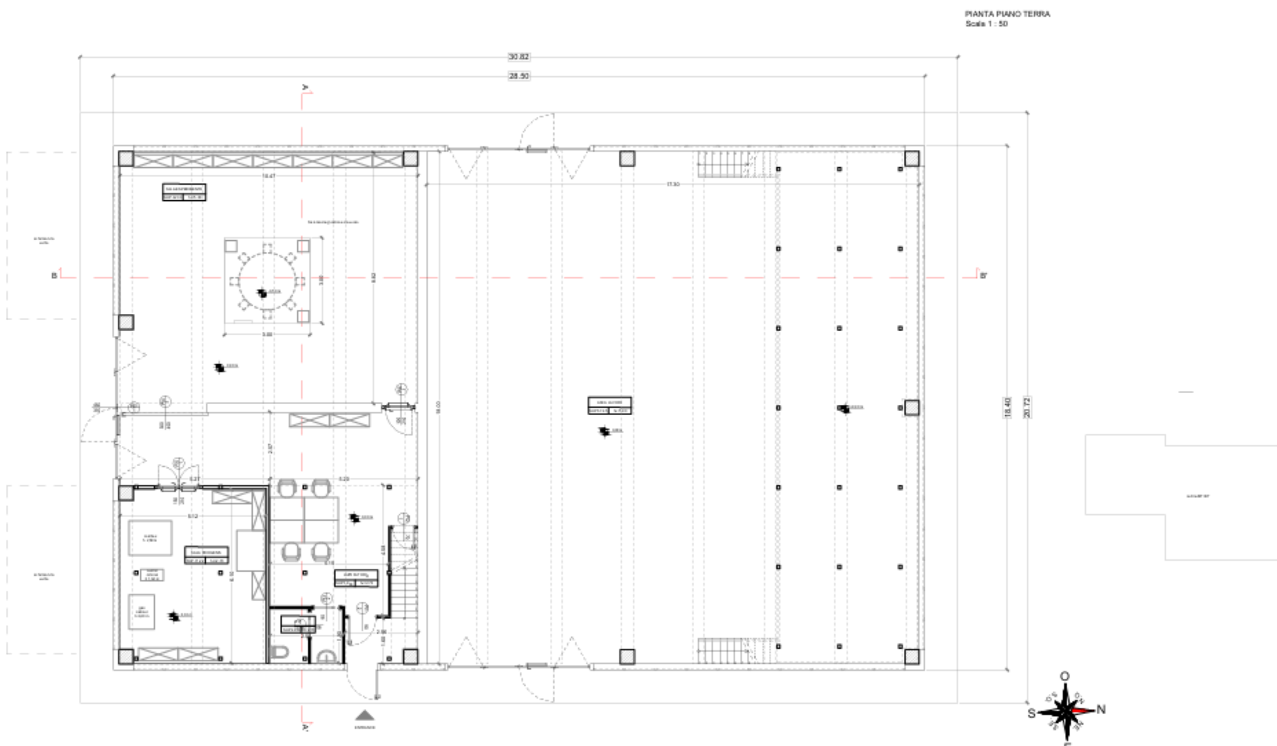
PIANTA PIANO TERRA
Scala 1 : 50
30.82
28.50
A
B
B'
17.30
18.40
20.72
A'
O
S
N
E

(b)

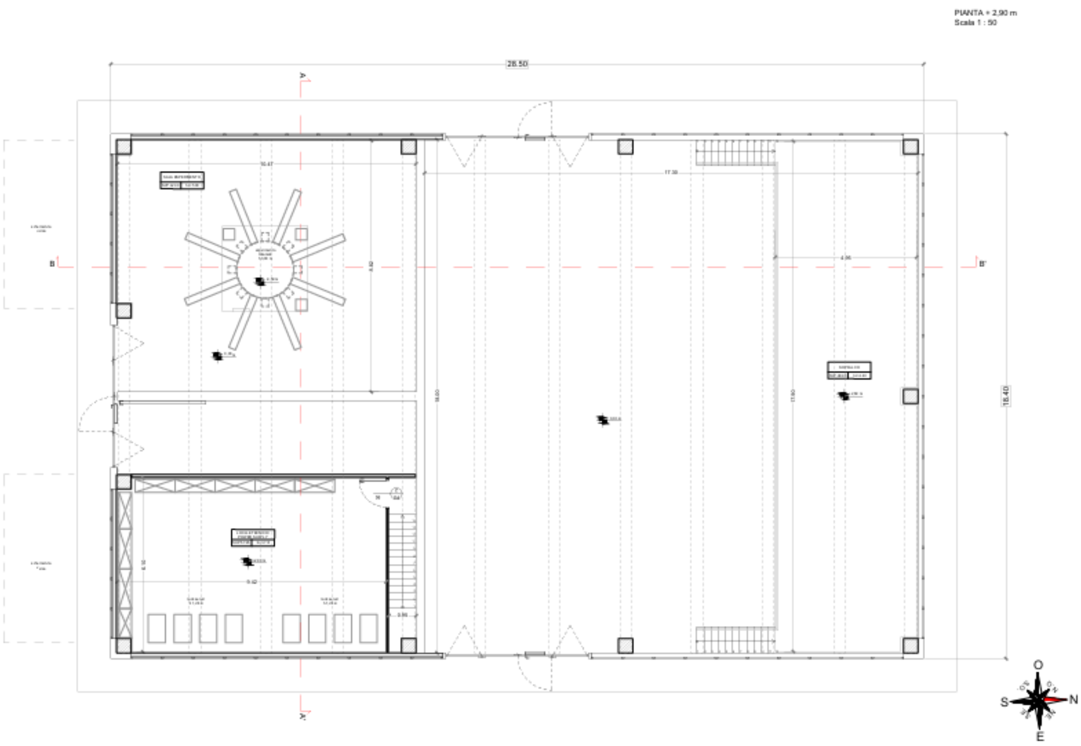

(c)

Fig. 43 (a) Current state of the warehouse, (b) Facility project approved – ground floor and (c) Facility project approved – first floor

5.2 Safety Analysis

In the following part are reported requirements and preventive actions to ensure safe conditions for TRUST-related experimental phases. This analysis is mandatory to the risk assessment associated with radio frequency and microwave electromagnetic fields, static magnetic fields, magnetic confinement nuclear fusion plant and cryogenic substances (D. Lgs. 81/2008 e s.m.i.).

The risk assessment requires knowledge of the probability of the triggering event and the subsequent performance of the protection systems. At present, there is no data on the failure rate of components for assessing the probability of an accident in the field of nuclear fusion, and even internationally, the specific database developed for fusion is based on data from typical equipment used in other areas of engineering (such as pipes, valves, ducts, etc.), which is in fact unrepresentative and only partially plausible. In the context of this experiment, an important activity is the characterisation of materials from the point of view of safety. For safety, it is referred as far as applicable to the general nuclear safety concept of current power reactor plants, which use fission, although there are specific differences in their implementation due to the physical and technological characteristics of fusion plants, and in any case the three safety objectives (general nuclear safety objective, radiation protection objective and technical safety objective) are to be achieved to ensure that the sources/components are kept under strict technical and administrative control.

- General nuclear safety objective: To protect individuals, society and the environment from harm by establishing and maintaining effective defences in nuclear facilities against radiological hazards (ionising and non-ionising).
- Radiation protection objective: To ensure that in all operating states radiation exposure within the facility or from any planned release of radioactive material from the facility is kept below prescribed limits and at the lowest reasonably achievable level, and to ensure mitigation of the radiological consequences of any accidents.
- Technical safety objective: to take all reasonably practicable measures to prevent accidents in nuclear facilities and to mitigate their consequences should they occur; to ensure with a high level of safety that, for all possible accidents considered in the design of the facility, including those of very low probability, the possible consequences from whatever source and in particular the radiological consequences are kept below the prescribed limits; and to ensure that the probability of accidents with severe radiological consequences is kept extremely low.

In TRUST the plasma reaction will be of the type H-H, so according to [5] and as described in Section 4.2, the plasma average electron temperature $T_{e,ave}$ of ~ 0.35 keV leads to a probability of nuclear reaction of ~ 0%. Therefore, no ionising radiation of the alpha type or neutron flux will be released, and the radiation produced inside the experiment (radius of 0.3m) would possibly produce a dose much lower than 1 mSv (the limit of Legislative Decree 101/20 for annual effective dose for non-exposed workers). It is possible to highlight as the average natural background in the Viterbo city area is approximately 4 mSv per year [90] resulting more critical respect the TRUST experiment. Moreover, due to the small amount of Hydrogen needed for the plasma pulse (approx. equal to 1 mg) also the explosion hazards are ~ 0 avoiding external elements from penetrating the VV.

The failure of magnetic systems can result in the occurrence of electric arcs which, by discharging their energy, can create significant damage to VV. In order to discharge the magnet's energy, protection, monitoring and fault detection systems must are foreseen to minimise the probability of arcs damaging the vacuum chamber walls. With regard to electromagnetic loads, these are negligible. Indeed, the main risks associated with the presence and use of static magnetic fields are: exposure to field levels that may be higher, even by several orders of magnitude, than the earth's magnetic field; uncontrolled movement of ferromagnetic objects attracted to the field. Following the guidelines on limits of exposure to static magnetic fields [91], the references limit for a continuous body exposure for non-exposed workers is 40 mT (limit that reaches even the 0.5 mT in case of people with pacemakers and/or defibrillators). In the worst operating condition, the magnetic field reached at the inner wall of the experimental hall (about 5m from the machine axis) is 0.3 mT. Three access zones are defined:

- Controlled access areas, zones where the stray field of magnetic induction is 0.5 mT (5 Gauss) or more [$B > 0.5$ mT].
- Respect zones, zones affected by stray field values of magnetic induction between 0.1 mT (1 Gauss) and 0.5 mT (5 Gauss) [0.1 mT $< B <$ 0.5 mT].
- Free-access areas, zones affected by stray field values of magnetic induction of less than 0.1 mT (1 Gauss) [$B < 0.1$ mT].

Thus, staying in areas affected by high field levels must be justified and optimised, i.e. made such that the operator is exposed to the lowest possible field level for the shortest time. These zones are defined in the absence of specific regulations, but in accordance with Ministerial Decree 2/08/91 on magnetic resonance diagnostic equipment, wherever there are static magnetic fields.

6. Conclusions

This thesis represents a significant contribution to the advancement of compact and scalable fusion reactor designs, with a focus on two complementary frameworks: the TRUST tokamak and the Alternative Magnetic Layout (AML). TRUST has been developed as a versatile, modular, and cost-effective platform that not only addresses critical engineering challenges but also serves as an essential tool for academic training and experimental validation. Its integration of advanced technologies, such as high-temperature superconductors and metamaterials, positions TRUST as a pioneering model for the next generation of tokamaks. The tokamak's adaptability and modular design allow for the testing of various configurations, fostering innovation and enabling collaboration with industrial partners to co-develop advanced engineering solutions. TRUST also demonstrates the critical role of academic tokamaks in bridging the gap between theoretical studies and practical applications, while contributing to the cultivation of a skilled workforce in fusion science and engineering. The AML framework complements TRUST by introducing a pre-conceptual reactor design that emphasizes compactness, simplicity, and cost-effectiveness. By reimagining the configuration of key components, such as the central solenoid and toroidal field coils, AML seeks to reduce the radial build of fusion reactors while maintaining efficient plasma confinement and operational stability. TRUST serves as a key experimental platform for validating AML-inspired concepts, enabling the practical assessment of its scalability and potential for application in larger fusion systems. This research combines advanced computational modelling with experimental validation to refine the designs of both TRUST and AML, providing a comprehensive understanding of the challenges and opportunities associated with compact fusion reactors. Plasma confinement, magnetic field performance, and material durability are systematically evaluated, and the results are benchmarked against conventional tokamak designs to highlight their advantages and limitations. This multi-faceted approach not only advances the state of the art in compact fusion technology but also provides a roadmap for future research and development. The findings of this thesis underline the importance of integrating academic research, industrial collaboration, and experimental validation in addressing the multifaceted challenges of nuclear fusion. By focusing on compact and adaptable designs, the TRUST and AML projects contribute to the broader vision of making fusion energy a practical and scalable solution to the global energy crisis. Future work should prioritize expanding the experimental capabilities of TRUST, refining AML concepts, and fostering deeper collaborations with industry to accelerate the transition from conceptual designs to operational fusion reactors. This thesis thus offers a significant step toward realizing the potential of nuclear fusion as a sustainable, reliable, and transformative energy source for future generations.

Bibliography

[1] International Energy Agency (IEA). (2024). *World Energy Outlook 2024.* Paris: IEA Publications.

[2] International Atomic Energy Agency (IAEA). (2024). *World Fusion Outlook 2024.* Vienna: IAEA Publications.

[3] Claessens, M. (2020). *ITER: The Giant Fusion Reactor: Bringing a Sun to Earth.* Springer.

[4] Stacey, W. M. (2010). *Fusion: An Introduction to the Physics and Technology of Magnetic Confinement Fusion.* Wiley.

[5] Wesson, J. (2011). *Tokamaks* (4th ed.). Oxford University Press.

[6] A W Morris *et al* 2022 *Plasma Phys. Control. Fusion* **64** 064002

[7] B. Bigot 2019 *Nucl. Fusion* **59** 112001

[8] S. Carusotti, et al., "Overview on the conceptual design and preliminary plasma scenario studies of university-class experiment TRUST", submitted to Fusion Eng. Des., 2024.

[9] C.F. Maggi et al 2024 *Nucl. Fusion* **64** 112012

[10] Francesco Romanelli *et al* 2024 *Nucl. Fusion* **64** 112015.

[11] F. Crisanti *et al* 2024 *Nucl. Fusion* **64** 106040

[12] Creely AJ, Greenwald MJ, Ballinger SB, et al. Overview of the SPARC tokamak. *Journal of Plasma Physics*. 2020;86(5):865860502.

[13] M. Scarpari, et al., "Development of SPARC plasma disruption database through electromagnetic predictive MAXFEA modelling", Fusion Eng. Des., Vol. 204, 2024.

[14] E.S. Marmar *et al* 2015 *Nucl. Fusion* **55** 104020

[15] K. Hanada, et al., "Overview of recent progress on steady state operation of all-metal plasma facing wall device QUEST", Nuclear Materials and Energy, vol. 27, 2021

[16] O. Grover, et al., "Remote operation of the GOLEM tokamak for Fusion Education", Fusion Eng. Des., vol. 112, 2016.

[17] S.J. Doyle, et al., "Magnetic equilibrium design for the SMART tokamak", Fusion Eng. Des., vol. 171, 2021.

[18] D. Kingham, et al., "The spherical tokamak path to fusion power: Opportunities and challenges for development via public–private partnerships", Phys. Plasmas, Vol. 31, 2024.

[19] J.R. Harrison *et al* 2024 *Nucl. Fusion* **64** 112017

[20] J.W. Berkery, et al., "NSTX-U research advancing the physics of spherical tokamaks", Nuclear Fusion, Volume 64, Number 11, 2024.

[21] S.A.M. McNamara *et al* 2024 *Nucl. Fusion* **64** 112020.

[22] R. Lombroni, et al., "Use of MAXFEA code in combination with ANSYS APDL to study the Electro-Magnetic behaviour of the new ST40 Inner Vacuum Chamber (IVC2) proposal during a plasma VDE", Fusion Eng. Des., vol. 192, 2023.

[23] S. Carusotti, et al., "Structural behaviour characterization of ST40 Inner Vacuum Chamber (IVC2) during a plasma VDE using ANSYS Workbench", Fusion Eng. Des., vol. 192, 2023.

[24] A.V. Müller, et al, "Tailored tungsten lattice structures for plasma-facing components in magnetic confinement fusion devices", Materials Today, Vol. 39, 2020.

[25] S. Carusotti, et al., "Preliminary study on Alternative Magnetic Layout (AML) for tokamaks reactors in the TRUST project framework", submitted to Fusion Eng. Des., 2024.

[26] G. Federici, "The European Programme Towards A Demonstration Fusion Reactor", Oral Contribution for 32nd Symposium on Fusion Technology (SOFT), 2022.

[27] G. Federici, "DEMO-related design activities in Europe", Oral Contribution for 15th International Symposium on Fusion Nuclear Technologies (ISFNT), 2023.

[28] U.S. Department of Energy (DOE), *Fusion Energy Strategy 2024*.

[29] C. Bachmann, et al., "Re-design of EU DEMO with a low aspect ratio", Fusion Eng. Des., vol. 204, 2024.

[30] https://tokamakenergy.com/ (access 31/01/2025)

[31] https://www.waltertosto.it/ (access 31/01/2025)

[32] https://www.asgsuperconductors.com/ (access 31/01/2025)

[33] https://ocem.eu/ (access 20/12/2024)

[34] Y. Sarazin *et al* 2020 *Nucl. Fusion* **60** 016010.

[35] M. Siccinio, et al., "Development of the plasma scenario for EU-DEMO: Status and plans", Fusion Eng. Des., Vol. 176, 2022.

[36] J.P. Freidberg, *Phys. Plasmas* 22, 070901 (2015).

[37] G. Federici, et al., "Relationship between magnetic field and tokamak size—a system engineering perspective and implications to fusion development", Nuclear Fusion, Volume 64, Number 3, 2024.

[38] C. Bachmann, et al., "Influence of a high magnetic field to the design of EU DEMO", Fusion Eng. Des., vol. 197, 2023.

[39] X. Sarasola, et al., "Parametric Studies of the EU DEMO Central Solenoid", IEEE Transaction on Applied Superconductivity, Vol. 33, 2023.

[40] L. Giannini, et al., "The MAgnet Design Explorer algorithm (MADE) for LTS, Hybrid or HTS toroidal and poloidal systems of a tokamak with a view to DEMO", Fusion Eng. Des., vol. 193, 2023.

[41] A. Portone, et al., "Design of superconducting tokamak magnet systems and applications to HTS", Fusion Eng. Des., vol. 193, 2023.

[42] G. Matsunaga, et al., "Achievement of precise assembly of the JT-60SA superconducting tokamak", Fusion Eng. Des., Vol 174, 2022.

[43] J.D. Weiss, et al., "Performance of low-loss demountable joints between CORC® cable-in-conduit-conductors at magnetic fields up to 8 T developed for fusion magnets", Supercond. Sci. Technol., Vol. 36, 2023.

[44] A. Van Arkel, et al., "Unlocking maintenance—architecting STEP for maintenance and realizing remountable magnet joints", Phil. Trans. R. Soc. A, Vol. 38, 2024.

[45] N. Mitchell, et al., "Superconductors for fusion: a roadmap", Supercond. Sci. Technol., Vol. 34, 2021.

[46] L. Giannini, et al., "An innovative coil fabrication and assembly process for the VNS tokamak based on in-situ winding", Fusion Eng. Des., Vol. 205, 2024.

[47] M. Claessens, "More Technical Challenges", In: ITER: The Giant Fusion Reactor, Copernicus Books, 2023.

[48] C. Lijun, et al., "Progress of Engineering Design of CFETR Machine Assembly", Fusion Science and Technology, Vol 78, 2022.

[49] M.L. Walker, et al., "Introduction to Tokamak Plasma Control", 2020 American Control Conference (ACC).

[50] S. Ding, et al., "A low plasma current (~ 8 MA) approach for ITER's Q= 10 goal.", Proc. 28th IAEA Fusion Energy Conference, 2021.

[51] H. Zohm, et al., "A stepladder approach to a tokamak fusion power plant", Nucl. Fusion, Vol. 57, 2017.

[52] S.J. Frank, et al., "Radiative pulsed L-mode operation in ARC-class reactors", Nucl. Fusion, Vol. 62, 2022.

[53] N. Asakura, et al., "Recent progress of plasma exhaust concepts and divertor designs for tokamak DEMO reactors", Nuclear Materials and Energy, Vol. 35, 2023.

[54] G: Federici, “Testing needs for the development and qualification of a breeding blanket for DEMO”, Nucl. Fusion, Vol. 63, 2023.

[55] G. Granucci, et al., “Roles of ECH system in DTT plasma operations”, Nucl. Fusion, Vol. 64, 2024.

[56] S. Ejima, et al., “Volt-second analysis and consumption in Doublet III plasmas”, Nuclear Fusion, Volume 22, 1982.

[57] Zoboli L., et al., “Multiscale structural assessment of toroidal field coils via reduced-order models”, Fusion Eng. Des., vol. 182, 2022.

[58] Y. Zhai, et al., “HTS Cable Conductor for Compact Fusion Tokamak Solenoids”, IEEE Transaction on Applied Superconductivity, Vol. 32, 2022.

[59] J.D. Weiss, et al., “Performance of low-loss demountable joints between CORC® cable-in-conduit-conductors at magnetic fields up to 8 T developed for fusion magnets”, Supercond. Sci. Technol., Vol. 36, 2023.

[60] M. Coatanéa, et al., “Selection of a quench detection system for the ITER CS magnet”, Fusion Eng. Des., Vol. 86, 2011.

[61] H. Utoh, et al., “SCONE code: Superconducting TF coils design code for tokamak fusion reactor”, J. Plasma Fusion Res. SERIES, Vol. 9, 2010.

[62] R. Wesche, et al., “Parametric study of the TF coil design for the European DEMO”, Fusion Eng. Des., Vol. 164, 2021.

[63] Yong Ren *et al* 2015 *Nucl. Fusion* **55** 093002.

[64] A. Fasoli, “Overcoming the Obstacles to a Magnetic Fusion Power Plant”, Phys. Rev. Lett. 130, 220001, 2013.

[65] A. Castaldo, et al., “Plasma Scenarios for the DTT Tokamak with Optimized Poloidal Field Coil Current Waveforms”, Energies, vol. 15, 2022.

[66] S.L. Gralnick, et al, “Analytic solutions for constant-tension coil shapes”, Journal of Applied Physics, 47, 1976.

[67] D.Q. Liu, et al., “Engineering design for the HL-2M tokamak components”, Fusion Eng. Des., vol. 88, 2013.

[68] S. Ito, et al., “Advanced high-temperature superconducting magnet for fusion reactors: Segment fabrication and joint technique”, Fusion Eng. Des., vol. 136, 2018.

[69] B. Lipschultz, et al., “Alcator C-Mod: A high-field divertor tokamak”, Journal of Nuclear Material, vol 162-164, 1989

[70] S.J. Doyle, et al., “Magnetic equilibrium design for the SMART tokamak”, Fusion Eng. Des., vol. 171, 2021.

[71] P.C. de Vries, et al., “ITER breakdown and plasma initiation revisited”, Nuclear Fusion, Volume 59, Number 9, 2019.

[72] Y. Gribov, et al., “Chapter 8: plasma operation and control”, Nuclear Fusion, Volume 47, Number 6, 2007.

[73] K. Hada, et al., “Analysis of ECRH Pre-Ionization for Plasma Start-Up in JT-60SA”, Plasma and Fusion Research, vol. 7, 2012.

[74] R. Khan, et al., “Development of microwave pre-ionization source for GLAST tokamak” Fusion Eng. Des., vol. 126, 2018.

[75] A. Scarabosio, “Outer target heat fluxes and power decay length scaling in L-mode plasmas at JET and AUG” Journal of Nuclear Mat

[76] P.C. Stangeby, “The plasma boundary of magnetic fusion devices” Institute of Physics Publishing Bristol and Philadelphia (2000).

[77] T. Eich, et al, “Inter-ELM power decay length for JET and ASDEX Upgrade: Measurement and comparison with heuristic drift-based model”, Physical Review Letters, Volume 107, 2011.

[78] M. Wischmeier, et al., “High density operation for reactor-relevant power exhaust”, Journal of Nuclear Materials, Volume 463, 2015.

[79] P. Innocente, et al., “Design of a multi-configurations divertor for the DTT facility”, Nuclear Materials and Energy, vol. 33, 2022.

[80] J.H. You, et al., “Limiters for DEMO wall protection: Initial design concepts & technology options”, Fusion Eng. Des., vol. 174, 2022.
[81] A. Sykes et al., “Overview and status of the ST40 high field spherical tokamak”, *Nuclear Fusion*, vol. 58, no. 1, 2018.
[82] A. Moret, et al., "Vertical instability analysis and control in the TCV tokamak," *Nuclear Fusion*, vol. 37, no. 6, pp. 825–834, 1997.
[83] G. Sias, et al, “Inter-machine plasma perturbation studies in EU-DEMO relevant scenarios: lessons learnt for EM forces prediction during VDEs”, Nuclear Fusion, Volume 62, Number 7, 2022.
[84] N. W. Eidietis et al., ‘The ITPA disruption database’, Nucl. Fusion, vol. 55, no. 6, p. 63030, 2015.
[85] R. Lombroni, et al., “Using MAXFEA code in combination with ANSYS APDL for the simulation of plasma disruption events on EU DEMO”, Fusion Eng. Des., vol. 170, 2021.
[86] F. Giorgetti, et al., “Vertical Displacement Events analysis using MAXFEA code in combination with ANSYS APDL in the final design stage of the DTT Vacuum Vessel”, Fusion Eng. Des., vol. 184, 2022.
[87] V. Vullo, “Circular cylinders and pressure vessels”, Springer Series in Solid and Structural Mechanics, Springer 2014.
[88] A. Mancini, “Mechanical and electromagnetic design of the vacuum vessel of the SMART tokamak”, Fusion Eng. Des., vol. 171, 2021.
[89] Appendix A to ITER SDC-IC, Materials Design Limit Data, Iter_222RLN (private communication).
[90] Giustini, F. et al. Radon Hazard in Central Italy: Comparison among Areas with Different Geogenic Radon Potential. Int. J. Environ. Res. Public Health 2022, 19, 666.
[91] HEALTH PHYSICS 74 (4):494-522; 1998